TRANSPORTATION RESEARCH RECORD 641

Stabilization of Soils

TRANSPORTATION RESEARCH BOARD

COMMISSION ON SOCIOTECHNICAL SYSTEMS
NATIONAL RESEARCH COUNCIL

NATIONAL ACADEMY OF SCIENCES
WASHINGTON, D.C. 1977

Transportation Research Record 641
Price $4.40
Edited for TRB by Frances R. Zwanzig

subject areas
61 exploration-classification (soils)
62 foundations (soils)
64 soil science

Transportation Research Board publications are available by ordering directly from the board. They may also be obtained on a regular basis through organizational or individual supporting membership in the board; members or library subscribers are eligible for substantial discounts. For further information, write to the Transportation Research Board, National Academy of Sciences, 2101 Constitution Avenue, N.W., Washington, D.C. 20418.

Notice
The project that is the subject of this report was approved by the Governing Board of the National Research Council, whose members are drawn from the councils of the National Academy of Sciences, the National Academy of Engineering, and the Institute of Medicine. The members of the committee responsible for the report were chosen for their special competence and with regard for appropriate balance.

This report has been reviewed by a group other than the authors according to procedures approved by a Report Review Committee consisting of members of the National Academy of Sciences, the National Academy of Engineering, and the Institute of Medicine.

The views expressed in this report are those of the authors and do not necessarily reflect the view of the committee, the Transportation Research Board, the National Academy of Sciences, or the sponsors of the project.

Library of Congress Cataloging in Publication Data
National Research Council. Transportation Research Board.
Stabilization of soils.

(Transportation research record; 641)
Includes bibliographical references.
1. Soil stabilization—Addresses, essays, lectures. 2. Roads—Subgrades—Addresses, essays, lectures. I. Title. II. Series.
TE7.H5 no. 641 [TE210.4] 380.5'08s [625.7'4]
ISBN 0-309-02670-9 78-9730

Sponsorship of the Papers in This Transportation Research Record

GROUP 2—DESIGN AND CONSTRUCTION OF TRANSPORTATION FACILITIES
Eldon J. Yoder, Purdue University, chairman

Compaction and Stabilization Section
Eugene B. McDonald, South Dakota Department of Transportation, chairman

Committee on Compaction
Charles M. Higgins, Louisiana Department of Highways, chairman
Mehmet C. Anday, Robert C. Deen, J. M. Hoover, Eugene Y. Huang, James E. Kelly, T. F. McMahon, William B. O'Sullivan, John R. Sallberg, Charles H. Shepard, William J. Sisiliano, Travis W. Smith, Robert J. Weaver, William G. Weber, Jr., Anwar E. Z. Wissa

Committee on Chloride Stabilization
B. Dan Marks, University of Tennessee, chairman
Gail C. Blomquist, Howard W. Fiedelman, William B. Greene, T. Allan Haliburton, Darryl L. Hearn, Ignat V. Kalcheff, R. C. Mainfort, Raymond K. Moore, Chester I. Schlarb, Walker L. Shearer, Frank C. Townsend

Committee on Lime and Lime-Fly Ash Stabilization
Marshall R. Thompson, University of Illinois at Champaign-Urbana, chairman
Mehmet C. Anday, Robert F. Ballard, Jr., James L. Eades, Kenneth A. Gutschick, C. W. Heckathorn, Thomas W. Kennedy, B. Dan Marks, Chester McDowell, W. C. Ormsby, Joseph H. Pound

Committee on Soil-Portland Cement Stabilization
J. M. Hoover, Iowa State University, chairman
Ara Arman, Merle D. Baker, H. H. Duval, Jr., Donald G. Fohs, K. P. George, Ali S. Kemahli, Thomas W. Kennedy, T. J. Larsen, Manuel Mateos-de-Vicente, Peter Nussbaum, E. Guy Robbins, Anwar E. Z. Wissa, Toyotoshi Yamanouchi

Committee on Soil-Bituminous Stabilization
Jon A. Epps, Texas A&M University, chairman
David D. Currin, Jack N. Dybalski, K. P. George, J. M. Hoover, Edwin H. Jones, Larry L. Kole, Sidney Mintzer, Raymond K. Moore, Charles G. Schmitz, Leonard J. Stern, B. A. Vallerga, Thomas D. White, Anwar E. Z. Wissa

Soil Mechanics Section
Lyndon H. Moore, New York State Department of Transportation, chairman

Committee on Strength and Deformation Characteristics of Pavement Sections
Richard D. Barksdale, Georgia Institute of Technology, chairman
Stephen F. Brown, Jim W. Hall, Jr., Amir N. Hanna, R. G. Hicks, Frank L. Holman, Jr., Ignat V. Kalcheff, Bernard F. Kallas, William J. Kenis, Thomas W. Kennedy, Kamran Majidzadeh, Fred Moavenzadeh, Quentin Robnett, Jatinder Sharma, Eugene L. Skok, Jr., Ronald L. Terrel, Peter J. Van de Loo

Soil and Rock Properties and Geology Section
David L. Royster, Tennessee Department of Transportation, chairman

Committee on Frost Action
Wilbur M. Haas, Michigan Technological University, chairman
Barry J. Dempsey, Wilbur J. Dunphy, Jr., L. F. Erickson, Glenn E. Johns, Thaddeus C. Johnson, Alfreds R. Jimikis, Miles S. Kersten, Clyde N. Laughter, George W. McAlpin, Richard W. McGaw, Stephen F. Obermeier, Marvin D. Oosterbaan, Robert G. Packard, Edward Penner, Harold R. Peyton, Alex Rutka

John W. Guinnee, Transportation Research Board staff

Sponsorship is indicated by a footnote at the end of each report. The organizational units and officers and members are as of December 31, 1976.

Contents

Subgrade Modulus on the San Diego Test Road

Michael P. Jones, Naval Facilities Engineering Command, Alexandria, Virginia
Matthew W. Witczak, Department of Civil Engineering, University of Maryland

The San Diego County Experimental Base Project, which was constructed in 1966 and continued until 1973, was a test road consisting of 35 different sections designed to measure the performance of granular and asphalt-bound base courses. This paper presents an analysis of the test-road subgrade and its variability. Multiple regression analysis has shown that the subgrade resilient modulus can be correlated with the soil moisture and degree of saturation and that the ratio of the laboratory modulus to the field modulus is near unity for high degrees of saturation. For lower degrees of saturation (80 to 85 percent), laboratory-compacted samples tended to have higher values of the modulus than did field-compacted samples. On the average, for treated base sections, the in-place modulus predicted from regression analysis gave excellent agreement with values of the modulus derived from Benkelman-beam deflections in a multilayer elastic analysis. Because of an apparently stiffer in situ response of granular base material than was predicted in the laboratory, similar comparisons for granular base sections were not good. The modulus of granular base materials averaged six times greater in the field than in the laboratory. The test-road subgrade was not uniform, but was highly variable between and within test sections. Resilient-modulus tests of undisturbed field cores had a coefficient of variation of the modulus of approximately 97 percent between test sections. The coefficient of variation within test sections averaged approximately 40 percent.

The San Diego County Experimental Base Project was a test road consisting of 35 different sections designed to measure the performances of granular and asphalt-bound courses. The objects of the experiment were to determine the specific thicknesses of various types of base courses required to give a desired level of performance, to relate the properties of the pavement to its observed performance, and to study deflection and strain behavior for translating performance results to other environments. The test road was completed in August 1966, and performance observations were continued until 1973.

The test road was designed for six different types of base at four levels of thickness. The bases included asphalt concrete, asphaltic-cement treated, cutback treated, emulsion treated, and California classes 2 and 3 aggregate. One additional type of base at two levels of thickness and two sections of a standard California design were also included. The thickness and quality of the asphalt-concrete surface and the quality of the clay subgrade were designed to be uniform throughout the length of the project.

Detailed descriptions of the design and construction of the road have been reported by Riley and Shook (1) and by Kingham (2). The performance of the test sections have been given by Hicks and Finn (3) and by Shook and Lambrechts (4). Hicks and Finn (3), in their performance study, cited considerable ambiguity in defining the resilient modulus of the subgrade with time and between test sections. The absence of subgrade-soil test data was a major obstacle in the development of fatigue relations from the data.

This paper presents an analysis of the subgrade modulus, the methods of its measurement, and the correlations and associated variability between and within test sections. The methods of measurement included laboratory tests on compacted and undisturbed specimens and modulus estimates determined from Benkelman-beam deflections and multilayered elastic theory. It also includes an analysis of the in-situ response of the unbound, granular base-course materials.

SUBGRADE CONSTRUCTION

The subgrade soil for all test sections was an A-7-6. Special contract provisions required that there be a minimum of 0.6 m (2 ft) of the clay under each test section. The original ground was excavated to a depth of 0.6 m (2 ft) below subgrade and, if a suitable clay existed at the bottom of the excavation, the clay was backfilled and compacted. If material other than clay was found at the bottom of the excavation, an additional 0.3 m (1 ft) of material was excavated before backfilling. The contract specifications required that the clay backfill be compacted to at least 90 percent of its maximum density within a moisture-content range of -2 to +3 percent of optimum.

Subgrade compaction-test results for each of the test sections have been reported by Kingham (2). All of the test sections were compacted in excess of the minimum of 90 percent. The variations in dry density among the test sections ranged from 1672 to 1901 kg/m^3 (104.4 to 118.7 lb/ft^3). The moisture contents ranged from 11.4 to 18.0 percent.

SUBGRADE RESILIENT MODULUS

The background of the resilient modulus test has been given by Seed, Chan, and Lee (5). In this test, the modulus of resilient deformation (M_R) is determined from repeated-load, triaxial compression tests. The modulus is computed as the ratio of the deviator stress to the resilient axial strain.

The modulus of fine-grained soils depends on both the deviator and the confining stresses, with the deviator stress being predominant. The modulus generally decreases with increasing deviator stress and decreasing confining pressure. The modulus is also significantly affected by the moisture content and the dry density of the soil.

Laboratory-Molded Samples

The resilient modulus of the subgrade soil was determined on laboratory-molded samples by the Asphalt Institute. Specimens 15.2 cm (6 in) in diameter and 30.5 cm (12 in) high were compacted at varying moisture contents according to the American Society for Testing and Materials Test Method D-1557. Two compactive forces [862 and 584 kJ/m^3 (18 000 and 12 000 ft·lb/ft^3)] were used. The deviator-stress levels were 41.4, 82.7, and 124.1 kPa (6, 12, and 18 lbf/in^2), and the ratios of the deviator stress to the confining stress were 3.0 and 1.5. Additional tests were conducted in an unconfined state. A complete summary of these test results has been given by Jones (6) and Kallas and Shook (7). The relation is between the M_R and the dry density versus the moisture content at the two compactive forces are shown in Figure 1.

To consider the effect of the overall physical state of the soil on the modulus, the degree of saturation (S) was computed and used in a multiple regression analysis with the modulus and the moisture content (Figure 2). To remove the influence of the stress state, all of the values of M_R used in the analysis corresponded to a deviator stress of 41.4 kPa (6 lbf/in^2) and a confining stress of

Figure 1. Effect of compactive effort on subgrade M_R (laboratory-molded samples).

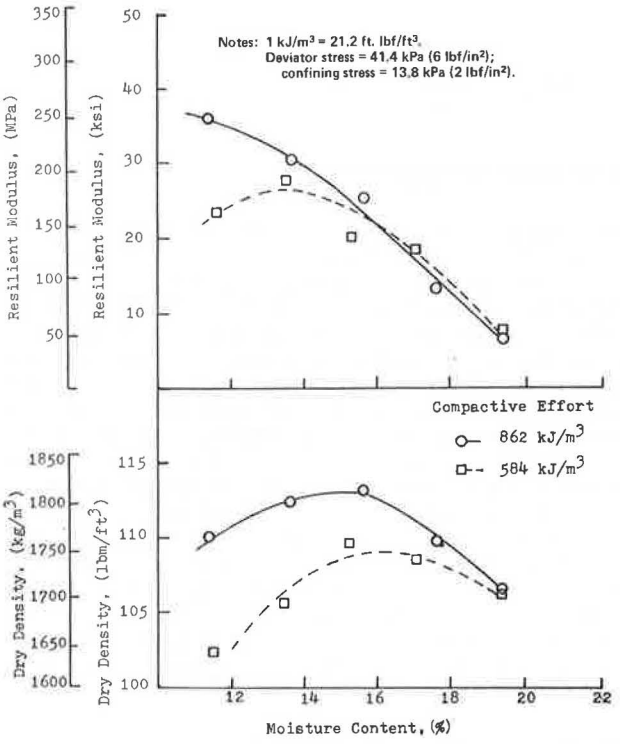

Figure 2. Relations between M_R, moisture content, and degree of saturation (laboratory-molded samples).

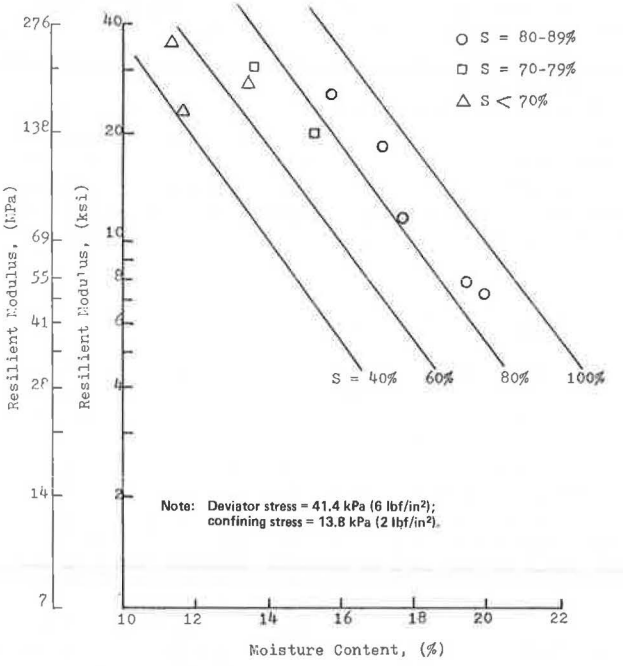

13.8 kPa (2 lbf/in²). The regression equation developed is given below.

$$\log M_R = -0.13\,282W + 0.013\,405S + 2.31\,909 \quad (n = 10 \text{ and } r = 0.97) \quad (1)$$

where W = percent moisture content. (SI units are not given for the variables in the equations in this paper because they were derived for U.S. customary units.)

A multiple variable model with limited test points may not, by itself, be statistically sound. However, the model selection was identical to the best-fit model developed from a larger data base of modulus tests on undisturbed specimens. The use of a similar model permitted comparisons between the two methods of prediction.

Undisturbed Field Samples

In 1970, undisturbed field samples from six test sections were tested for resilient modulus by the Asphalt Institute. In April and May of 1973, an extensive subgrade sampling program was conducted by San Diego County. The Asphalt Institute determined the M_R, moisture content, and dry density of undisturbed field samples from representative areas. These tests were conducted over a range of stress states; the complete test results have been given by Jones (6) and Kallas and Shook (7). Table 1 summarizes the test results for the subgrade for a deviator stress of 41.4 kPa (6 lbf/in²) and a confining stress of 13.8 kPa (2 lbf/in²). Figure 3 shows the range of test results at two different states of stress.

The effects of moisture and saturation on the M_R of the field samples were similarly examined. The values of the M_R from the first and second 0.3 m (1 ft) of the subgrade were combined for the 1970 and 1973 test series for the multiple regression analysis (Figure 4). The stress state chosen was the same as that chosen for the laboratory-molded samples. The derived relationship is shown below.

$$\log M_R = -0.111\,109W + 0.021\,699S + 1.17\,869 \quad (n = 97 \text{ and } r = 0.67) \quad (2)$$

The general pattern of Figure 4 is similar to the relationship developed from the laboratory-molded samples (Figure 2). A comparison of the two regression models is shown in Figure 5. There is good agreement at high degrees of saturation within the limits of moisture contents obtained (approximately 12 to 20 percent).

At high saturation levels, the modular ratio of laboratory-molded to field samples is near unity, which increases confidence in the use of laboratory-compacted samples for the evaluation of in situ modulus. However, for lower degrees of saturation, unconservative estimates of the field modulus may also be obtained with laboratory-compacted samples.

Specific reasons for this have been difficult to ascertain. However, Seed and others (5) have found that the method of compaction and the degree of saturation are only two of the many variables that affect the elastic modulus of clay. When cohesive soil samples are com-

Table 1. Tests on undisturbed field samples (April and May 1973).

Subgrade Depth[a] (m)	No. of Samples	Moisture Content (%) Mean	Moisture Content (%) Standard Deviation	Dry Density (kg/m³) Mean	Dry Density (kg/m³) Standard Deviation	Resilient Modulus (MPa) Mean	Resilient Modulus (MPa) Standard Deviation
0 to 0.30	44	16.9	2.1	1818.3	72.1	203.4	198.6
0.30 to 0.61	35	15.5	2.9	1792.6	73.7	182.7	160.6

Notes: 1 MPa = 145 lbf/in²; 1 m = 3.28 ft; 1 kg/m³ = 0.0624 lb/ft³.
Deviator stress = 41.4 kPa; confining stress = 13.8 kPa.

[a]Outer wheel path.

pacted at low degrees of saturation in the laboratory, little or no significant shearing strain is induced by any of the conventional methods of compaction, which results in the soil attaining a flocculated structure. When samples are compacted at a high degree of saturation (approximately greater than 80 percent), both kneading and impact compaction cause shear deformations that result in a more dispersed soil structure. For static compaction procedures, a flocculent structure occurs for all levels of saturation. Dispersed structures generally have higher deformations in the resilient-modulus test and consequently lower moduli.

The mean values of the degree of saturation for both the laboratory-molded samples and the initial undisturbed field samples were nearly identical (74 versus 75 percent), and one would not expect very large differences in the computed results with the two regression models.

Figure 3. Subgrade M_R test results (undisturbed specimens).

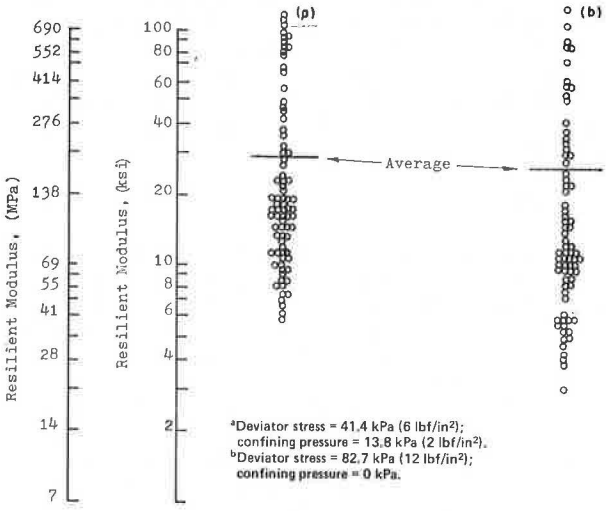

Figure 4. Relations between M_R, moisture content, and degree of saturation (undisturbed field samples).

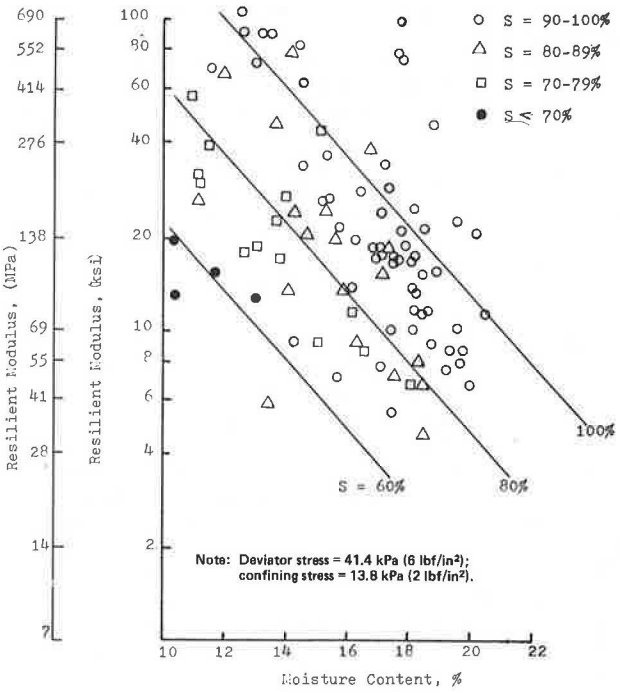

However, the impact type of laboratory compaction does not precisely simulate the in-service condition. As was shown by Jones (6), the mean subgrade saturation increased with time from the as-built value (74 percent) to a value greater than 90 percent. The structure of the subgrade soil particles was probably more flocculent for the entire period of service. One-half of the laboratory-molded samples were impact-compacted at a saturation level greater than 80 percent and would therefore exhibit a dispersed structure. These differences in soil structure may somewhat explain the differences in the two regression models.

The initial subgrade-compaction data for each test section were input into the two regression equations to predict the initial, in-situ subgrade M_R in each test section. The predicted values derived from Equations 1 and 2 for the treated and granular base sections will be summarized.

Derivation of Subgrade Moduli From Deflections

A major element in the San Diego measurements program was the measurement of the pavement-surface deflections with a Benkelman beam. The deflection measurements were made at least once a year over the entire test road and at more frequent intervals in test sections having high deflections. The measurements were obtained with a dual-tire-configuration, 80-kN (18 000-lbf/in²) axle load. The average pavement temperatures were also recorded.

A multilayer, linear-elastic system and the computer program, NLAYER, described by Michelow (8) were used to compute subgrade modulus values from the deflections. The elastic properties of all other pavement materials, determined from laboratory testing, were used as input to the analysis.

The basic approach used to develop a history of the subgrade modulus versus time for each test section was to develop a family of curves for each test section that related the computed deflection from the NLAYER program to the subgrade modulus and the temperature corresponding to an elastic modulus of the bound materials. By using these curves with the measured deflections and temperatures, an effective subgrade modulus was determined at which the measured deflections equaled the predicted deflections.

Figure 5. Relation between M_R of laboratory-molded and undisturbed field samples.

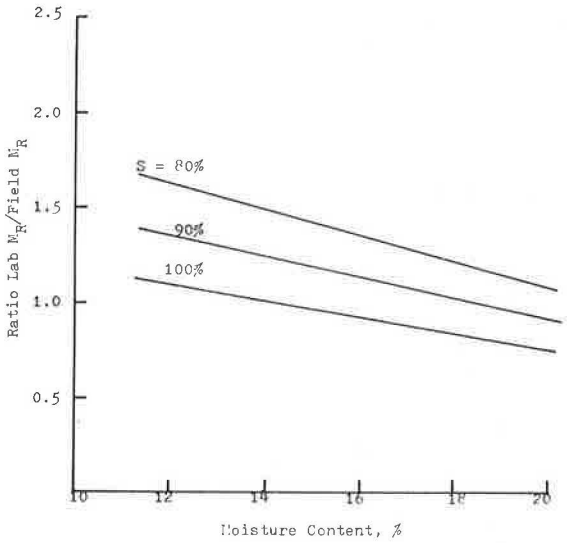

For pavement base-course materials having stress-dependent moduli, a layered-stress iteration procedure was used. The modulus of granular material and of emulsion and cutback-treated base in an uncured state can be expressed by the equation $M_R = k_1\theta^{no}$; where k_1 and no. are experimentally derived constants and θ is the first stress invariant.

The laboratory-derived values of k_1 and no. for unbound granular materials when tested at optimum moisture are given below (6, 7).

Aggregate Material	k_1	no.
Class 2 base	1880	0.64
Class 3 base	2101	0.57
Class 4 subbase	1944	0.59

The initial series of computer solutions for the class 2 and class 3 granular-base sections using the values of k_1 and no. given above gave exceedingly high values of deflection within the base. The ranges of computed deflections varied from the measured field deflections, particularly in the earlier stage of the project, leading to the conclusion that the base moduli values for granular materials in the field were higher than those determined from laboratory testing. A new M_R versus θ relationship, $M_R = 4000\,\theta^{0.5}$, was then selected for the analysis. This relationship differed only slightly from that used by Hicks and Finn (3) in their analysis of the San Diego data. (Later in this paper the actual in-situ response of the granular materials will be discussed more fully.)

Partial results of the deflection versus modulus analysis are given in Table 2. The derived moduli for the untreated base sections are significantly higher than those for the treated base sections, even though a higher M_R versus θ relationship than that predicted in the laboratory was used in the analysis.

Table 3 shows that the subgrade modulus values for the granular base sections do not compare well with the values predicted from the previously given regression models and the subgrade compaction tests. The high values predicted from the deflection analysis may be the result of the NLAYER-program prediction of high deflections within the base. It appears, therefore, that the granular base exhibits a stronger response in the field than was indicated by laboratory tests or the assigned modulus function ($M_R = 4000\,\theta^{0.5}$).

The values of the mean initial modulus given in Table 2 for the treated base sections also show some variance between the asphalt-concrete and asphalt-cement-treated bases versus those composed of the emulsion and cutback-treated materials. However, the differences among the treated bases are much smaller than the differences between the treated and untreated bases. The asphalt-concrete and asphalt-cement-treated bases are less complex and can be analyzed as two-layer systems in which the percentage of cure and the stress state are insignificant. However, an accurate measure of the in-situ modulus of the emulsion and cutback-treated bases is dependent on reliable estimates of both the percentage of cure and the in-situ stress state. Consequently, these sections would probably have the most reliable measure of subgrade M_R, which would be (initially) about 172 400 kPa (25 000 lbf/in^2). The difference between this value and the average modulus for all treated sections [138 600 kPa (20 100 lbf/in^2)] is relatively small and may be within the range of error introduced in the deflection-derived modulus study.

Table 2. Predicted initial subgrade modulus from deflections.

Type of Base	Derived Subgrade Modulus (MPa)	
	Mean	Standard Deviation
Asphalt concrete	183.4	40.7
Asphalt-cement treated	166.9	57.2
Emulsion treated	116.5	40.7
Cutback treated	100.7	11.7
Class 2	326.8	175.1
Class 3	370.9	75.2
Standard California design	362.0	24.1
All treated	138.6	51.0
All granular	350.9	117.2

Note: 1 MPa = 145 lbf/in^2.

Table 3. Initial subgrade M_R from three methods of measurement.

Section and Method of Measurement	M_R (MPa)	
	Mean	Standard Deviation
Treated base		
Benkelman-beam deflections	138.6	51.0
Regression model from undisturbed field samples[a]	138.6	53.1
Regression model from laboratory-molded samples[a]	224.1	64.1
Granular base		
Benkelman-beam deflections	350.9	117.2
Regression model from undisturbed field samples[a]	121.3	22.1
Regression model from laboratory-molded samples[a]	217.2	65.5

Note: 1 MPa = 145 lbf/in^2.
[a] All regression models based on a deviator stress of 41.4 kPa and a confining stress of 13.8 kPa.

Comparisons

Table 3 gives a comparison of the predicted initial M_R values and the standard deviations computed for each of the prediction methods for both treated and unbound base sections. For the treated base sections, the mean values of M_R computed from the deflection measurements are in excellent agreement with the mean values predicted by the regression model from the field cores. However, the mean values of the deflection-derived M_R for granular sections do not compare well, and these values are not considered representative of the actual subgrade stiffness.

For the treated base sections, the mean values of the initial M_R determined from the laboratory-molded samples are about 50 percent higher than those predicted by deflections or by the field cores (Figure 5). The mean subgrade saturation at the time of compaction was about 75 percent, and the mean moisture content was about 14 percent. Thus, from Figure 5, one would expect higher predicted values from the laboratory samples. However, cohesive subgrades tend to gain moisture with time, and their saturation levels approach 90 to 100 percent. This was true on the San Diego Test Road. Consequently, in terms of the longer term or ultimate subgrade modulus in the field, tests on laboratory-molded samples should give reasonable estimates.

SUBGRADE VARIABILITY

Analysis of the M_R values from tests on field cores and those values derived from deflections gave results indicative of the large variations in the test-road subgrade. For example, the results of the 1973 field-sampling program, summarized in Table 1, showed the coefficient of variation (CV) of the modulus in the top of the subgrade, between test sections, to be 97 percent. When analyzed for variability within test sections, the field cores had a mean CV of the M_R of 40 percent in the top half of the subgrade.

The standard deviations of the deflection measurements within test sections were also used to estimate the magnitude of the subgrade variability. From the family of curves used to develop moduli from deflections, the range in M_R corresponding to the range of plus and

minus one standard deviation of deflection was determined. From this analysis, a mean standard deviation and CV of the M_R was computed for the initial deflection-measurement period and for each deflection measurement in the pavement history. The computed average values of the CV within test sections for the entire length of the test road are given below.

At	Average Values (%)	
	From Deflections	From Field Cores
Project initiation	17	—
Project termination	38	40

(The value given from the deflection measurement at project termination represents the average for all deflection measurement periods, and the value given from the field cores at termination is from the 1973 sampling program.)

A number of inferences can be drawn from this table. The variation of the initial subgrade M_R as measured by deflections is within reasonable limits. Although a small number of test sections showed high variations, the overall mean CV of 17 percent is within the normal limits of control of pavement construction. The values of CV at the time of the project termination indicate that the variability has increased with time. This high degree of variability has undoubtedly occurred because of nonuniform changes in the physical state of the clay soil. The mean CV of the modulus as determined from field samples agrees well with the mean value computed from deflections, i.e., 40 percent from field cores versus 38 percent from deflections. The values computed from deflections represent the average variation for all periods of the deflection measurement. Thus, the high variability in the subgrade probably existed earlier in the project history than is indicated by the 1973 coring program.

The variations of the in-situ subgrade M_R are generally much greater than the variations created by differences in stress state. Test data for eight of the subgrade cores taken in 1973 were randomly chosen and their CV of M_R computed over five different states of stress. The average for the eight cores was 18 percent. Thus, the influence of stress state in the determination of the in-situ modulus is secondary when compared to the physical variations in the soil. This can also be seen in Figure 3, where the range of core-test results is significantly greater than the range in average results due to differing states of stress.

The San Diego Test Road was a controlled experiment, and the subgrade was designed and constructed to be a constant in the experiment. The wide variations that have, in fact, existed must cast doubt on the meaning of the relative performance observations and records. Only through an extensive analysis of the performance, properly weighted against the subgrade stiffness and its variation, can any meaningful conclusions relative to type of base be drawn.

Table 4. Estimated stiffness function of granular base.

Type of Base	Section	Assigned Subgrade M_R (MPa)	k_1[a]	k_1 (field)/k_1 (laboratory)
Class 2 aggregate	1	88.3	22 000	11.7
	10	115.1	7 600	4.0
	11	117.9	11 100	5.9
	14	126.9	7 000	3.7
	24	156.5	10 700	5.7
Class 3 aggregate	8	108.9	15 400	7.3
	18	138.6	7 200	3.4
	26	162.7	18 200	8.7
Avg				6.3

Note: 1 MPa = 145 lbf/in^2.

[a]Value of k_1 in the expression $M_R = k_1\theta^{0.5}$ that gives measured surface deflections equal to calculated surface deflections.

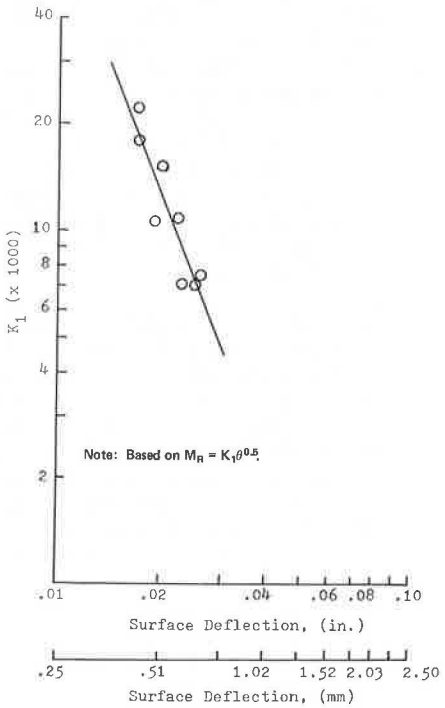

Figure 6. Variation of computed granular-base M_R with deflections.

ESTIMATED MODULUS OF GRANULAR BASE SECTIONS

The results of the derivation of subgrade modulus values from deflections indicate that granular base material exhibits a stronger response in the field than is indicated by laboratory testing. The initial modulus values of the subgrade derived from deflections averaged 136 MPa (20 100 lbf/in^2) for treated base sections and 346 MPa (50 900 lbf/in^2) for granular base sections. The function $M_R = 4000\,\theta^{0.5}$ was used in the analysis for all granular materials.

To ascertain the modulus of the granular base sections that was being exhibited in the field, new values of subgrade M_R were assigned to eight of them. The object of the analysis was to determine the value of k_1 in the expression $M_R = k_1\theta^{0.5}$ such that the computed deflections were equal to the measured deflections. By using the NLAYER program and a trial-and-error procedure, the analysis was conducted for the initial deflection-measurement period.

The computed values of k_1 are given in Table 4. Analysis of these values indicates no evident dependence on the type of base, thickness, or location in the test road. The derived values were, however, related to the surface deflections, as shown by Figure 6 and Equation 3.

$$\log k_1 = -2.4529 \log \Delta + 7.2931 \quad (r = 0.91) \qquad (3)$$

This figure, which indicates decreasing k_1 with increasing deflection, suggests that the modulus function of the base cannot be taken as a unique value, but varies with the pavement section. Each of the derived values exceeds the laboratory values by a substantial factor. The average of the derived values of k_1 for the eight sections analyzed was 12 400. This compares with the 1880 determined in the laboratory for class 2 material and

the 4000 used in the previous derivation of subgrade modulus values. As shown in Table 4, the ratio of k_1 for field to laboratory conditions ranged from 3 to 12, with an average near 6.

The high computed k_1-values help to explain why the computed subgrade modulus values in granular base sections are considerably higher than those in the treated base sections. The use of a higher k_1-value in the previous derivations would have reduced the magnitude of the subgrade modulus to values consistent with those derived for the other test sections.

It has not been the intent of this study to ascertain the reasons for the seemingly high values of k_1. Laboratory M_R tests approximate as closely as possible the loading conditions that are believed to exist in the field. These results are important, however, in that they suggest that the field behavior of granular base pavements is more complex than previously believed and that multilayer elastic analysis underpredicts the in-situ state of stress. This is an area that needs further research. The implications of the high response of granular bases is extremely important in the use of rational design procedures based on limiting values of tensile and compressive strains.

CONCLUSIONS

The following conclusions are presented.

1. The M_R of a cohesive subgrade soil is dependent on the physical soil state. Multiple regression models using moisture content and degree of saturation were developed to predict the modulus for both laboratory compacted and undisturbed field samples. A comparison of the two regression models indicates that the ratio of laboratory M_R to field M_R is generally equal to unity for high degrees of saturation ($S > 90$ percent) for the range of moisture contents obtained.
2. For lower degrees of saturation ($S < 80$ to 85 percent), the laboratory-compacted samples may have higher values of M_R than do undisturbed field samples having identical physical soil states. Although more research is needed, it is believed that variations in the clay structure, produced by differing methods of compaction, may cause the variations in the measured modulus.
3. The best estimate of the mean initial subgrade modulus for the entire test road is about 138 000 to 172 500 kPa (20 000 to 25 000 lbf/in^2).
4. For test sections made of asphalt-treated base materials, the mean deflection-derived subgrade modulus of 138 000 kPa (20 000 lbf/in^2) agreed well with the mean value of modulus predicted from the regression models developed from direct laboratory testing of field samples.
5. In general, the deflection-derived values of the initial subgrade modulus for both emulsion and cutback-treated base sections averaged about 69 000 kPa (10 000 lbf/in^2) lower than those derived for asphalt-concrete and asphalt-cement-treated base sections. This indicates that, for bases having temperature and stress dependency and state-of-curing effects on the modulus, the treated bases may have been exhibiting a lower response than that determined from laboratory modulus evaluation.
6. Resilient-modulus testing of undisturbed cores taken 7 years after the test road was opened to traffic showed that the CV of the modulus between test sections was 97 percent.
7. The CV of the modulus within test sections averaged 17 percent initially, but increased with time. The average CV over the project life (approximately 7 years), as determined from surface deflections, was 38 percent. This value is in excellent agreement with the CV of 40 percent determined from laboratory testing of undisturbed cores.
8. Variations of the subgrade modulus due to the physical state of the soil are of much greater significance in analyzing pavement performance than is the range in modulus values due to differing stress states normally imposed in the laboratory.
9. In the derivation of the subgrade modulus from deflection measurements, for the granular-base test sections, the comparison between the derived moduli and those determined from direct laboratory testing on field cores was very poor. For these types of bases, the stress-dependent function for modulus of the base, determined from laboratory tests, tended to underpredict the in-situ response of the granular material. When the apparent in-situ granular moduli were recomputed from the initial surface deflections, an adjusted value of k_1 ($M_R = k_1\theta^{0.5}$) ranged from 7000 to 22 000 with a mean of 12 400. In general, the ratio of the k_1-term derived from the field to that found in the laboratory ranged from about 3 to 12 with an average near 6.

ACKNOWLEDGMENTS

We wish to acknowledge the financial and technical support of the Asphalt Institute, which made this research possible. Particular gratitude is expressed to James Shook and Bernard Kallas of the institute staff.

REFERENCES

1. J. C. Riley and J. F. Shook. San Diego County Experimental Base Project: Design and Construction. Asphalt Institute, College Park, Md., Res. Rept. 67-4 (RR 67-4), June 1967.
2. R. I. Kingham. Full-Scale Experimental Base Construction in San Diego County. ASCE, Preprint of paper presented at Meeting on Transportation Engineering, San Diego, Calif., Feb. 1968.
3. R. G. Hicks and F. N. Finn. Prediction of Pavement Performance From Calculated Stresses and Strains at the San Diego Test Road. Proc., AAPT, Vol. 43, 1974, pp. 1-40.
4. J. F. Shook and J. R. Lambrechts. Performance of Full-Depth Asphalt Bases on San Diego County Experimental Base Project. TRB, Transportation Research Record 521, 1974, pp. 47-59.
5. H. B. Seed, C. K. Chan, and C. E. Lee. Resilience Characteristics of Subgrade Soils and Their Relation to Fatigue Failures in Asphalt Pavements. Proc., 1st International Conference on the Structural Design of Asphalt Pavements, Univ. of Michigan, Aug. 1962, pp. 611-636.
6. M. P. Jones. Analysis of the Subgrade Modulus and Pavement Fatigue on the San Diego Test Road. Univ. of Maryland, College Park, MS thesis, 1975.
7. B. F. Kallas and J. H. Shook. San Diego County Experimental Base Project. Asphalt Institute, College Park, Md., Res. Rept. 77-1, Nov. 1977.
8. J. Michelow. Analysis of Stresses and Displacements in an N-Layered Elastic System Under a Load Uniformly Distributed on a Circular Area. California Research Corp., Richmond, Sept. 1963.

Publication of this paper sponsored by Committee on Strength and Deformation Characteristics of Pavement Sections.

Fatigue Behavior of Cement-Treated Materials

L. Raad,* Department of Civil Engineering, University of Illinois at Urbana-Champaign
C. L. Monismith and J. K. Mitchell, Department of Civil Engineering and Institute of Transportation Studies, University of California, Berkeley

Fatigue-failure criteria based on the Griffith failure theory have been developed to describe the behavior of cement-treated pavement materials subjected to repeated multiaxial stress applications. These criteria are represented by two relationships, one for curing periods of 4 weeks and the other for curing periods of 10 weeks, that show the variation of the maximum stress level as a function of the number of stress applications required to cause failure. The stress level is defined in terms of the applied principal stresses and the initial tensile strength. For a given set of applied stress pulses, there will be a maximum value of stress level. Fatigue failure occurs when the tensile strength decreases from its initial value to the maximum value of the stress level. The number of stress applications to cause failure can thus be expressed as a function of the stress factor and the tensile strength. This relationship is independent of the duration and frequency of the applied stress pulses. The proposed criteria agree well with fatigue data from a number of investigations, which indicates their general validity.

In recent years, there have been a number of laboratory studies to determine the fatigue response of cement-stabilized materials. The data developed from these studies have been used to establish design criteria for improved use of cement-treated materials in pavement structures for both highway and airfield pavements. Table 1 summarizes the criteria developed from a number of investigations using repeated-load tests on (a) simply supported beams in flexure [e.g., Pretorius (1), Otté (2), Irwin (3), Scott (4), and Mitchell and Shen (18)], (b) beams resting on an elastic foundation [e.g., Larsen and others (5)], and (c) specimens in direct uniaxial tension or compression [e.g., Bofinger (6)].

These criteria, however, have the following limitations:

1. They have been developed by using the results of simple flexure and direct tension tests in which the critical state of stress at the point at which cracking initiates is either uniaxial or biaxial rather than triaxial as is an actual pavement structure, and therefore a different layer thickness might be selected by using a maximum strain criterion than by using a maximum stress criterion (7);
2. The effects of variations in the frequency, shape, and duration of the stress or strain pulse have not been considered;
3. The additional repetitions required to propagate a crack through the cement-stabilized base after it initiates (8) have not been accounted for in a number of these criteria; and
4. The fatigue behavior of cement-treated materials subjected to compound loading has not been investigated, although the linear summation of cycle ratios has been proposed as a reasonable hypothesis for cumulative damage.

In this paper, the Griffith failure theory (9) is used to develop an analytical model of the fatigue behavior of cement-treated materials subjected to triaxial stress pulses. The results of laboratory tests (8) are used to define fatigue criteria suggested by this analytical model.

Predictions using these criteria are compared with published fatigue data. Verification of these criteria is important because the model from which the criteria were developed can be used to establish an analytical approach for the design of cement-stabilized layers in pavement sections that accounts for both crack initiation and propagation in the layers.

FATIGUE-FAILURE CRITERIA

Failure Under Static Loading

Griffith (9) derived a criterion for failure under a two-dimensional state of stress by assuming that fracture is caused by stress concentrations at the tips of minute Griffith cracks or starter flaws that are presumed to occur in the material and that it is initiated when the maximum stress near the tip of the most favorably oriented crack reaches a value characteristic of the material. The Griffith criterion for failure can be written as

$$(\sigma_1 - \sigma_3)^2/(\sigma_1 + \sigma_3) = 8T_0 = \sigma_c \qquad (\sigma_1 + 3\sigma_3 \geq 0) \tag{1}$$

and

$$\sigma_3 = -T_0 = -\sigma_c/8 \qquad (\sigma_1 + 3\sigma_3 \leq 0) \tag{2}$$

where

σ_1 = major principal stress,
σ_3 = minor principal stress,
T_0 = tensile strength, and
σ_c = unconfined compressive strength.

(Compressive stresses are positive; tensile stresses are negative.) The relationships given in Equations 1 and 2 were derived by assuming that the starter flaws in the material remained open under the action of the applied stresses, σ_1 and σ_3.

The strength of cement-treated materials has been studied under triaxial loading conditions (i.e., with σ_2 equal to σ_3) by, e.g., Pretorius (1), Nash and others (10), and Abboud (11), and under biaxial loading conditions (σ_2 equal to 0) by Bresler and Pister (12). Figure 1 presents a plot of this data in normalized form (i.e., σ_1/σ_c versus σ_3/σ_c, where σ_c = unconfined compressive strength). [The data reported by Bresler and Pister (12) are for a concrete material that can be considered similar to soil-cement; they have been included because they are the only known data available in this range of loading conditions.] The information shown in Figure 1 indicates that the Griffith criterion is applicable for values of $\sigma_3/\sigma_c < 0.10$, but that for $\sigma_3/\sigma_c > 0.10$, a modified criterion developed by McLintock and Walsh (15) that assumes that the starter flaws in the material are closed could be used in the form of $\sigma_1 = 5\sigma_3 + \sigma_c$.

As will be seen, the Griffith crack approach appears applicable to the description of cement-treated soils under the various combinations of σ_1 and σ_3 that are likely to be encountered in a treated layer. It also offers the advantage of requiring knowledge of only the unconfined compressive strength for its application.

Table 1. Design criteria for soil-cement bases using present analytical approaches.

Material	Dynamic Test	Suggested Criteria: Parameter	Number of Repetitions: N	10⁶	Unlimited	Reference
Soil-cement Silty clay	Direct tension	Maximum tensile stress	—	—	18 lbf/in²[a]	Bofinger (6)
Soil-cement Eliot sand mixture Vicksburg silty clay	Flexural beam	Maximum flexural stress or strain level[b]	—	—	0.50	Mitchell and Shen (18)
Soil-cement Granular soil A-1, A-2-4, A-2-5, A-3 Fine-grained soil A-2-6, A-2-7, A-4, A-5	Flexural beam on elastic foundation	Radius of curvature (R)	R[c]	—	—	Larsen, Nussbaum, and Colley (5)
Cement-treated	Flexural beam	Maximum flexural-strain level[b]	—	0.33	0.25	Otté (2)
Soil-cement A-1-b, A-2-4, A-3, A-4	Flexural beam	Maximum flexural-stress level[b]	S[d]	0.67	—	Scott (4)
Cement-treated Gravelly sand Vicksburg lean clay	Flexural beam	Energy density (lb in/ft³)[a,e]	—	0.0018 (gravelly sand) 0.0030 (lean clay)	—	Irwin (3)
Cement-stabilized	Flexural beam	Maximum flexural strain (ϵ_t in/in × 10⁻⁶)[a]	N[f]	50 in/in × 10⁻⁶	—	Mitchell and others (7)

[a] These criteria were designed for U.S. customary units only; therefore SI units are not given.
[b] Ratio of applied stress or strain to value at failure in static testing.
[c] $R = R_c N^a h^{1/4}/(2.1h - 1)$ where R = radius of curvature under a given wheel load (in), h = thickness of base (in), N = number of repetitions, a = 0.025 for granular soil or 0.05 for fine-grained soil, and R_c = critical radius of curvature for a base of thickness h.
[d] S = 94.4 - 4.71 log N.
[e] Energy density for a linear elastic material under a given state of triaxial stresses is given by $U_d = (1/2E)(\sigma_1^2 + \sigma_2^2) + \sigma_3^2 - (\mu/E)(\sigma_1\sigma_2 + \sigma_2\sigma_3 + \sigma_1\sigma_3)$, where σ_1, σ_2, and σ_3 are the principal stresses; μ = Poisson's ratio; and E = modulus of elasticity.
[f] $N = 142^{20.3/\epsilon}$.

Figure 1. Failure envelope for cement-treated soils.

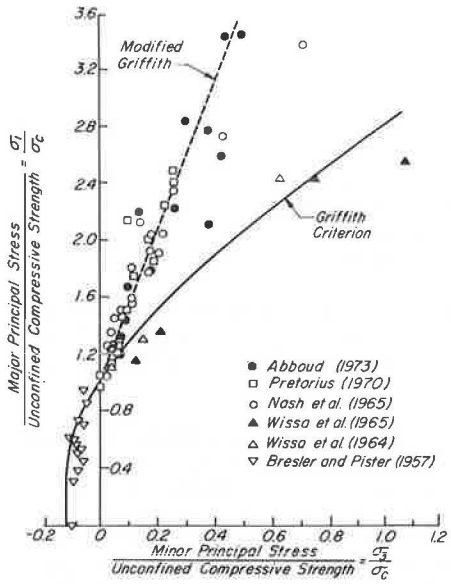

Analytical Fatigue Model

Confining pressures (σ_3) in cement-treated bases are generally small because such base materials support traffic loads in flexure, and the overburden pressure is low. Thus, Griffith's failure theory rather than the modified Griffith theory is applicable [i.e., $\sigma_3/\sigma_1 \leq 1/13$ (8)].

At any point in the base, the stress state generated by a moving wheel load can be represented by the principal stresses (σ_1, σ_2, and σ_3). Because these stresses are repeatedly applied under the action of traffic loads, the strength of the cement-treated material will decrease until failure occurs. It may be hypothesized that the decrease in strength is caused by a reduction in bond strength between the soil, aggregate, and cement.

Mathematically, this strength reduction can be described as follows. Let F be a stress factor defined as

$$F = (\sigma_1 - \sigma_3)^2/8(\sigma_1 + \sigma_3) \quad (\sigma_1 + 3\sigma_3 \geq 0)$$
$$F = -\sigma_3 \quad (\sigma_1 + 3\sigma_3 \leq 0) \qquad (3)$$

Failure will take place when the tensile strength of the material decreases from an initial value (T_i) to a value (T') equal to the maximum value of the stress factor (F_{max}), which is defined by the σ_1 and σ_3 pulses as shown in Figure 2.

The decrease in tensile strength for a clayey, gravel soil-cement is a function of F_{max} and is independent of the frequency, shape, and duration of the applied principal-stress pulses. The variation of tensile strength with the number of repetitions of stress applications for a given F_{max} is shown schematically in Figure 3.

The strength decrease illustrated in Figure 3 can be defined in terms of a rate (a) given by

$$a = (\log T_i - \log T')/(\log N_f - \log 1)$$
$$= (\log T_i - \log F_{max})/\log N_f$$
$$= \log [1/(F_{max}/T_i)]/\log N_f \qquad (4)$$

where N_f = number of repetitions to failure.

The parameter a can be determined by measuring the slope of the function that represents the decrease in tensile strength with number of stress repetitions. For a given F_{max}, there corresponds a given value of a. The variation of a as a function of the maximum stress level (i.e., F_{max}/T_i) for a clayey, gravel soil-cement is shown in Figure 4.

These relationships were determined from repeated-load triaxial tests on a soil-cement consisting of a well graded gravel [19-mm (¾-in) maximum particle size] combined in a 5 to 1 ratio with silty clay (1, 8). A water content of 7.5 percent and 5.5 percent cement were used to prepare samples that were then cured in a humid room for varying periods of time. The magnitude, frequency,

and duration of the applied σ_1 and σ_3-stress pulses were varied, and the decrease of tensile strength was found to depend only on F_{max}/T_i.

From the definition of a, the number of stress repetitions to failure (N_f) can be written as

$$\log N_f = \log [1/(F_{max}/T_i)]/a \quad (5)$$

and therefore, the number of stress repetitions to failure can be determined for a given a and F_{max}/T_i. The relation that describes the variation of F_{max}/T_i with N_f defines the fatigue-failure criterion for a cement-treated material. The values for a and F_{max}/T_i are obtained from Figure 4 and used in Equation 5 to establish a relationship between F_{max}/T_i and N_f as shown in the following table and in Figure 5. The relationships shown in Figure 5 were also examined relative to their applicability to various other cement-treated soils.

Figure 2. Variation of F for given σ_1 and σ_3 pulses.

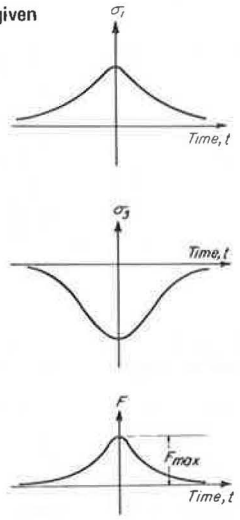

Figure 3. Variation of tensile strength with number of stress applications for a given F_{max}.

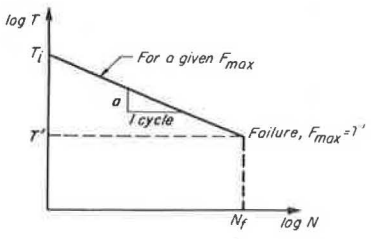

N_f	F_{max}/T_i Samples Cured 4 Weeks	Samples Cured 10 Weeks
10^{35}	0.20	0.47
10^7	0.55	0.71
10^6	0.58	0.73
10^5	0.62	0.75
10^4	0.67	0.78
10^2	0.78	0.84
1	1.00	1.00

COMPARISON OF EXPERIMENTAL FATIGUE DATA AND THE FATIGUE-FAILURE CRITERIA

The fatigue data used to evaluate the criteria are given in Table 2 and include the following variables: (a) type of stabilized material, (b) cement content, (c) frequency of applied stress pulses, and (d) curing age.

Comparisons of the experimental and analytical results are shown in Figures 6 to 10. The ratio of the applied stress to the initial strength (i.e., the maximum stress level) is plotted versus the number of repetitions to failure. As noted in Table 2, different tests were used to obtain the fatigue data, including (a) rotating cantilever beam (13), (b) simply supported beam (1, 3, 4, 6), and (c) repeated compression (14). To use Symons' data, which is presented as applied stress expressed as a percentage of static strength versus number of repetitions to failure, F_{max} was taken equal to the applied tensile stress, and T_i was assumed to be the applied stress at N_f equal to one repetition. Analysis of the data shown in Figures 6 to 10 leads to the following conclusions.

1. The fatigue data obtained by testing at different frequencies (200 to 500 and 2800 revolutions/min) of applied stress pulses agree reasonably well with the fatigue-failure criteria in materials ranging from well graded sand to silty clay (Figures 6 to 8). Thus, the fatigue-failure criteria are appropriate for the prediction of the fatigue failure of cement-treated soils independent of the loading frequency.
2. The fatigue criteria for a curing age of 4 weeks agree well with the fatigue data for cement-treated materials that have a curing age of up to 4 weeks (Figures 6 to 9), and the criteria corresponding to a curing age of 10 weeks agree with the data for a curing age of 10 or more weeks (Figure 10).
3. There is reasonable agreement between the experimental values and those that correspond to the suggested analytical criteria, independent of the type of stabilized soil and the cement content (Figures 6 to 10).

Figure 4. Variation of a with $(F_{max})/T_i$.

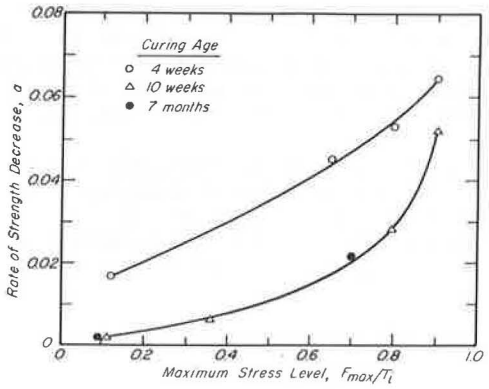

Figure 5. Suggested fatigue-failure criteria for cement-treated soils.

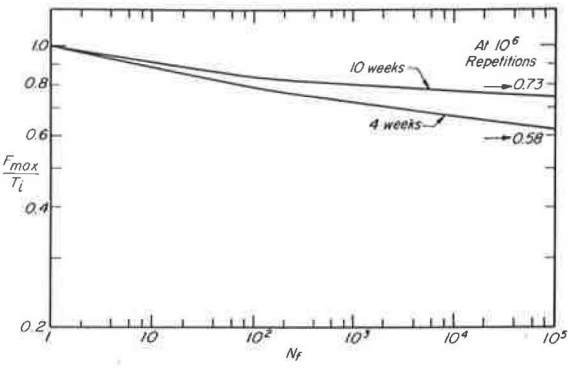

Table 2. Fatigue data for cement-treated soils.

Material	Cement Content (%)	Water Content[a] (%)	Curing Age (d)	Dry Density (Mg/m^3)	Repeated Load Test	Reference
Well graded sand	6 to 14	9 to 11	7 to 28	1.99	Rotating cantilever	Symons
Uniformly graded sand	12 to 16	13	7	1.65	Rotating cantilever	Symons
Silty clay	6 to 14	19	7	1.68	Rotating cantilever	Symons
Crushed rock	4 to 8	8	7	2.03	Rotating cantilever	Symons
A-2-4, A-4, A-3, A-1-6	6.5 to 8.5	7 to 11	365	1.78 to 2.18	Flexural beam	Scott
A-2-4, A-4	6.7 to 8.4	10.7 to 12.4	28	1.78 to 1.89	Flexural beam	Scott
Lean clay	10	15.7	14 to 28	1.73	Flexural beam	Irwin
Gravelly sand	6	6.2	21	2.15	Flexural beam	Irwin
Clayey gravel	5.5	7.5	90	2.19	Flexural beam	Pretorius
Silty clay	8 to 16	38	14	1.39	Flexural beam	Bofinger
Uniform sand	6	9	2 to 14	1.84	Direct compression	Gregg

Note: 1 Mg/m^3 = 62.4 lb/ft^3.
[a]Mixing content.

Figure 6. Comparison of fatigue data for cement-treated (6 to 14 percent cement) well graded sand (7 and 28 d curing) at different loading frequencies with suggested fatigue-failure criterion.

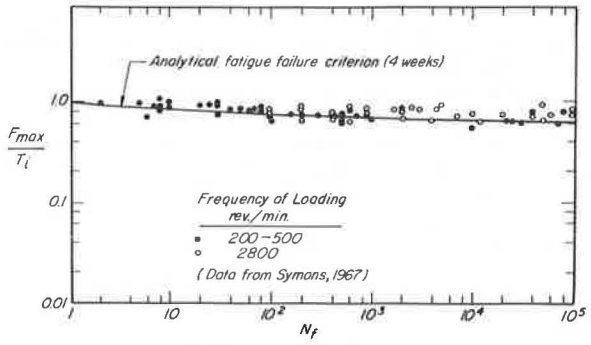

Figure 7. Comparison of fatigue data for cement-treated (12 to 16 percent cement) uniformly graded sand (7 d curing) at different loading frequencies with suggested fatigue-failure criterion.

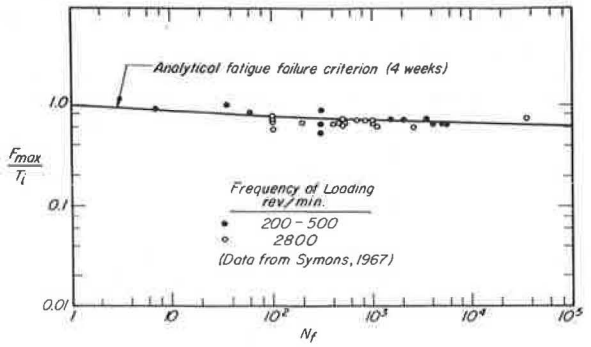

Figure 8. Comparison of fatigue data for cement-treated (6 to 14 percent cement) silty clay (7 d curing) at different loading frequencies with suggested fatigue-failure criterion.

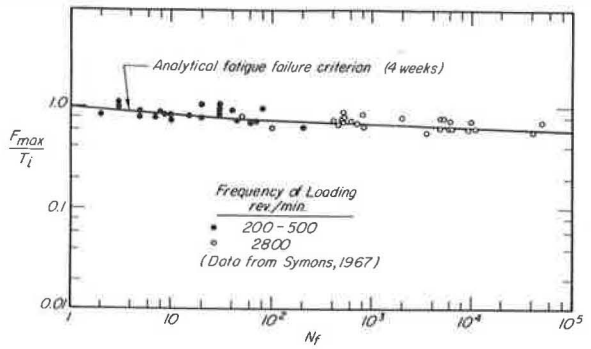

Figure 9. Comparison of fatigue data for cement-treated soils (<4 weeks curing) with suggested fatigue-failure criterion.

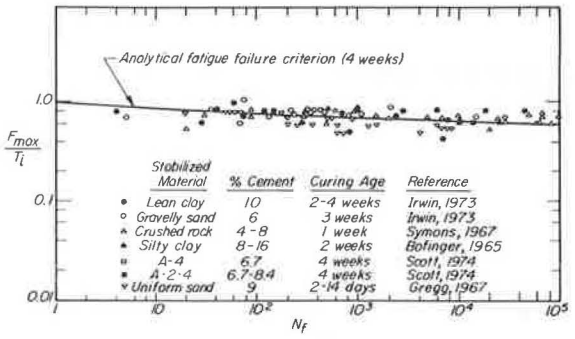

Figure 10. Comparison of fatigue data for cement-treated soils (>10 weeks curing) with suggested fatigue-failure criterion.

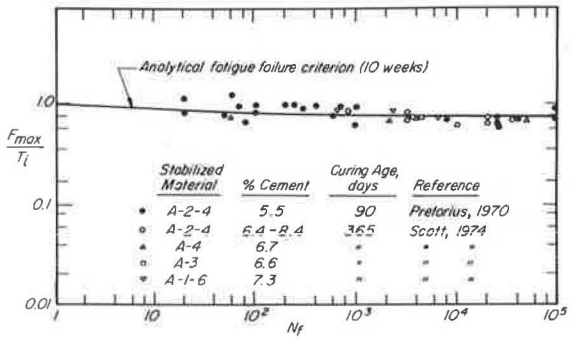

SUMMARY

Fatigue-failure criteria corresponding to curing ages of 4 and 10 weeks have been developed for a clayey, gravel soil-cement by using an analytical fatigue model based on the Griffith failure theory. In these criteria, the number of repetitions to failure is expressed in terms of the maximum stress level applied, and the resulting relationship is independent of pulse duration, frequency, and shape.

The suggested criteria fit the available fatigue data for cement-treated soils, for different curing ages, independent of type of material, cement content, and frequency of applied loads, which indicates the possible applicability of these criteria for cement-treated soils in general.

REFERENCES

1. P. C. Pretorius. Design Considerations for Pavements Containing Soil-Cement Bases. Univ. of California, Berkeley, PhD dissertation, April 1970.
2. E. Otté. A Tentative Approach to the Design of Pavements Using Cement-Treated Layers. Paper presented at the Symposium on Cement-Treated Crusher-Run Bases, National Institute for Road Research, Johannesburg, Sough Africa, Feb. 1973.
3. L. H. Irwin. Evaluation of Stabilized Soils in Flexural Fatigue for Rational Pavement Design. Texas A&M Univ., College Station, PhD dissertation, May 1973.
4. J. L. M. Scott. Flexural Stress-Strain Characteristics of Saskatchewan Soil-Cements. Saskatchewan Department of Highways and Transportation, Regina, Technical Rept. 23, Dec. 1974.
5. T. J. Larsen, P. J. Nussbaum, and B. E. Colley. Research on Thickness Design for Soil-Cement Pavements. Research and Development Laboratories, Portland Cement Association, Bulletin D142, Jan. 1969.
6. H. E. Bofinger. The Fatigue Behavior of Soil-Cement. Australian Road Research, Vol. 2, No. 4, June 1965.
7. J. K. Mitchell, P. Dzwilewski, and C. L. Monismith. Behavior of Stabilized Soils Under Repeated Loading: A Summary Report With a Suggested Structural Design Procedure. U.S. Army Engineer Waterways Experiment Station, Vicksburg, Miss., Rept. No. 6, June 1974.
8. L. Raad. Design Criteria for Soil-Cement Bases. Univ. of California, Berkeley, PhD dissertation, 1976.
9. A. A. Griffith. Theory of Rupture. Proc., 1st International Congress for Applied Mechanics, Delft, Netherlands, 1924.
10. J. K. T. L. Nash, F. M. Jardin, and J. D. Humphrey. The Economic and Physical Feasibility of Soil-Cement Dams. Proc., 6th International Conference on Soil Mechanics and Foundation Engineering, Montreal, 1965.
11. M. M. Abboud. Mechanical Properties of Cement-Treated Soils in Relation to Their Use in Embankment Construction. Univ. of California, Berkeley, PhD dissertation, 1973.
12. B. Bresler and K. S. Pister. Failure of Plane Concrete Under Combined Stresses. Trans., ASCE, Vol. 122, 1957, pp. 1049-1059.
13. I. F. Symons. A Preliminary Investigation to Determine the Resistance of Cement-Stabilized Materials to Repeated Loading. U.K. Transport and Road Research Laboratory, Crowthorne, England, RRL Rept. LR 61, 1967.
14. J. S. Gregg. The Significance of Compressive, Tensile, and Flexural Strength Tests in the Design of Cement-Stabilized Pavement Foundations. Paper presented at the 4th Regional Conference on Soil Mechanics and Foundation Engineering, Cape Town, South Africa, Dec. 1967.
15. F. A. McClintock and J. B. Walsh. Friction on Griffith Cracks Under Pressure. Proc., 4th U.S. National Congress of Applied Mechanics, 1962.
16. A. E. Z. Wissa and C. C. Ladd. Effective Stress-Strength Behavior of Compacted Stabilized Soils. Department of Civil Engineering, MIT, Res. Rept. No. 64-32, Soils Publ. No. 164, July 1964.
17. A. E. Z. Wissa, C. C. Ladd, and T. W. Lambe. Effective Stress-Strength Parameters of Stabilized Soils. Proc., 6th International Conference on Soil Mechanics and Foundation Engineering, Montreal, 1965.
18. J. K. Mitchell and C. K. Shen. Soil-Cement Properties Determined by Repeated Loading in Relation to Bases for Flexible Pavements. Proc., 2nd International Conference on the Structure and Design of Asphalt Pavements, Univ. of Michigan, 1967, pp. 348-373.

Publication of this paper sponsored by Committee on Strength and Deformation Characteristics of Pavement Sections.

**Mr. Raad was at the Department of Civil Engineering, University of California, Berkeley, when this research was performed.*

Stabilization of Expansive Shale Clay by Moisture-Density Control

E. B. McDonald, South Dakota Department of Transportation

Stabilization of expansive Pierre shale has been a continuing problem in South Dakota for many years. A procedure has been developed to produce a roadbed with very few differentials that uses special undercutting to a depth of 1.83 m (6 ft), replacement of subgrade by selected materials, rigid control of moisture to achieve low density at a high moisture content, and lime treatment in the upper 15.2 cm (6 in) of subgrade. A density of 92 percent of the maximum American Association of State Highway and Transportation Officials T 99 test value and a moisture content of 3 percent above the optimum were set as targets. The high degree of stability of roads constructed by this procedure is shown by the very good roughness-index ratings. The average roughness index, based on a 0 to 5 rating system, is 4.34 for the full length of 209.2 km (130 miles) of surfacing. The projects observed and tested for this study have been in service from 5 to 8 years.

A good road is one that is stable from the subgrade depth to the top of the surfacing. To achieve this type of stability, it is necessary to design each component so as to use the best materials and techniques available. Stability, especially in the subgrade, is dependent on the environment in which the material is located. All of the components of the road structure must be able to resist the deteriorating effects of climatic cycles and traffic loads. A road structure is usually divided into four component parts—subgrade, subbase, base, and bituminous mat or wearing course. In a rigid design, it is composed of a concrete surfacing and a base. The subgrade is the native material below the imported materials.

Subgrade stabilization is usually carried out by the incorporation of some type of stabilizing agent into the soil. However, there are other things that can be done to improve the natural stability of fills and the upper portions of cut sections before incorporating stabilizing additives into the subgrade.

Subgrade soil is by nature differentiated, especially in the upper A horizon. It is highly responsive to moisture and thermal changes. The B horizon is more pervious to water, which moves within this zone in channels of least resistance or in a differential manner, resulting in variable support values. The C horizon is even less permeable than the B horizon and reacts differently than do the two upper horizons. Obviously, for the road surfacing to remain stable, differentials in the subgrade support must be minimized as much as possible. This stabilization can be accomplished by blending and mixing the various soil horizons into a more uniform mass.

This report deals primarily with experience in South Dakota in the design and construction of 209 km (130 miles) of I-90 on highly expansive Pierre shale. However, although these methods of stabilization and construction procedures were applied to the problems of Pierre shale, they could also be applied successfully to other types of expansive soils in other parts of the country. The paper also presents the results of postconstruction testing and the ridability of the surfacing, as of June 1975.

HISTORICAL BACKGROUND

The Materials and Soils Program of the South Dakota Division of Highways has long recognized the problems connected with the design of road surfaces on the highly expansive Pierre shale. Over many years, changes have been made in the methods of design and the construction procedures in an attempt to reduce the expansion of the soils and its resultant effects.

The Missouri River divides South Dakota almost equally into two distinct land forms. The soils of each half have quite different physical characteristics, such as liquid limits, plasticity indexes, volume changes, and bearing values. The upper mantle of soil in the eastern half of the state is composed chiefly of glacial till, silt clays, clay silts, and sand silts. The western half of the state, except in the Black Hills area, is composed of Pierre shale and weathered Pierre shale clay, commonly referred to as gumbo. A small area near the south-central Nebraska border is predominantly sand, and some small areas on the northwest corner have thin sandstone overlays. The mineral composition of the bentonitic shale is largely montmorillonite. The physiographic features associated with this geology are shown in Figure 1.

Pierre shale was laid down west of the Missouri River in South Dakota in the Mesozoic Era (1). The shale structures are the result of several sea intrusions over a period of millions of years and are composed of layers of interbedded, highly plastic, colloidal clays and silts, with some areas containing layers of nearly pure bentonite. This deposition varies in thickness from a meter or two to a hundred or more. The layers are differentiated with respect to degree of weathering, volume changes, and water susceptibility. The upper portion of the deposition is weathered to a fine, homogeneous till-like clay from 0.305 to 4.6 m (1 to 15 ft) in thickness. The next portion is weathered to an open-jointed condition that readily admits surface water when the upper soil and clay till are removed. The inorganic colloidal clays and the bentonite are susceptible to large volume changes when they are subjected to prolonged alternate dry and wet cycles, such as are prevalent in western South Dakota. The expansive pressure of the clay derived from Pierre shale in some areas is nearly 689 kPa (100 lbf/in^2) (Figures 2 and 3).

A short history of the design and performance of highways built in these expansive soils before the use of deep undercutting and moisture and compaction control is given to enable the reader to better understand the reasons for using drastic undercutting methods. Before 1952, asphaltic mats, 3.8 to 5.1 cm (1.5 to 2 in) thick, and base gravel, 0.10 to 0.15 m (4 to 6 in) thick, were used as a surfacing over the Pierre shale. Several short sections of plain 0.15 and 0.20-m (6 and 8-in) thick portland-cement-concrete pavements were placed on the shale near Pierre, Winner, and Chamberlain. Both of these types of surfacing distorted badly in 3 to 5 years. This distortion was not due to the traffic, but to the expansive soil that warped the surfaces to such a degree that traffic soon finished the breakup.

After observing the poor results of these thinner designs, thicker pavement surfaces were constructed by using 7.6 to 10.2-cm (3 to 4-in) mats over 0.13 to 0.20 m (5 to 8 in) of base course and 0.15 to 0.38 m (6 to 15 in) of subbase. At the same time, procedures were implemented to control the subgrade moisture, undergrade cut sections up to 0.30 m (12 in), scarify an additional 0.15 m (6 in) of soil, and recompact the scarified and undercut soil. The undercut soil was replaced with selected soil where possible. In more recent years, cut sections have been undercut to the toe of the in-slopes. The undercut soil is either returned to the cut and recompacted or replaced with selected soil.

Observations of the roads built by using these methods indicated a certain degree of success in reducing the severity of warping in areas containing highly expansive soil. The majority of these roads have an adequate riding surface, although there is still a certain amount of undesirable roughness. This roughness is found in areas where there is as much as 0.76 m (30 in) of subbase material under the base and mat. The same conditions have also developed where extremely thick bases were used under concrete.

PRELIMINARY FIELD STUDIES AND LABORATORY TESTS

The preliminary soil investigations by the highway division consisted of the development of a continuous soil profile from field measurements of the types of soil along each project. Tests were made on samples of the various soils encountered, and a careful performance study was made of an existing highway, US-16, that parallels the entire length of I-90 (Figure 1). Areas requiring considerable maintenance because of differential swell, usually in cut sections, were investigated by digging a series of closely spaced holes and determining the position and extent of the in-place soil types and the nature of each layer. In-place moisture and density tests of the upper portion of the subgrade soil, which was covered by asphalt concrete and the soil-aggregate base course, were also taken from the existing road. Large differentials in liquid limits and volume changes over very short distances were found not only in a longitudinal direction for 1.5 to 4.6 m (5 to 15 ft), but also in very thin vertical layers of 0.15 to 0.46 m (6 to 18 in). The quantity of available topsoil [usually the top 0.15 m (6 in) of sodded areas] and the availability of weathered soil suitable for topping the upper 0.91 m (3 ft) of the entire subgrade were estimated. This material is usually found in the upper 0.31 to 1.5 m (1 to 5 ft) of the natural terrain.

The degree of variations and the high incidence of change in the physical properties of the interbedded soils required a method by which soils from one zone could be

Figure 1. Physiographic divisions of South Dakota.

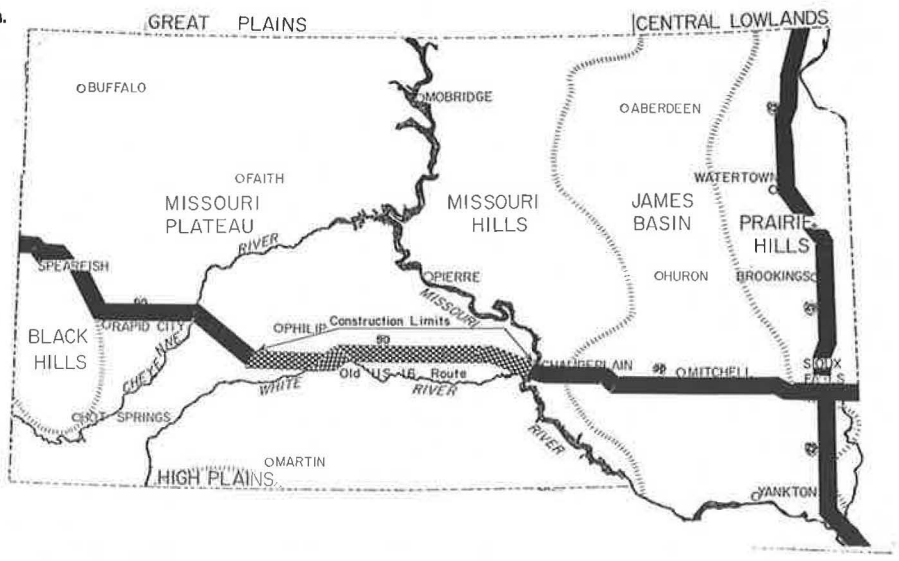

Figure 2. Expansion pressures of South Dakota soil (standard AASHTO compaction T-99).

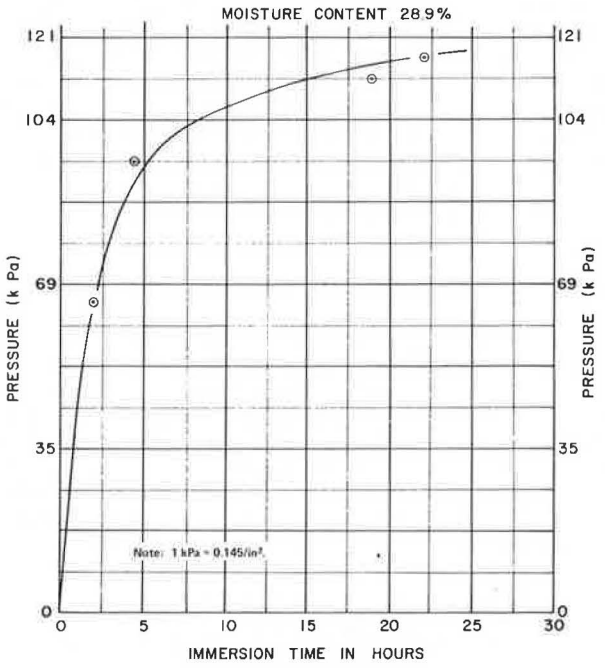

Figure 3. Expansion pressures of South Dakota soil (modified AASHTO compaction T-180).

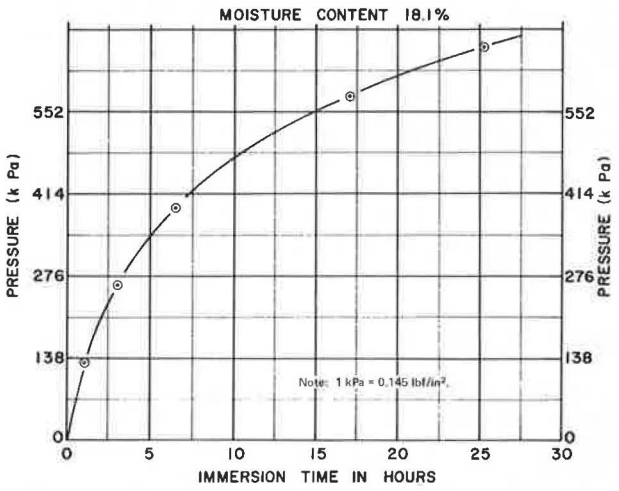

salvaged or stockpiled for use in the upper portion of the roadbed. In certain areas, the soils in the upper 1.2 or 1.5 m (4 or 5 ft), exclusive of sod, were naturally fairly well blended. A series of moisture, density, and swell tests were run to determine the moisture and density combination that would produce the least amount of swell and still allow construction traffic. The weathered shale in the upper layer of soil had a lower swell potential than did the lower layer of jointed shale. The least amount of swell occurs when the weathered soil is compacted at approximately 3 percent above optimum, at 92 percent of the AASHTO T 99 test. The test data for the two samples described below and given in Figures 4 and 5 show that the swell potential of the weathered shale is less than half that of the jointed shale (1 kg/m^3 = 0.062 lb/ft^3). These tests were one of the important factors in the decision to construct rigid as well as flexible pavements on the Pierre shale.

Property	Weathered	Jointed
Location	Fort Pierre area	Fort Pierre area
Optimum moisture, %	23.5	30.9
Max density, kg/m^3	1538	1309
Liquid limit, %	49.8	111.0
Plastic index, %	27.4	80.3

PRECONSTRUCTION PLANNING

Before the grading plans were prepared, there was considerable discussion about the types of pavement that could economically be placed and maintained over the expansive soils west of the Missouri River in South Dakota. The final decision was to use a 0.21-m (8-in) thickness of continuously reinforced concrete pavement on 15.2 cm (6 in) of lime-stabilized base course on the 209-km (130-mile) section between Cactus Flat and Chamberlain, except for an 18-km (11-mile) section westward from the Missouri River Bridge at Chamberlain and a 24-km (15-mile) section westward from Vivian. These sections of roadway are constructed of deep-strength asphalt because it was believed that the maintenance problems would be less

in these highly bentonitic-soil areas in the event that the deep undercutting and moisture and density controls were not adequate to contain the heaving.

Before the specifications for these projects were written, it was recommended that, in addition to the normal undercutting procedures, there be an additional 0.61 (2 ft) of undercutting and that the placement of soil use the energy-input method, which controls the number of roller passes per layer of soil placed. Special field-control crews to maintain strict supervision of the selected-soil placement were also recommended.

Main-line undercutting for the top 0.91 m (3 ft) of earth subgrade was designated for the full roadbed width, shoulder slope to shoulder slope. The backfill material for the top 0.91 m (3 ft), including the adjacent fill areas, is composed of selected subgrade topping. The undercut area below the top 0.91 m (3 ft), to a depth of 1.83 m (6 ft), is confined to the area between the subgrade shoulder lines. This lower 0.91 m (3 ft) forms a trench 15.9 m (52 ft) wide, shoulder to shoulder, and 0.91 m (3 ft) deep (Figure 6).

Four soil inspectors who had experience in grade construction were chosen from various districts of the department. These inspectors were given a course of instruction in the central laboratory dealing specifically with construction items as they related to soil selection, moisture and density control, soil identification, special tests, and interpretation of the specifications and special provisions.

These men worked directly under the resident engineer and acted in an advisory capacity about the grading operations as they related to the selection of the topping soil and the identification and disposal of highly plastic soils. They were responsible for the determination of the undercutting that was needed in addition to that shown on the plan and the deletion of undercut where it was deemed unnecessary. It was their responsibility to document all such changes.

SUBGRADE CONSTRUCTION

The specifications required that the upper 0.91 (3 ft) of subgrade, in both cuts and fills, be constructed of weathered soil selected for that purpose. The lower 0.91 to 1.83-m (3 to 6-ft) zone of the entire subgrade was constructed of normal soil, using higher moistures and lower minimum densities than for the underlaying embankment. One inspector was assigned to each working area of a project. There was usually more than one contractor on a project, and individual inspectors were always assigned to each contractor.

The inspectors kept daily diaries and recorded all of the activities connected with the grading work. The specifications required that the soil be broken down or pulverized so that approximately 50 percent would pass a 6.35-cm (2.5-in) sieve to achieve an adequate and uniform moisture content and to prepare each individual lift for compaction. The specifications also required that a minimum of one density test be taken for each 0.8 km (0.5 mile) of road per lane for each zone or layer.

The inspectors were directly in charge of these operations and enforced the requirements. Many liquid-limit tests were run to determine the areas of least expansive soil for use as the selected subgrade topping and for backfilling. The inspectors worked several kilometers ahead of the grading operations and supervised the location of topping material and determined the quantity available. They also supervised the placement of the selected soil in the upper 0.91 m (3 ft) of the subgrade, both in cuts and fills. In areas where extremely high bentonitic materials were encountered, the soil inspectors identified the unsuitable soil, recommended its removal, and supervised additional undercutting and backfilling. Although it was preferred to meet the target value limits, test values were acceptable if within the minimum specification requirements.

To meet the density limits of the specifications, the energy-input method was used to control the work. It was expected that four uniform coverages of the roller would be needed to meet the stipulated density requirements. However, a minimum of two coverages were required, with additional coverages as determined by the engineer and contractor, based on the results of random density tests. Frequent moisture and pulverization tests were taken to ensure that the moisture was adequately dispersed (4).

STUDIES

Costs

On the average, a total of 198 000 m^3 (259 000 yd^3) of excavation and selected-soil topping were handled for each kilometer of grade built at a cost of approximately $123 000/km ($197 000/mile). The total cost of grading the 209 km (130 miles) of projects was $25 716 306.

These costs were taken from the abstract bid items. The undercutting and borrow items were included in the unclassified excavation. The majority of the projects listed in this report were graded during 1967 to 1970. The bid prices on unclassified excavation, at that time, ranged from $0.21 to 0.28/$m^3$ ($0.16 to 0.21/$yd^3$). The selected-soil topping was bid as low as $0.145/$m^3$ ($0.11/$yd^3$). Figure 7 shows the surfacing costs for 13 continuous-reinforced-concrete surfacing projects and for 3 full-depth asphalt-concrete surfacing projects. These costs include shaping, the lime treatment of the base, and materials for shoulders.

Test Data

The average moisture and density tests indicate that the moistures and densities were reasonably close to the goals set. However, an in-depth investigation of the subgrade on one project showed that the results were not quite as close as the construction tests indicated. A review of 89 tests taken from the upper 1.83-m (6-ft) zone of this project shows an average density of 99.5 percent of the AASHTO T 99 test and a moisture content of about 2 percent above optimum. There is no doubt that the moisture content results are due to the loss of a certain amount of moisture during the compaction process and that the increase in density was due to construction equipment. A total of 41 281 985 m^3 (53 991 610 yds^3) of soil was processed and compacted on these projects. Adherence to the specifications effectively produces, as nearly as possible, a uniformly blended subgrade with a uniform moisture content. A resumé of the moisture and density tests and the volume of soil excavated is given in Table 1.

Ridability

Roughness-index measurements have been made on these projects since they were constructed. These data are shown in Figure 8 and indicate that the special moisture and density controls used appear to have retarded the adverse effects of the expansive soil through 1975. The earliest project constructed, which is now 8 years old, is located from Cactus Flat eastward. The most recently constructed project, which is adjacent to the Missouri River, was completed in 1973.

At present, some sharp bumps have appeared in the pavement because of fault lines in the shale. These oc-

curred where it was not feasible to cut enough to eliminate the fault blocks. The bumps are especially noticeable just west of the Missouri River and in areas near Kadoka, Stamford, and Murdo.

The average roughness index for the full length of the 16 projects tested is 4.34. This is a very good rating, considering that several of the projects are 8 years old. The project built in the Missouri River trench has the poorest index rating (4.15). It is also one of the newer projects, having been built in 1972.

In general, the ridability is extremely good when it is considered that in the past it was not possible to maintain

Figure 4. Special swell tests on weathered shale.

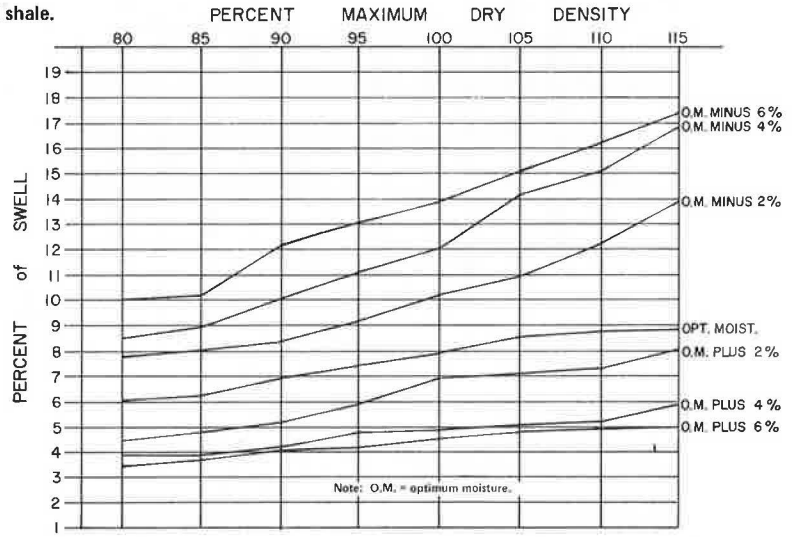

Figure 5. Special swell tests on jointed shale.

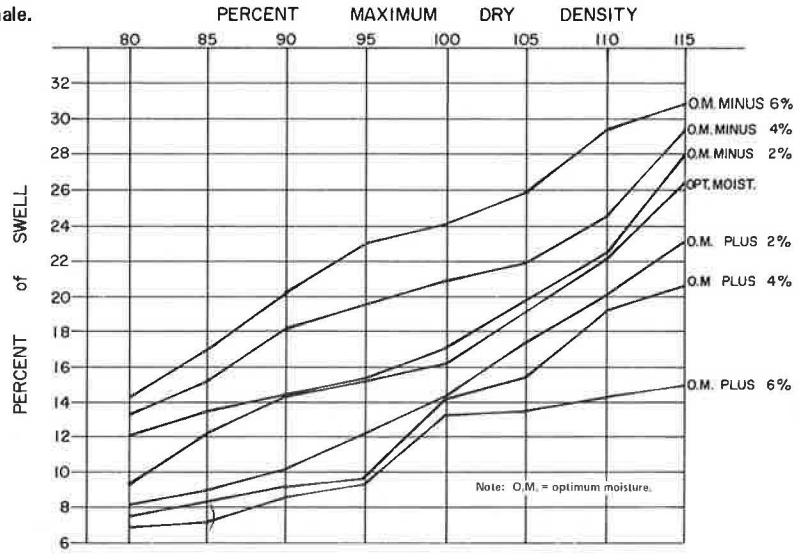

Figure 6. Typical grading section.

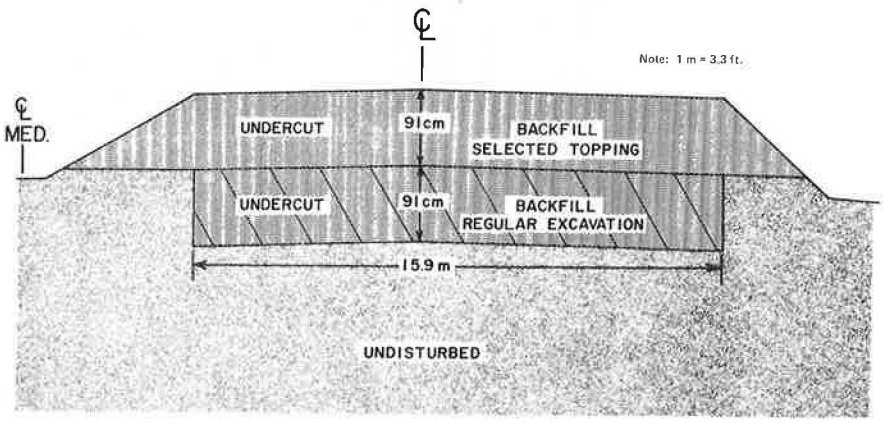

Figure 7. Cost study.

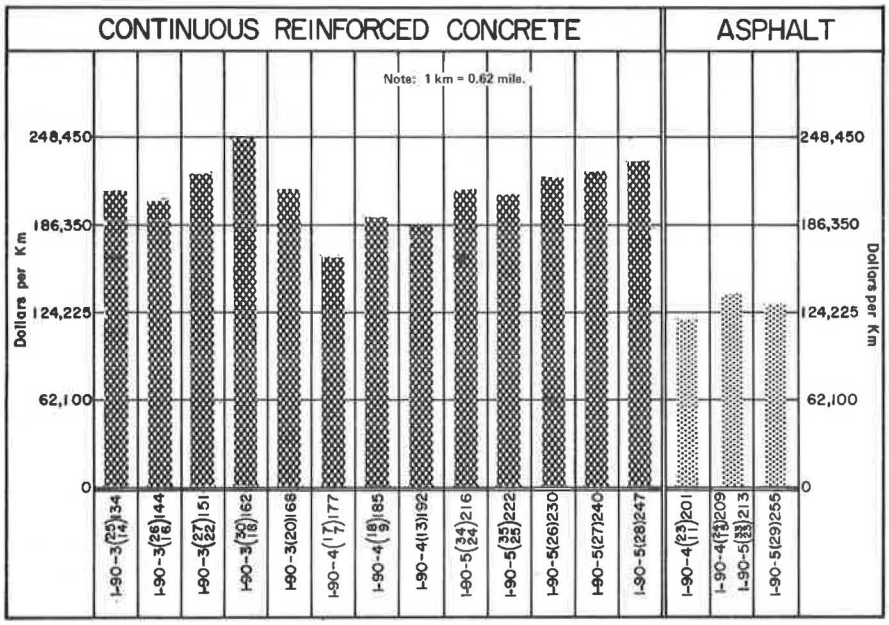

Table 1. Construction test data.

Project	County	Length (km)	No. of Tests	Percentage of T-99 Test Density		Percentage Moisture Above Optimum		Volume Excavated (m^3)
				Upper Half of Zone	Lower Half of Zone	Upper Half of Zone	Lower Half of Zone	
I-90-3(14)134	Jackson	16.0	2 750	96	97	2.0	1.8	2 218 378
I-90-3(16)144	Jackson	11.8	1 337	96	98	2.0	1.5	1 368 539
I-90-3(22)151	Jackson	15.8	1 338	97	95	1.4	1.8	2 426 788
I-90-3(18)162	Jackson	10.3	946	98	98	1.5	1.0	1 407 278
I-90-3(20)168	Jackson	14.2	494	100	100	0.6	0.7	2 827 064
I-90-4(7)177	Jones	12.9	972	99	98	2.2	1.8	2 330 844
I-90-4(9)185	Jones	11.4	968	99	97	2.0	1.7	2 689 159
I-90-4(13)192	Jones	13.7	1 706	99	98	2.5	2.5	3 045 705
I-90-4(11)201	Jones	12.8	1 032	97	99	2.7	2.8	2 449 058
I-90-4(19)209	Jones	6.5	877	101	100	2.9	2.8	2 005 524
I-90-5(23)213	Lyman	4.8	651	101	100	2.9	2.8	1 487 406
I-90-5(24)216	Lyman	9.9	1 268	100	98	3.5	2.8	2 573 478
I-90-5(25)222	Lyman	11.9	877	98	98	2.3	2.4	2 487 287
I-90-5(26)230	Lyman	15.5	1 068	97	100	3.2	2.8	2 711 396
I-90-5(27)240	Lyman	11.7	699	97	99	2.6	2.9	1 988 870
I-90-5(28)247	Lyman	12.9	770	97	99	1.5	1.7	2 274 840
I-90-5(29)255	Lyman	17.4	2 600	99	98	0.0	1.0	5 011 967
Total		209.5	21 851	—	—	—	—	41 303 581
Avg		—	—	98	98	2.1	2.0	—

Note: 1 km = 0.62 mile; 1 m^3 = 35.3 ft^3.

Figure 8. Roughometer analysis (1975).

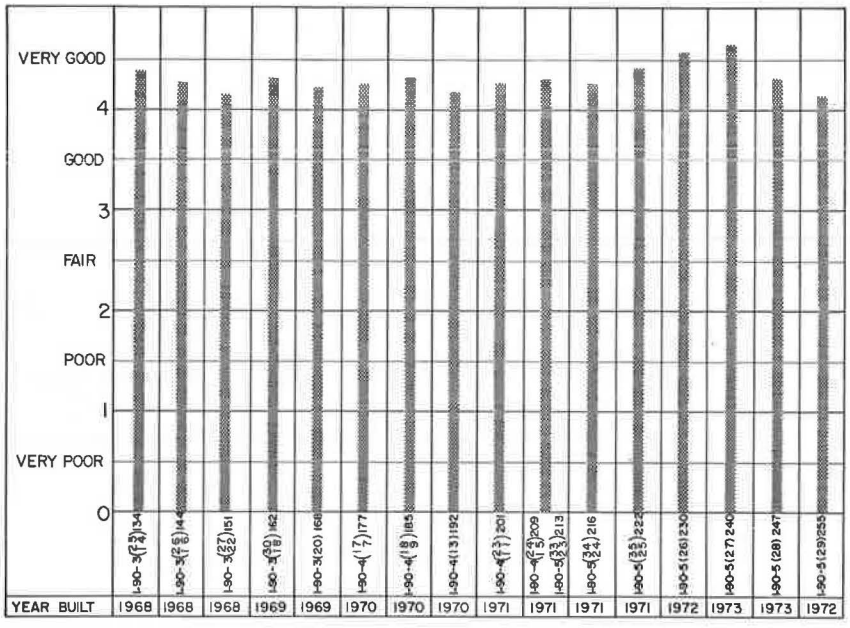

anything approaching this rating beyond 3 or 4 years.

CONCLUSIONS

It appears that much of the objectionable differentials in the Pierre shale that caused road-surface roughness in the past have been alleviated.

1. It is possible to achieve relatively good density and moisture control by designating the number of roller passes and making frequent moisture tests.
2. The control of special undercutting and soil selection can be managed by the use of specially trained crews assigned to the work.
3. Extreme warping and heaving of the subgrade over narrow fault lines appears to be reduced by deep undercutting of expansive shale and replacement of it with soil having a lower liquid limit.
4. At this time, the ridability of the surfacing is extremely good and better than on similar highways constructed through Pierre shale without deep undercutting and rigid control of compaction efforts and moisture application.
5. The use of lime treatment in the upper 0.15 m (6 in) of the subgrade and a lime-treated base is effective in preserving the moisture content of the subgrade over an extended period of time, which contributes to improved ridability.
6. At the present time, the maintenance costs for the highways listed in this report are very low; however, long-range maintenance costs are time dependent.

Although the methods discussed in this report will not be completely effective in correcting the differentials usually encountered in Pierre shale, the indications, after 5 to 8 years, are that the ridability will generally be much better over a longer period of time at lower maintenance costs.

REFERENCES

1. Mineral and Water Resources of South Dakota. U.S. Geological Survey, Committee Report to 88th Congress, 2nd Session, 1964, pp. 17-28.
2. Treatment of Expansive Soils for I-90 in South Dakota. Woodward-Clyde-Shemond and Associates, Denver, May 1965.
3. Review and Comments on Woodward-Clyde Report. H. Allen, Bethesda, Md., June 1965.
4. Moisture and Density Control on I-90 Projects I-90-(34) to I-90-(55) (1969-1974). R. Wold, Pierre, S.D., Resumé Repts., 1969-1974.

Publication of this paper sponsored by Compaction and Stabilization Section.

Factors Affecting Unconfined Compressive Strength of Salt-Lime-Treated Clay

Johnny M. Ozier,* Law Engineering Testing Company, Birmingham, Alabama
Raymond K. Moore, Department of Civil Engineering, Auburn University

Statistical procedures were used to analyze the effects of salt content, lime content, curing time, curing temperature, molding-water content, and soil type on the unconfined compressive strength of compacted specimens. A modified central-composite, second-order, rotatable experiment design and analysis of variance techniques were used to determine the significant main effects, curvilinear effects, and linear interactions at an alpha level of 1 percent. The following effects and interactions were significant at an alpha level of 1 percent: (a) main effects—salt content, lime content, curing temperature, curing time, molding-water content, and soil type and (b) interactions—lime content and salt content, lime content and curing temperature, lime content and molding-water content, salt content and curing temperature, curing temperature and molding-water content, curing temperature and soil type, curing time and soil type, and lime content and salt content and curing temperature. An engineering interpretation of each is given. A coded multiple regression model was developed to the estimate unconfined compressive strength in terms of the statistically significant main effects and interactions.

A combination stabilization strategy—the use of salt in conjunction with the lime treatment of clay soil—has been studied to determine whether small amounts of sodium chloride can be used to accelerate the stabilization phase of the lime-soil treatment process. Previous research by Mateos and Davidson (1) indicated that small amounts of sodium chloride are beneficial to the lime-fly ash treatment of Ottawa sand. The relationship between immersed compressive strength and sodium chloride content was parabolic, with maximum strengths at 7, 28, and 120 d curing times at a sodium chloride content of 1 percent. They also reported that 1 percent sodium chloride in conjunction with either calcitic hydrated lime or dolomitic monohydrate lime and fly ash produced higher compressive strengths than those observed for lime-fly ash-treated dune sand and friable silt without sodium chloride. A 6.1°C (43°F) curing temperature was shown to be detrimental to lime-fly ash-sodium chloride treatment of dune sand.

Thornburn and Mura (2), in a review of the literature of salt stabilization, have summarized several studies that used various inorganic salts with lime and lime-fly ash stabilization. This review did not note any specific reference to the effects of sodium chloride on the lime treatment of clay, although other compounds, such as sodium carbonate, have been used successfully to in-

crease the 28-d strength of lime-treated clay (3).

More recent investigations by Marks and Haliburton (4, 5) and by Drake and Haliburton (6) have been specifically designed to study the effects of sodium chloride on the lime treatment of clay soil and have indicated that there is an optimum percentage of salt beyond which further addition decreases the compressive strength. They also reported that small amounts of salt accelerate formation of the stabilization compounds associated with lime treatment. This acceleration of the formation of the pozzolanic compounds would reduce the relatively long time periods required for the development of the cured strength, which is especially significant in areas with short construction seasons and a limited number of months having sufficiently high soil-curing temperatures.

The object of this study was to develop additional information about the effects of mixture design, construction, and environmental variables, and their interactions on the unconfined compressive strength of sodium chloride-lime-treated clay soil.

MATERIALS AND SOILS

The sodium chloride used was common, noniodized table salt. The lime used was a commercial grade, hydrated, high-calcium lime, processed to have a maximum particle size of 0.037 mm (no. 400 sieve).

Permian red clay (PRC) is a medium plastic, cohesive soil of marine origin found in central Oklahoma with a distinctive red color produced by iron oxide. The PRC used in this experiment was taken from a depth of approximately 3 m (10 ft) below the ground surface on the Oklahoma State University campus in Stillwater, air-dried, and crushed to finer than 0.42 mm (no. 40 sieve). The mineralogical composition indicated that 50 to 75 percent of the PRC is chlorite, 10 percent is mica, and the remainder is illite and smectite.

The Black Belt soils of Alabama are located in a narrow strip running east to west through the south central portion of the state and are characterized by a high volume-change potential. The Houston clay (HC) used in this experiment was sampled at a depth of 38 to 76 cm (15 to 30 in) in a pasture near Downs, Alabama, air-dried, and crushed finer than 0.42 mm (no. 40 sieve).

Houston clay was created by the decomposition of Selma chalk and marine deposits of the Cretaceous age (7) and is visually identified by its grey-yellow color interspaced with modules of calcareous materials and its high plasticity (8). Smectite constitutes about 65 percent of the clay in the Alabama Houston soils and 30 to 45 percent of the whole soil in the Houston profile. Kaolinite is the second most abundant clay mineral, constituting about 25 percent of the clay fraction. Other clay minerals present are mica, vermiculite, small amounts of quartz, and trace quantities of intergrade chlorite (7). The physical properties of the clays used are given below (0.074 and 0.002 mm = no. 200 and no. 10 sieves respectively).

Property	PRC	HC
Specific gravity	2.75	2.72
Liquid limit, %	49.8	61.2
Plastic limit, %	14.2	19.2
Plasticity index, %	35.6	42.0
Percent finer than 0.074 mm	90	90
Percent finer than 0.002 mm	39	36

EXPERIMENT DESIGN

A modified five-factor, central-composite, rotatable experiment design was used for both soil types (9). A full factorial was selected within this experiment design so that all main effects, linear interactions, and quadratic effects could be analyzed. This type of experiment design has been successfully used previously (10). The factors and levels used in the experiment are given below [the lime, salt, and molding-water contents are measured as air-dried weight of soil; °C = (°F - 32)/1.8].

	Level				
Factor	-2	-1	0	+1	+2
Lime content	0	2.0	4.0	6.0	8.0
Salt content	0	1.0	2.0	3.0	4.0
Molding-water content	10.0	12.5	15.0	17.5	20.0
Curing time, d	–	10	20	30	–
Curing temperature, °C	–	4.4	23.9	43.3	–

Before completion of the analysis of variance, the estimates of experimental error obtained from the center points were compared for each soil type to determine whether the variances within the two populations were homogeneous. The two estimates of experimental error indicated homogeneity and, therefore, the analysis of variance was pooled. Thus, soil type was treated as a sixth variable, and its main effect and all linear interactions involving it as a quantitative variable were analyzed.

SPECIMEN PREPARATION AND TESTING

Lime, salt, and soil were weighed out in separate containers at predetermined levels to minimize the time required for specimen preparation. The compacted specimens were prepared by measuring the proper amount of distilled water; selecting the proper preweighed quantities of salt, lime, and soil and dry mixing them; adding the water; and blending by hand until a uniform appearance was attained. Next, the soil was compacted by using a Harvard miniature compaction mold and a scaled model of the ASTM D-698 compaction hammer. The specimens were extruded from the compaction mold, weighed, wrapped to minimize moisture loss, identified, and stored at the desired curing temperature until the test day. Immediately before testing, the specimens were removed from their temperature chambers and weighed. The unconfined compression testing procedure used a strain rate of 1 percent/min. The remains of the entire sample were used to determine its moisture content for the determination of its dry unit weight.

STATISTICAL INFERENCES

The analysis of variance results are given in Table 1. No quadratic effects were found to be significant at an alpha level of 1 percent. Each significant effect will be individually discussed in the following sections. A multiple regression equation to predict the unconfined compression strength in terms of the mixture, construction, and environmental variables studied is presented.

Main Effects

Salt Content

Figure 1 shows that increasing the salt content from 1 to 3 percent decreases the unconfined compressive strength. Previous research (5) had indicated that an optimum salt content below 3 percent maximizes the unconfined compressive strength obtained in salt-lime treatment, and the data in Figure 1 indicate a similar trend.

Thornburn and Mura (2) have reported that increasing the salt content of a soil increases the dry unit weight, and this experiment indicated a similar trend. Therefore,

an increase in dry unit weight cannot be the reason why an increased salt content caused a decreased strength. A more plausible explanation for the lower strengths associated with higher salt contents is that the excess quantity of salt recrystallizes in the cementitious gels, which may disrupt the crystalline structure of the pozzolanic products and reduce the unconfined compressive strength.

Lime Content

Figure 2 shows that increasing the lime content from 2 to 6 percent increases the unconfined compressive strength. The 2 percent level of lime provides an adequate quantity of calcium to modify the soil, but leaves very little for the formation of pozzolanic compounds. The 6 percent level provides adequate calcium for both modification and the formation of strength-producing cementitious compounds.

Curing Temperature

As is shown in Figure 3, increasing the curing temperature from 4.4 to 43.3°C (40 to 110°F) causes a large increase in the unconfined compressive strength. Increased temperatures accelerate the rate of the strength-producing chemical reactions between the lime and the soil. The high-temperature curing produces large increases in strength (however, the specimens were wrapped and sealed to minimize moisture loss).

Curing Time

Figure 4 shows that as the curing time is increased from 10 to 30 d, the unconfined compressive strength increases, which illustrates the beneficial effect of longer curing periods. However, substantial strengths were developed by the end of 10 d.

Molding-Water Content

Figure 5 shows that increasing the molding-water content from 12.5 to 17.5 percent increases the unconfined compressive strength. Because the specimens were sealed, significant amounts of moisture were not lost during curing. The lower level of moisture does not provide an adequate quantity of water for the stabilization reactions; however, the 17.5 percent level of moisture provides the additional water needed for the formation of pozzolanic compounds.

Soil Type

As is shown in Figure 6, the two types of soil used in this research have significantly different mean unconfined compressive strengths. Because of differences in clay mineralogy, HC has a much higher cation exchange capacity and a larger specific-surface area than does PRC. This creates several differences in the lime, salt, and moisture requirements of the two soils. First, the quantity of lime required to modify and stabilize HC is greater than that necessary for the modification and stabilization of PRC. Second, because of the differences in the specific-surface areas of the two clays and the different water requirements required to develop the diffused double water layers, it would be expected that HC would require more molding water than does PRC, which has a lower specific-surface area. Therefore, at identical moisture contents, more free water will be available in PRC to participate in the stabilization reactions than will be available in HC.

The confounding effect of the dry unit weight is also present in these data. The mean dry unit weight of the PRC specimens was 1514 kg/m^3 (94.6 lb/ft^3) as compared to 1322 kg/m^3 (82.6 lb/ft^3) for the HC specimens. The difference in dry unit weights will contribute to the increased unconfined compressive strengths observed in the PRC as compared to the HC.

Linear Interactions

Lime Content and Salt Content

Figure 7 illustrates one of the most important interactions investigated in this research: A 2 percent lime content and a 3 percent salt content produces slightly higher unconfined compressive strengths than does a 2 percent lime content and a 1 percent salt content; however, a 6 percent lime content and a 1 percent salt content produces a much higher unconfined compressive strength than does a 6 percent lime content and a 3 percent salt content. There are several possible explanations for this apparent contradiction. The lower level of lime (2 percent) is very near the quantity required for modification of the soils; therefore, very little if any, calcium will be available for the production of pozzolanic compounds. This suggests that the quantity of salt added would far exceed the quantity of lime available for stabilization of the soil. This excess salt could then only fill the voids, adding strength through increased density, but not through chemical reactions with the soil itself. Also, if the lime content is low, the salt is present in much too great a quantity to act solely as a catalyst in the formation of pozzolanic compounds. At a 6 percent lime content, the decrease in strength of the soil with a corresponding increase in the level of salt strongly suggests that not only is there an optimum quantity of salt, but also that excessive salt can be detrimental to the development of unconfined compressive strength.

Lime Content and Curing Temperature

At a lime content of 2 percent, an increase in curing temperature causes an increase in strength (Figure 8), and at a lime content of 6 percent, a change in the temperature from 4.4 to 43.3°C (40 to 110°F) causes a larger increase in the strength of the specimens because the chemical reactions involved in the formation of the pozzolanic compounds are greatly accelerated at the higher temperature. The lime content of 2 percent supplies very little calcium for the formation of these compounds after the modification reactions have taken place. A lime content of 6 percent supplies a surplus of calcium after modification that is available for the chemical reactions that increase the unconfined compressive strength.

Lime Content and Molding-Water Content

At a 2 percent lime content, an increase in molding-water content from 12.5 to 17.5 percent increases the unconfined compressive strength (Figure 9). At a 6 percent lime content, the increase in strength as the molding-water content is increased is larger than that at a 2 percent lime content.

This interaction shows the positive effect of increased molding water and lime contents on the unconfined compressive strength. The 17.5 percent molding-water content provides more of the water for the required development of pozzolanic compounds when sufficient calcium is present.

Salt Content and Curing Temperature

Figure 10 shows that increasing the salt content from 1 to 3 percent at a curing temperature of 4.4°C (40°F) produces little change in the unconfined compressive strength. The same increase in salt content at 43.3°C (110°F) produces a decrease in the unconfined compressive strength. The unconfined compressive strengths for each salt content were higher at a 43.3°C (110°F) curing temperature than at a 4.4°C (40°F) curing temperature, again because the chemical reactions are accelerated at a higher temperature. The decrease in the unconfined compressive strength when the salt content is increased further illustrates the detrimental effect of excessive salt.

Table 1. Analysis of variance for unconfined compressive strength.

Source of Variation	Degree of Freedom	Mean Squares	F-Value[a]	Significance Level (%)
Total	63	—	—	—
Salt content	1	3 546	17	1
Lime content	1	50 421	245	1
Curing temperature	1	154 814	751	1
Curing time	1	7 151	34	1
Molding-water content	1	14 841	72	1
Soil type	1	25 824	125	1
Lime content and salt content	1	7 884	38	1
Lime content and curing temperature	1	31 964	155	1
Lime content and molding-water content	1	3 234	16	1
Salt content and curing temperature	1	4 132	20	1
Curing temperature and curing time	1	4 124	20	1
Curing temperature and molding-water content	1	11 348	55	1
Curing temperature and soil type	1	16 738	81	1
Curing time and soil type	1	3 242	16	1
Lime content and salt content and curing temperature	1	3 934	19	1
Residual	48	—	—	—
Center points	11	206.31	—	—

[a]Critical F-value: F(1, 11, 0.01) = 9.65.

Figure 1. Effect of salt content on unconfined compressive strength.

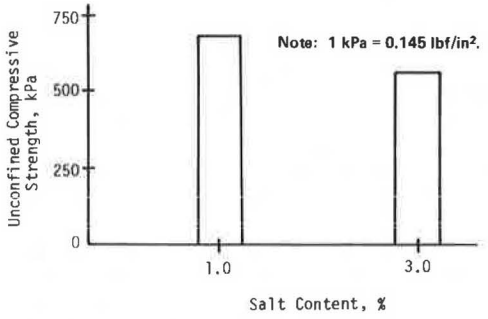

Figure 2. Effect of lime content on unconfined compressive strength.

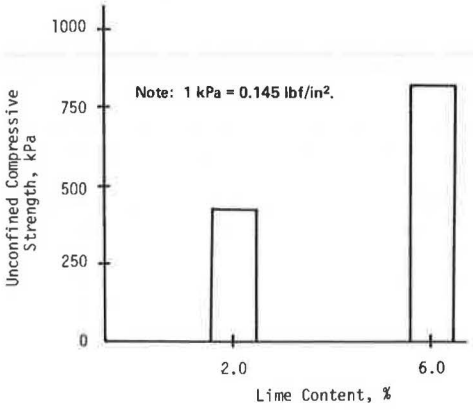

Figure 3. Effect of curing temperature on unconfined compressive strength.

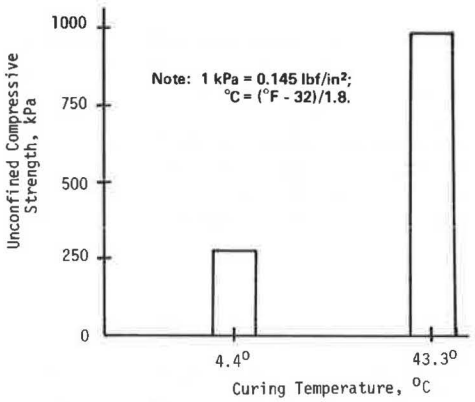

Figure 4. Effect of curing time on unconfined compressive strength.

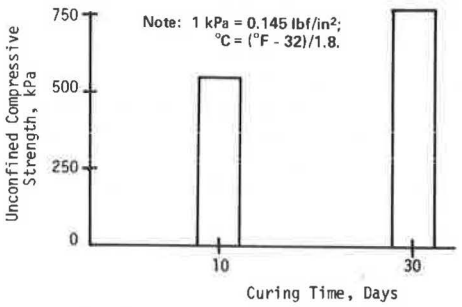

Figure 5. Effect of molding-water content on unconfined compressive strength.

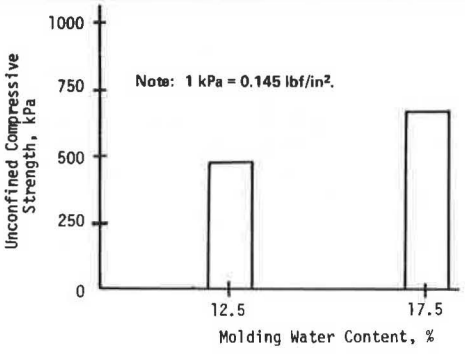

Curing Temperature and Curing Time

As shown in Figure 11, at a curing temperature of 4.4°C (40°F), there is little change in the unconfined compressive strength as the curing time is increased from 10 to 30 d, but at a curing temperature of 43.3°C (110°F), an

increased unconfined compressive strength is observed when the curing time is increased from 10 to 30 d. This indicates that little chemical activity takes place at 4.4°C (40°F) for the two curing times used and that both increased curing time and increased curing temperature increase the unconfined compressive strength.

Figure 6. Effect of soil type on unconfined compressive strength.

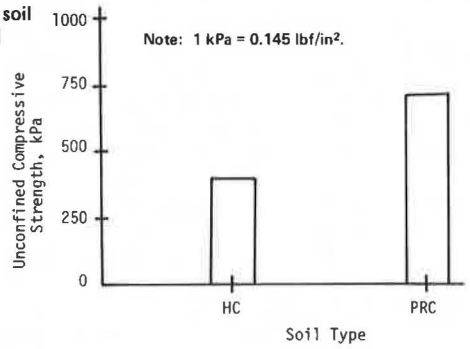

Figure 7. Effect of interaction between lime content and salt content on unconfined compressive strength.

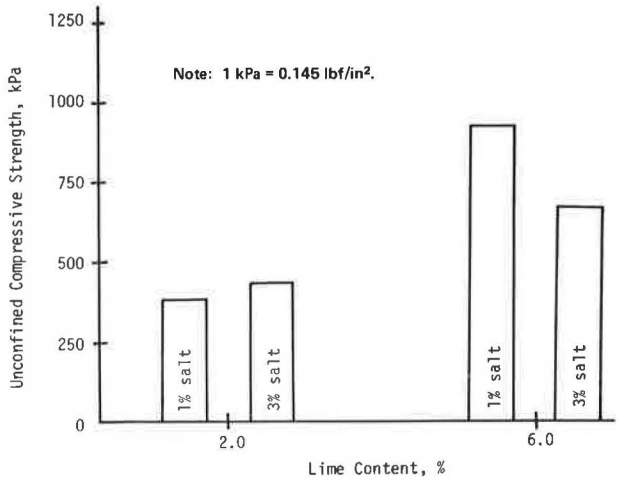

Figure 8. Effect of interaction between lime content and curing temperature on unconfined compressive strength.

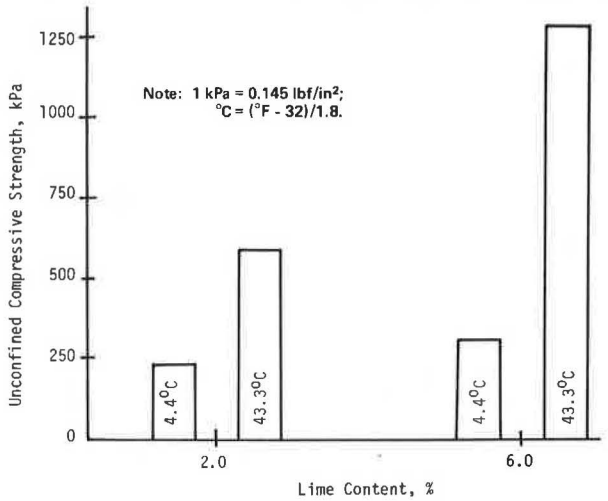

Curing Temperature and Molding-Water Content

As shown in Figure 12, at 4.4°C (40°F), there is a small increase in the unconfined compressive strength with increased moisture content. However, the unconfined compressive strength substantially increases at a 43.3°C (110°F) curing temperature when the molding-water content is increased from 12.5 to 17.5 percent. As previously discussed, at 4.4°C (40°F), the formation of cementitious compounds is slower than at 43.3°C (110°F). A combination of high levels of molding-water content and temperature produces increased unconfined compressive strength, which illustrates the need for water in the production of the pozzolanic products.

Curing Temperature and Soil Type

Figure 13 shows that at 4.4°C (40°F), PRC has a slightly greater unconfined compressive strength than does HC; however, at 43.3°C (110°F), the difference is large.

The difference in the unconfined compressive strengths of the two soils can be partially explained by the differ-

Figure 9. Effect of interaction between lime content and molding-water content on unconfined compressive strength.

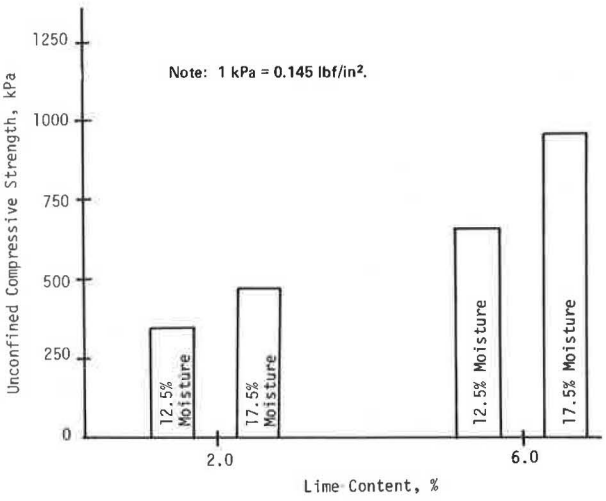

Figure 10. Effect of interaction between salt content and curing temperature on unconfined compressive strength.

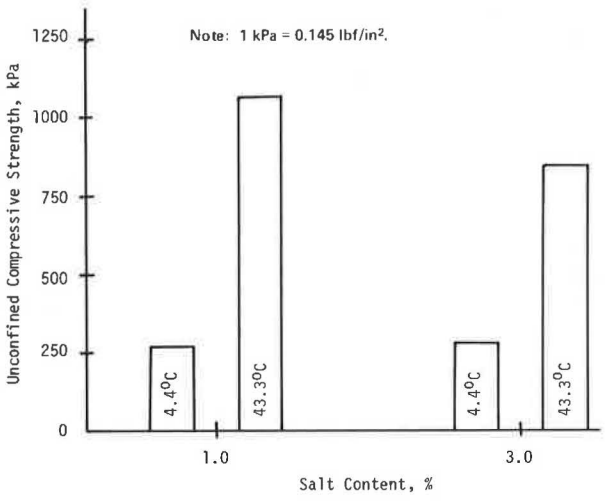

ence in their dry unit weights. That difference should explain the difference in their unconfined compressive strengths at low temperatures, even when chemicals have been added, because virtually no strength-producing stabilization reactions take place at 4.4°C (40°F).

At 43.3°C (110°F), the difference between the strengths of the two soils can no longer be explained without considering their mineralogical properties. Because HC could very well have a specific-surface area four to five times larger than that of PRC, one would expect that it would require much more chemical to treat HC than is required for PRC. Hence, the PRC would have a larger increase in the unconfined compressive strength at the higher curing temperature for the levels of lime content, moisture content, and salt content used.

Curing Time and Soil Type

As is illustrated in Figure 14 for a curing time of 10 d, PRC develops a higher unconfined compressive strength than does HC. This is also true for a curing time of 30 d, and the difference in strength of the two clays is much greater. This interaction strengthens the postulate that the quantity of lime required to stabilize HC is greater than that required to stabilize PRC and that soil type is confounded with dry unit weight.

Lime Content, Salt Content, and Curing Temperature

At a curing temperature of 4.4°C (40°F), the average unconfined compressive strength increases as the lime content is increased from 2 to 6 percent and as the salt content is decreased from 3 to 1 percent (Figure 15). These increases are very small, but there is a much larger average strength increase at 43.3°C (110°F) as the lime content is increased from 2 to 6 percent and the salt content is decreased from 3 to 1 percent.

This interaction illustrates a response surface among several of the suggested hypotheses. First, lower temperatures retard and higher temperatures accelerate the formation of strength-producing compounds. Second, excessive quantities of salt appear to be detrimental to the stabilization process. The response surface created by the 43.3°C (110°F) curing temperature slopes toward higher percentages of lime and lower percentages of salt for the development of higher unconfined compressive strengths. The major inference from this effect is

Figure 11. Effect of interaction between curing temperature and curing time on unconfined compressive strength.

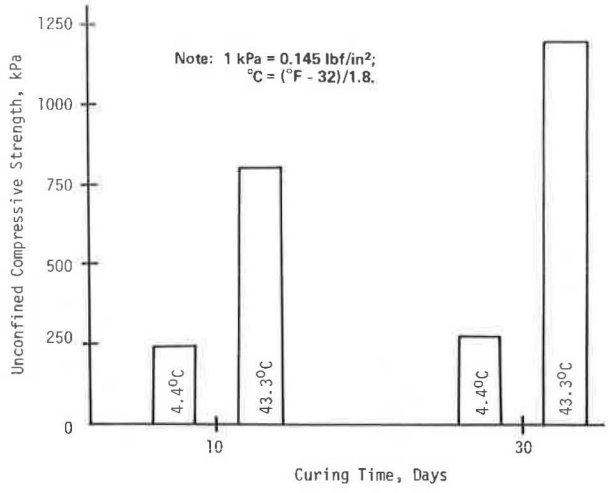

Figure 12. Effect of interaction between curing temperature and molding-water content on unconfined compressive strength.

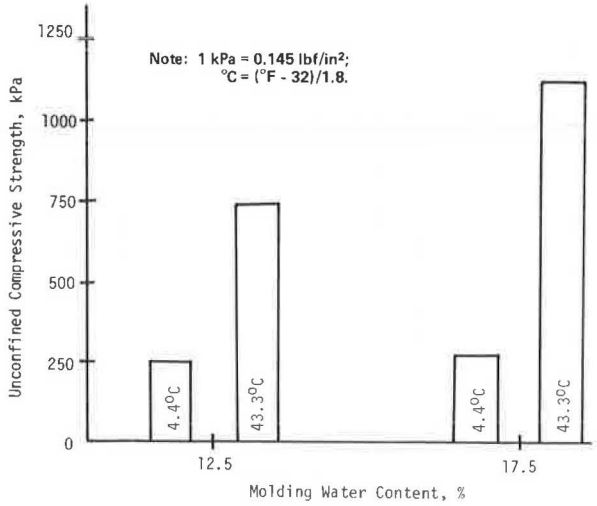

Figure 13. Effect of interaction between soil type and curing temperature on unconfined compressive strength.

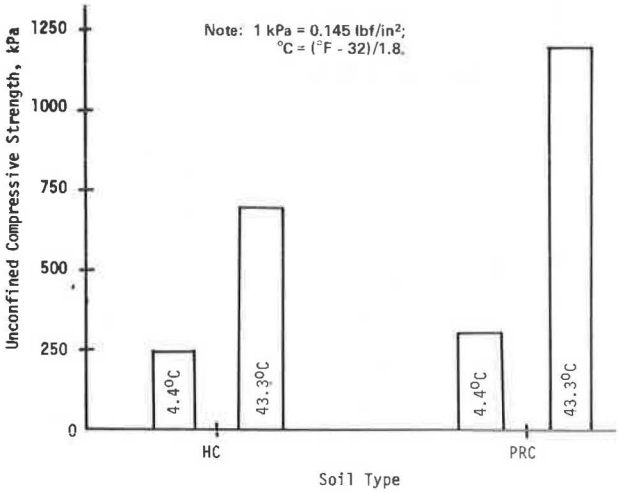

Figure 14. Effect of interaction between soil type and curing time on unconfined compressive strength.

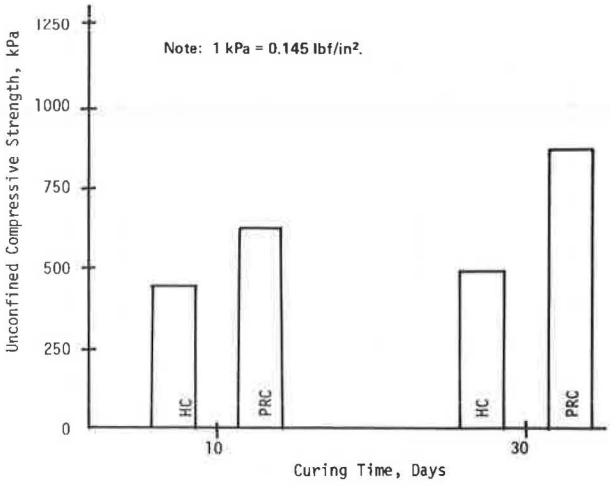

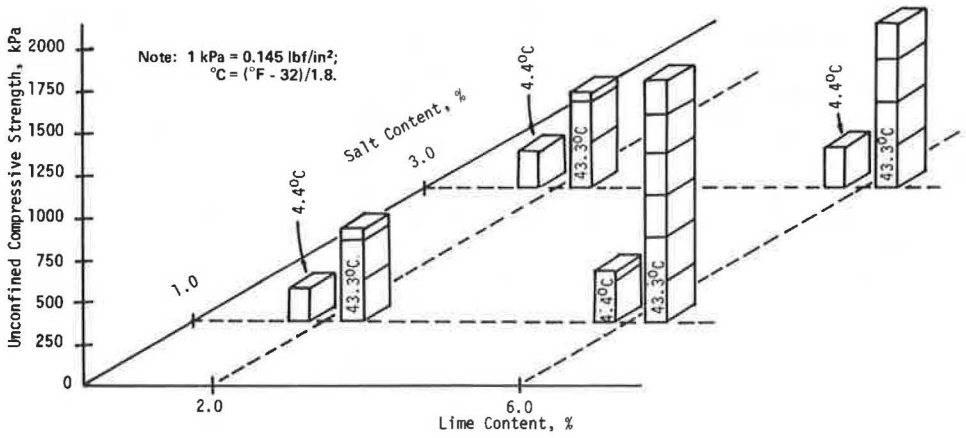

Figure 15. Effect of interactions among lime content, salt content, and curing temperature on unconfined compressive strength.

that there is an optimum salt content that maximizes unconfined compressive strengths in lime-treated clays and that this is probably less than 3 percent if sufficient lime is present for the development of pozzolanic compounds.

Prediction Equations

A multiple linear regression was used to generate a coded prediction equation that included all of the main effects, two-factor interactions, and three-factor interactions found to be significant at an alpha level of 1 percent.

$$S = 88.22 - 7.44A + 28.07B + 49.18C + 10.57D + 15.23E + 20.09F - 11.10AB - 8.03AC + 22.35BC + 7.11BE + 8.02CD + 13.32CE + 16.17CF + 7.12DF - 7.84ABC \quad (1)$$

where

S = unconfined compressive strength,
A = salt content,
B = lime content,
C = curing temperature,
D = curing period,
E = molding water content, and
F = soil type.

The coded levels given in Table 1 are used.

The standard error of estimate of the equation is 173.4 kPa (24.9 lbf/in^2), and R^2 is 0.9246. The equation has a lack of fit at an alpha level of 2.5 percent and is valid only for predictive purposes within the factor space studied, which is a function of the factors and levels studied. Any attempt to extrapolate beyond the factor space with regression equations may introduce conditions that were not investigated and result in erroneous predictions.

CONCLUSIONS

All six factors studied in this research were found to be significant as main effects at an alpha level of 1 percent with respect to the unconfined compressive strength. No quadratic effects were found to be significant; however, eight two-factor linear interactions and one three-factor linear interaction were significant at an alpha level of 1 percent. Those main effects and interactions were

1. Main effects: salt content, lime content, curing temperature, curing time, molding-water content, and soil type and
2. Interactions: lime content and salt content, lime content and curing temperature, lime content and molding-water content, salt content and curing temperature, curing temperature and curing time, curing temperature and molding-water content, curing temperature and soil type, curing time and soil type, and lime content, salt content, and curing temperature.

Each of the effects and interactions had a positive regression coefficient except salt content, lime content and salt content, and salt content and curing temperature. A positive coefficient implies that the dependent variable—unconfined compressive strength—is increased as the quantity of the independent variable is increased. For the range of the variables used in this research, the unconfined compressive strength was increased by

1. Increased lime content,
2. Decreased salt content,
3. Increased curing temperature,
4. Increased curing time,
5. Increased molding-water content, and
6. Using PRC rather than HC.

The results of this experiment are indicative of the complexity involved in combination stabilization processes.

REFERENCES

1. M. Mateos and D. T. Davidson. Further Evaluation of Promising Chemical Additives for Accelerating Hardening of Soil-Lime-Fly Ash Mixtures. HRB, Bulletin 304, 1961, pp. 32-50.
2. T. H. Thornburn and R. Mura. Stabilization of Soils With Inorganic Salts and Bases: A Review of the Literature. HRB, Highway Research Record 294, 1969, pp. 1-22.
3. C. C. Ladd, Z. C. Moh, and T. W. Lambe. Recent Soil-Lime Research at the Massachusetts Institute of Technology. HRB, Bulletin 262, 1960, pp. 64-85.
4. B. D. Marks and T. A. Haliburton. A Salt-Lime Soil Stabilization Feasibility Study. School of Civil Engineering, Oklahoma State Univ.; Oklahoma Research Program Project Agreement No. 6, Final Rept., 1970.
5. B. D. Marks and T. A. Haliburton. Acceleration of Lime-Clay Reactions With Salt. Journal of the Soil Mechanics and Foundations Division, Proc., ASCE, Vol. 98, No. SM4, April 1972, pp. 327-340.
6. J. A. Drake and T. A. Haliburton. Accelerated Curing of Salt-Treated and Lime-Treated Cohesive Soils. HRB, Highway Research Record 381, 1972, pp. 10-19.

7. Chemical, Mineralogical, and Engineering Properties of Alabama and Mississippi Black Belt Soils. Alabama and Mississippi Agricultural Experiment Stations and Soil Conservation Service; Southern Cooperative Series No. 130, Auburn Univ., Auburn, Ala., Feb. 1968.
8. Soil Survey of Macon County, Alabama. U.S. Department of Agriculture and Alabama Department of Agriculture and Industries, Series 1937, No. 11, 1944.
9. W. B. Cochran and G. M. Cox. Some Methods for the Study of Response Surfaces. Experimental Designs, Wiley, New York, 2nd Ed., 1957.
10. R. K. Moore, T. W. Kennedy, and J. A. Kozuh. Tensile Properties for the Design of Lime-Treated Mixtures. HRB, Highway Research Record 351, 1971, pp. 112-114.

Publication of this paper sponsored by Committee on Chloride Stabilization.

**Mr. Ozier was at the Department of Civil Engineering, Auburn University, when this research was performed.*

Laboratory Study of the Effectiveness of Cement and of Lime Stabilization for Erosion Control

George Machan,* L. R. Squier, Inc., Lake Grove (Portland), Oregon
Sidney Diamond, School of Civil Engineering, Purdue University
Edmond Leo,* Geo Testing, Inc., San Rafael, California

Soils ranging in texture from sand to heavy clay can be rendered effectively resistant to the soil erosion caused by raindrop impact by treatment with as little as 1 percent portland cement or hydrated lime. Erosion resistance was evaluated in a standard rainstorm sequence in which 8.2 cm (3.25 in) of rain was applied for 1 h on each of two successive days. Compacted but otherwise unstabilized soils lost 1 to 2.5 g/cm^2 (0.014 to 0.035 lb/in^2) of exposed surface, equivalent to 45 to 110 tons/acre, in this standard test. Incorporation of stabilizer and appropriate curing before exposure decreased this erosion loss to about 0.11 g/cm^2 (0.0016 lb/in^2), equivalent to 5 tons/acre, for fully compacted specimens. Cement-treated soils tested after only modest compaction maintained their erosion resistance, but lime-treated soils were adversely affected by reduced levels of compaction. These laboratory test results do not necessarily predict practical field performance, because the effects of running water erosion, of the incomplete mixing characteristic of field incorporation of stabilizers, and of cycles of temperature change, wetting and drying, and freezing and thawing have not been tested.

Accelerated soil erosion at construction sites is a serious environmental problem in many parts of the United States. The present methods of erosion control are not uniformly effective.

For many years, soils have been stabilized for use as highway or airfield subgrade materials by treatment with portland cement or hydrated lime.

The present work is based on the idea that treatment of soils exposed on construction sites with small amounts of cement or lime might be useful in preventing erosion. The use of these stabilizers would be relatively expensive in terms of the usual costs of erosion control, but it might provide effective erosion resistance and be a useful alternative to conventional methods, particularly where erosion may lead to especially harmful or serious consequences.

EVALUATION METHODS

Characterizing the erosion resistance of a particular soil or treated soil is, in the final analysis, a field-scale problem. Nevertheless, laboratory assessment based on measurement of the soil lost in controlled artificial-rainstorm tests should be helpful in screening the effectiveness of various kinds of erosion-control treatments on various soils. The present paper reports the results of tests on a range of Indiana soils treated with small amounts of hydrated lime or portland cement, compacted, and cured to various degrees before exposure to a standardized laboratory rainstorm sequence and discusses the extent to which such laboratory results might reflect field effectiveness.

The apparatus used measured the resistance of 10.2-cm (4-in) diameter test specimens exposed to a standard rainstorm sequence of approximately 7.6 cm (3 in) of rain delivered in 1 h, followed by a 23-h rest period, and then by another rain cycle of the same kind. Equipment quirks prevented the delivery of exactly 7.6 cm (3 in) of rainfall in 1 h, and 8.2 cm (3.25 in) was standardized on. The rainfall device delivered droplets of uniform size and spatial distribution that had a kinetic energy approximating that of the average drop in natural storms of the same intensity.

In the tests, the surfaces of the specimens were maintained at a 5° angle to the horizontal to prevent ponding. Three replicate specimens were exposed simultaneously, and the actual amount of rainfall delivered was monitored by rain gauges between the specimens. The soil removed from each specimen was collected and dried and weighed for the quantitative assessment of the amount of erosion. Erosion was expressed in terms of weight loss per unit area of exposed specimen surface.

The apparatus and test procedures have been described previously (1).

SOILS AND STABILIZERS USED

Four natural Indiana soils were chosen to provide examples of a full range of textural classes from a heavy, montmorillonite-bearing clay soil to a predominantly sandy soil with only about 3 percent clay. They are described in Table 1.

The stabilizers used were a type 1 portland cement of normal chemical and other characteristics and a reagent-grade hydrated lime (calcium hydroxide). While reagent-grade hydrated lime is somewhat more effective than most commercial limes, the differences are not usually of major consequence.

EROSION RESISTANCE OF UNSTABILIZED SOILS

The erosion resistance of the untreated soils used as blanks against which the effects of the stabilizers could be evaluated were measured by using the same procedures of specimen preparation, except that no stabilizers were incorporated and hence no curing was required. The procedure consisted of air drying the soil and then compacting it to the approximate standard Proctor (ASTM designation D 698-method A) unit weight at optimum moisture content. Some deviation of compaction technique was necessary to adapt the method to the specimen size used, which was considerably smaller than the standard Proctor specimen.

The results of the erosion tests on these compacted but otherwise unstabilized soils are given below (1 g/cm^2 = 0.0142 lb/in^2).

Soil	Loss (g/cm^2)
Romney clay	1.08
Blue clay till	1.70
Tan till	2.24
Glacial outwash	2.53

The losses varied from slightly over 1 g/cm^2 (0.014 lb/in^2) for the heavy clay soil (Romney clay) to more than 2.5 g/cm^2 (0.035 lb/in^2) for the sandy soil (glacial outwash). The field equivalents of these losses are about 50 and 110 tons/acre.

The higher erosion of the sandier soils agrees with the expectations developed from long-term field tests (2), which suggests that soils with high contents of fine sand and silt erode most rapidly.

One of the projected uses for these erosion-control treatments would be on highway slopes too steep for effective compaction by heavy equipment. Consequently, one of the objects of the present study was to provide information on the effectiveness of stabilization treatments where the treated soil is compacted only lightly, or perhaps not at all. To provide blanks for such experiments, the effect of the degree of compaction on the erosion loss of unstabilized soils was assessed.

In this assessment, specimens were tested in which the compactive effort was reduced in stages by decreasing both the number of blows and the height of fall of the compaction hammer from that prescribed for the standard Proctor compaction. This produced unit weights down to about 80 percent of the standard Proctor unit weight, which corresponds roughly to the field densities of the undisturbed soils. In all cases, the moisture content was adjusted to be approximately optimal for the compactive effort actually applied. Details of the procedures followed have been described previously (3).

The results of the rainstorm-exposure tests indicated that fully compacted soils suffered more erosion (i.e., were less erosion resistant) than did lightly compacted soils of the same type. Over the range of unit weights explored (from 100 to about 80 percent of the standard Proctor), the loss for the heavy clay soil (Romney clay) decreased from 1.1 to 0.2 g/cm^2 (0.016 to 0.0028 lb/in^2). The effect was generally less pronounced for the other soils; the loss for the blue clay till decreased from 1.7 to 1.0 g/cm^2 (0.024 to 0.014 lb/in^2), that for the tan till decreased from 2.3 to 0.7 g/cm^2 (0.032 to 0.0099 lb/in^2), and that for the sandy glacial outwash decreased from 2.5 to 1.9 g/cm^2 (0.032 to 0.027 lb/in^2) over the same range of decreasing unit weights.

The explanation for this appears to depend on the effect of compaction on the permeability and the swelling behavior of the soil. If sufficient permeability exists after compaction (i.e., for lightly compacted soils of lower unit weight), the soil appears to resist swelling and dispersion of its particles under the impact of the raindrops.

Conversely, clay-bearing soils rendered relatively impermeable by full compaction tend to swell, disperse, and erode under raindrop impact. Predominantly sandy soils are less affected by variations in the degree of compaction because they are highly permeable in any case; however, there is so little interparticle bonding that the impact of the drops causes rapid particle detachment and erosion of the silt and sand grains.

These results are the basis for assessment of the erosion losses of the same soils after treatment with stabilizers. The degree to which the stabilization treatment reduces erosion loss compared to that of the same soil compacted in the same way in the absence of the stabilizer provides a working assessment of the effectiveness of the treatment.

EFFECTIVENESS OF PORTLAND CEMENT TREATMENT

Both hydrated lime and portland cement depend for their stabilizing effect on a chemical reaction with individual soil grains. Such reactions are not instantaneous and require curing at a high relative humidity and a reasonable temperature for some hours or days after mixing and compaction. Curing in laboratory tests is normally carried out in a fog room at a controlled temperature, even though such conditions may not be duplicated in the field.

In the tests with portland cement, the specimens were mixed and compacted at the optimum moisture content and then cured in a fog room at approximately 21°C (70°F) for 3 d or longer before being exposed to the artificial rainstorm.

Preliminary results had indicated that all of the soils might be effectively stabilized against erosion in the standard erosion-test rainstorm sequence by the addition of as little as 1 percent cement by weight of soil. This percentage was used in all cases, with additional tests carried out at higher levels of cement content where indicated.

The erosion-test results for specimens treated with 1 percent portland cement compacted to the full standard Proctor unit weight and cured for various periods are shown in Figure 1. (In this and the succeeding figures, the erosion plotted at zero curing time actually represents the erosion of blank specimens compacted to the same unit weight as the series indicated.)

These results show that the erosion of all four soils tested decreased to the order of 0.1 g/cm^2 (0.0014 lb/in^2) after 3 d of fog-room cure. The particles actually detached at this level of erosion loss come mostly from the edges of the specimens. The bulk of the specimens appear to be essentially undisturbed; thus, this level of treatment effectively stabilizes the soils against erosion.

A number of additional tests were carried out with specimens mixed with 1 percent cement, but compacted under reduced compactive efforts to lower unit weights. These tests did not encompass a full spectrum of reduced compactive efforts, but the following results were obtained.

The blue clay till and glacial outwash soils lightly compacted to unit weights of about 80 percent of the standard Proctor unit weight were effectively stabilized

[their erosion losses were about 0.1 g/cm^2 (0.0014 lb/in^2)] after 7 d of fog-room curing.

The tan till soil compacted to 90 percent of the standard Proctor unit weight (the only level explored) was effectively stabilized after 3 d of fog-room curing.

The Romney clay soil, the heavy montmorillonitic clay material, had a low erosion loss when compacted to 80 percent of the standard Proctor unit weight even without added stabilizer. This loss [0.2 g/cm^2 (0.0028 lb/in^2)] was not improved on by adding 1 percent portland cement and compacting to the same level, regardless of curing time allowed. Apparently heavy clays that are not effectively compacted require more cement for any improvement in erosion resistance to occur. A special test was conducted with 3 percent cement and compaction to 80 percent of the standard Proctor unit weight, and complete stabilization in terms of erosion loss was attained after 7 d fog-room curing.

EFFECTIVENESS OF HYDRATED-LIME TREATMENT

Fog-room curing was even more important for the development of resistance to erosion of lime-treated soils; specimens were cured up to 28 d.

Again based on preliminary results, a treatment level of 1 percent of stabilizer by weight of soil was reasonably effective; this amount was used in all tests except those where it was clear that higher levels were needed.

The results of erosion trials on specimens mixed with 1 percent lime, compacted to standard Proctor unit weight, and cured in a fog room for up to 28 d are shown in Figure 2.

Most of the soils tested showed lower erosion-loss levels after lime treatment, but fully effective stabilization requires more than the 3-d curing period that is sufficient with portland cement. Curing in the fog room for 7 d before exposure yields satisfactory results, however, except for the Romney clay soil.

This soil was not effectively stabilized against erosion loss by a 1 percent lime treatment, regardless of the curing period allowed. Presumably a larger percentage of lime is required for this heavy montmorillonitic soil.

The effect of reduced compaction was more complicated for lime treatment than for cement treatment, and varied somewhat for the different soils tested.

The glacial outwash soil developed adequate resistance to erosion when the compacted density was reduced to 90 percent of the standard Proctor unit weight, but the erosion resistance development required 28 d of fog-room curing. At a lower unit weight (78 percent of the standard Proctor value), complete erosion resistance was not attained even after 28-d curing. These results are shown in Figure 3.

The tan till soil was even more sensitive to the degree of compaction: Specimens compacted to as much as 90 percent of standard Proctor unit weight showed appreciable erosion loss even after 28 d of curing.

As shown in Figure 4, the blue clay till soil was stabilized against erosion loss at a unit weight of 96 percent of the standard Proctor value after 7 d of curing and at a unit weight of 90 percent of the standard Proctor value after 28 d of curing. However, further reduction of unit weight prevented entirely effective erosion resistance even after 28 d of curing.

The Romney clay soil had previously been found to show only a small soil loss when prepared without stabilizer at reduced levels of compactive effort. As shown in Figure 5, the addition of 1 percent of lime generated no improvement in the erosion resistance of lightly compacted specimens, regardless of the curing time allowed. It is clear that a greater amount of stabilizer is required for this heavy clay soil at low unit weights. Specimens mixed with 3 rather than 1 percent of lime were effectively stabilized after only 7-d curing.

Generalizing on the results of the tests with lime-treated soils, it appears that treatment with 1 percent lime is as effective as treatment with 1 percent portland cement, but the curing time required to develop effective erosion resistance is longer, and the sensitivity to reduced compaction is greater. At reduced unit weights comparable to those of the natural soils, effective stabilization by treatment with 1 percent lime seems unattainable.

CHARACTERIZATION OF STABILIZED SOILS

The soils treated with portland cement and with lime were in no sense converted to massive, concrete-like materials. While a modest strength, sufficient to permit careful handling, was produced, the original particulate character of the soils was largely retained, and the compacted and cured specimens were usually porous and permeable.

The erosion resistance developed is apparently due to the formation of a calcium silicate hydrate gel around some of the soil grains and as a mesh linking adjacent grains together (4). This results in the generation of water-stable aggregations of particles that do not break down under the impact of raindrops. These changes are the effect of irreversible chemical reactions and hence would seem permanent.

An earlier report (3) compared these test results with those for specimens of a silty clay soil on which a full stand of Alta fescue grass had been grown to maturity. The erosion loss of such specimens averaged 0.5 g/cm^2 (0.070 lb/in^2) in the standard rainstorm sequence, which is significantly higher than most of the losses reported for properly compacted and cured cement and lime-stabilized soils, even at the 1 percent level of stabilizer. Thus, at least under laboratory conditions, the stabilization treatments tested here are more effective in conferring erosion resistance than is a stand of grass.

Table 1. Characteristics of experimental soils.

Soil	Unified Soil Classification	Percentage Clay (<0.002 mm)	Type of Clay Mineral	Liquid Limit (%)	Plasticity Index (%)	Maximum Unit Weight[a] (kg/m^3)	Field Density (kg/m^3)
Romney clay	CH	48	Montmorillonite	68	39	6.1	4.6
Blue clay till	SC	20	Illite, chlorite, kaolinite, montmorillonite	23	10	7.8	6.0
Tan till	SM	5	Illite, chlorite	19	4	7.8	6.4
Glacial outwash	GM-GC	3	Illite, chlorite, vermiculite, montmorillonite	21	5	7.4	5.8

Note: 1 kg/m^3 = 0.062 lb/ft^3; 0.002 mm = No. 10 Sieve.

[a]ASTM D 698-70 method A.

IMPLICATIONS FOR FIELD USE

Success in stabilizing small soil specimens against erosion loss in a laboratory test rainfall does not necessarily mean that the same methods will be successful in a field-scale treatment. There are a number of differences between the kind of laboratory-scale testing described here and actual field situations. A few of these merit specific discussion.

First, the specimens were tested only against the impact effects of raindrops. Actual soil erosion involves at least two mechanisms, one that is due to raindrop impact and results primarily in sheet erosion, and another that is due to the tractive force of running water, especially on long steep slopes, and results in rill and gully formation. There is evidence, however, that the mechanisms that involve impact effects exert control in the sense that the impact effects are a necessary precurser to rill erosion. For example, Young and Wiersma (5) found that in field-scale experiments where soil loss was primarily by rill erosion, preventing impact effects by placing a screen above, but out of contact with, the soil reduced soil loss by 90 percent or more. They concluded that 80 to 85 percent of the soil lost in the experiments without the screen was first detached by rainfall impact and then transported down the rills by running water effects.

A second difference between these laboratory tests and field-scale use is that of the completeness of mixing attainable in the two situations. Laboratory-scale mixing is more efficient and complete than any feasible field-scale method of incorporation of the stabilizer. In consequence, it is likely that a significantly higher content of stabilizer would be required to ensure the presence of at least the amount needed at all points throughout the material.

Third, the curing procedure used does not have an

Figure 1. Effect of 1 percent portland cement treatment on erosion loss of soils as a function of curing period.

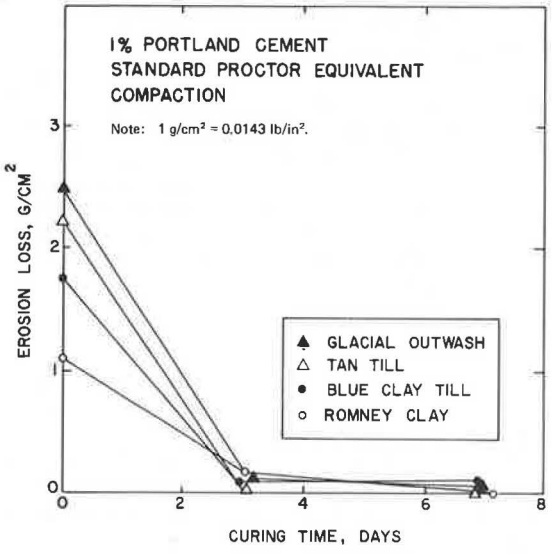

Figure 2. Effect of 1 percent lime treatment on erosion loss of soils as a function of curing period.

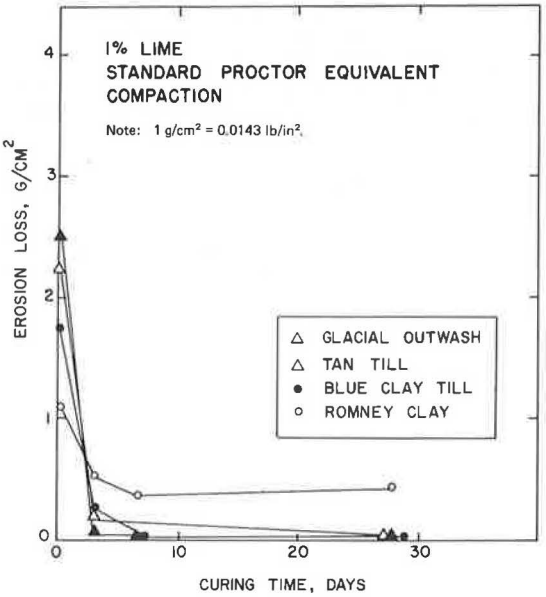

Figure 3. Effect of 1 percent lime treatment on erosion loss of sandy soils compacted at reduced compactive effort as a function of curing period.

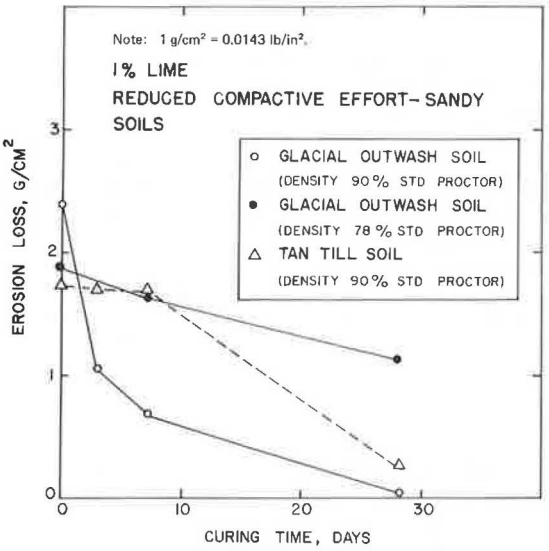

Figure 4. Effect of 1 percent lime treatment on erosion loss of blue clay till soil compacted at reduced compactive efforts as a function of curing period.

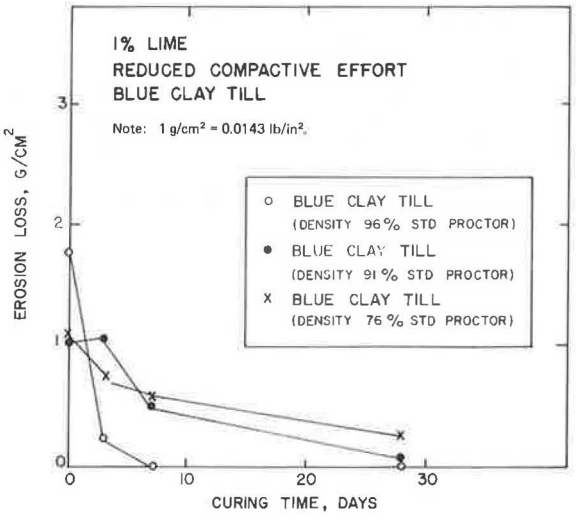

Figure 5. Effect of lime treatment on erosion loss of Romney clay soil compacted at reduced compactive effort as a function of curing period.

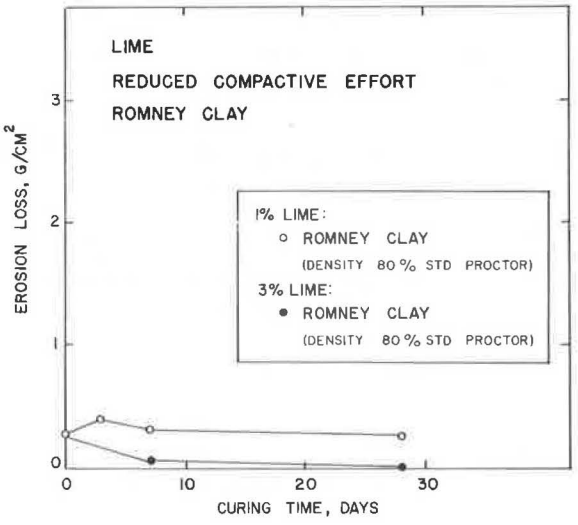

exact counterpart in field-scale applications, although expedient means of field curing stabilized soils are widely used in the application of lime and cement to soil stabilization for subgrades.

Finally, the permanence of the treatment in field exposures where temperatures cycle daily, where wetting and drying cycles occur frequently, and most important, where freezing and thawing occur might be questioned. The chemical reactions resulting in the binding together of the particles are irreversible, but whether this binding is sufficiently strong to overcome the environmental forces tending to disruption in practical cases remains to be seen.

CONCLUSIONS

1. Standard, laboratory rainfall tests showed that both type 1 portland cement and reagent-grade hydrated lime used at levels of 1 percent by weight of soil, in specimens that were thoroughly mixed, compacted, and cured before testing, provided effective control against erosion caused by raindrop impact (except in a heavy montmorillonite clay soil that required more stabilizer).
2. The portland cement treatments were effective after only 3 d of room-temperature fog-room curing; hydrated lime seemed to require a week or more of curing for the development of full effectiveness.
3. The reduction in the unit weight of soil specimens produced by reduced compactive efforts in specimen preparation did not seriously interfere with the development of erosion resistance with portland cement, but delayed, and in some cases prevented, the development of full erosion resistance with lime.
4. Soils stabilized by either treatment retained most of their natural soil characteristics and were not rendered impermeable or greatly strengthened.
5. Only the erosion resistance with respect to the impact effects of raindrops was tested. The erosion resistance to the tractive force of running water was not tested. However, there is reason to believe that soils stabilized with respect to falling-drop impact should be at least partly resistant to running-water effects.
6. The erosion resistance developed has been tested only with laboratory-scale specimens not subject to temperature, wetting and drying, or freezing and thawing cycles before exposure to the rainstorm. Whether such resistance is permanent in field-scale exposure is a subject for further testing.

ACKNOWLEDGMENTS

This work was carried out with the support of the Federal Highway Administration and the Indiana State Highway Commission and is a contribution from the Joint Highway Research Project, Purdue University.

The successful prosecution of this research was made possible in large part through the development of the sophisticated and effective test rainstorm installation by Mitsunori Kawamura, whose contribution to this work is gratefully acknowledged.

The assistance of Mark Levy and Janet Lovell in the experimental program is acknowledged with thanks.

The contents of this report reflect our views and we are responsible for the facts and the accuracy of the data presented herein. The contents do not necessarily reflect the official views or policies of the Indiana State Highway Commission or the Federal Highway Administration. This report does not constitute a standard, specification, or regulation.

REFERENCES

1. S. Diamond and M. Kawamura. Soil Stabilization for Erosion Control. Joint Highway Research Project, Purdue Univ., Rept. JHRP-74-12, 1974.
2. W. H. Wischmeier, C. B. Johnson, and B. V. Cross. A Soil Erodability Nomograph for Farmland and Construction Sites. Journal of Soil and Water Conservation, Sept.-Oct. 1971, pp. 189-192.
3. G. Machan. Stabilization of Soils for Erosion Control on Construction Sites. Joint Highway Research Project, Purdue Univ., Rept. JHRP-75-5, 1975.
4. M. Kawamura and S. Diamond. Stabilization of Clay Soils Against Erosion Loss. Clays and Clay Minerals, Vol. 23, 1975, pp. 444-451.
5. R. A. Young and J. L. Wiersma. The Role of Rainfall Impact on Soil Detachment and Transport. Water Resources Research, Vol. 9, 1973, pp. 1629-1636.

Publication of this paper sponsored by Committee on Soil-Portland Cement Stabilization.

**Mr. Machan and Mr. Leo were at the School of Civil Engineering, Purdue University, when this research was performed.*

Compaction Energy Relationships of Cohesive Soils

J. R. Bell, Department of Civil Engineering, Oregon State University

The energy requirements of laboratory methods of compaction that produce similar results with a sandy silty clay soil of low plasticity were investigated. The purposes were to provide insight into compaction energy relationships, to give a preliminary indication of the possible benefits of improved field compaction equipment design and operation, and to suggest directions for future studies. Three methods of compaction—impact, static, and kneading—were studied. The soil was compacted at three energy levels by the impact method, and for one energy level, nine combinations of rammer mass, number of tamps, and height of drop were used. The moisture versus unit weight relationships for the basic impact method were reproduced by a static compaction method and by a kneading method and the compaction energies determined. The compacted specimens were tested for as-compacted undrained strength. The static method is always the most efficient for the soil tested, but the relative efficiencies of the other methods vary with the moisture content of the soil, the rammer force per unit area, and the rate and duration of loading. In this study, the most efficient method was always at least three times as efficient as the least efficient method with respect to the energy required to produce the same dry unit weight. A view of the compaction process for cohesive soils that considers energy and distinguishes between penetration due to densification and plastic deformation is presented.

It is frequently possible to meet a given set of compaction specifications with a wide range of equipment and field procedures. To select the most efficient equipment and method requires knowledge of the inputs of compaction energy per unit volume of soil that are required to produce end products having comparable properties by different compaction methods. It also requires knowledge of the efficiencies of different types of field compaction equipment and of the procedures used in applying useful compaction energy to soil. This report presents the results of a preliminary study of the energy requirements of various laboratory methods of compaction that produce comparable results. The purposes of the study are to provide a better understanding of the compaction energy relationships for cohesive soils, a preliminary indication of the possible benefits of improved field compaction equipment, and information for planning further research.

Three laboratory compaction methods—impact, static, and kneading—were studied using one soil. The soil used was a sandy silty clay of low plasticity. The results from this soil are compared with data from the literature by other investigators for other cohesive soils. From the point of view of efficiency in field compaction, it is necessary to consider equipment factors relative to the efficiency of transferring energy from some source to the soil as well as the energy that must be applied to the soil itself to obtain the desired results. This investigation considers only the relationship between the desired end product and the energy applied to a unit volume of soil (the compactive effort).

It is traditional to compare compaction on the basis of density. However, with cohesive soils, different methods of compaction may yield different soil grain structures at the same density (1), and different densities and moisture contents may be required to obtain comparable end properties by different methods. A comparison of the energy per unit volume to obtain a given density may not be a true evaluation of relative efficiencies. Therefore, the compactive efforts required by each method were compared with respect to dry unit weight and as-compacted undrained shear strength.

LITERATURE REVIEW

Considerable, but still incomplete, information about the compaction-energy requirements of cohesive soils is available in the literature. Some of this is summarized briefly below, and a more complete review has been given by Johnson and Sallberg (2).

Several investigations of the effects of the magnitude and distribution of compactive effort in the impact test are reported in the literature. A study relating compactive effort, dry unit weight, and compaction moisture content by Dhawan and Bahri (3) showed that, under conditions drier than the optimum moisture content, increased energy per unit volume results in higher densities. This is true even at high compactive efforts. Under conditions wetter than the optimum moisture content, however, increasing the energy input above some relatively low value does not increase the density because the additional effort is consumed in remolding the soil at constant volume. It is this remolding that produces the different grain structures of cohesive soils compacted above and below the optimum water content (1).

There have been several studies of the details of how a given effort is applied to the soil. Sowers and Kennedy (4) found that the most important factor influencing the effectiveness of a given impact compactive effort was the percentage of the total energy that was applied in each tamp. In studies of the effects of force, velocity, energy, and momentum of the rammer, Proctor (5) showed that for constant compactive effort per unit volume of soil, the variation in dry unit weight due to rammer force was small. Maclean and Williams (6) also found that for constant applied energy, the effect of the force of the rammer was very small. Contrary to Proctor, however, they found that the lighter rammer gave slightly higher unit weights. Maclean and Williams also studied the effects of rammer force at constant momentum and found only a slightly greater effect than for constant energy. Sowers and Kennedy (4) used rammers ranging from 24.5 to 111.2 N (5.5 to 25.0 lbf) and heights of drop from 76.2 to 457 mm (3 to 18 in) and concluded that neither rammer force, velocity, nor momentum had discernible effects on impact compaction effectiveness with respect to dry unit weight.

There are no known data for the moisture and unit weight versus energy relationships for static compaction. Some factors affecting efficiency may be the ratio of the diameter of the specimen to its length, the rate of compression, the time of load application, and whether compression is from both ends or one.

Several studies have been made of the effects of the number of layers, the number of tamps per layer, the foot pressure, and the dwell time on the kneading compaction process. Typical of the results of these studies are those of Seed and Monismith (7), who showed that increasing the number of layers or of load applications per layer has the same general effect as in the impact test, and increasing the foot pressure has the same effect as increasing the rammer force in the impact test. McRae and Rutledge (8) found that increasing the time the foot pressure was maintained on the soil shifted the line of optimum toward the zero air-voids line.

Sankaran and Muthukrishnaiah (9) have compared the

energy consumed in laboratory impact and kneading compactions under moisture contents drier than optimum. They concluded that the impact method is more efficient in terms of both dry density and strength. They also found that, for any given molding-water content drier than the optimum, there was a critical compactive effort for each compaction method. Below this critical compaction effort, the as-compacted undrained strength was a linear function of the compactive effort. Above this effort, the strength increased very little with increased compactive effort.

LABORATORY STUDIES

This is a preliminary study; therefore, only one soil and only each method of impact, static, and kneading compaction were studied. Because of the large amount of data (nearly 90 specimens were compacted and tested), typical results only are presented.

Test Soil

The soil was sieved through a 4.75-mm (no. 4 U.S. standard) sieve. The portion passing was air dried, thoroughly mixed, and stored until needed for testing. This soil had 61 percent passing the 0.074-mm (no. 200) sieve; its liquid and plastic limits were 24 and 19 percent respectively. The soil was a sandy silty clay of low plasticity having a unified classification of CL-ML.

For all tests, the air-dried soil was carefully mixed by hand with distilled water to as nearly the desired moisture content as possible and stored in air-tight containers for a curing period of not less than 24 h before compaction. A fresh soil sample was used for each specimen.

Shear Test Method

The undrained strength relationships for all of the specimens were measured to detect any differences in soil structure that might result from the different compaction procedures. A direct shear test was used for these investigations because the sample could be cut from the center third of the cylinder of compacted soil so as to not include the contact planes between the layers in which the soil was compacted.

After compaction, the soil was extruded from the compaction mold, and a sample 63.5 mm (2.5 in) in diameter by 25.4 mm (1.0 in) high was carefully trimmed from the center of the cylinder. The sample was placed in the direct-shear machine, a normal stress of 47.9 kPa (1000 lbf/ft^2) was applied to it, and it was sheared at a rate of 0.01 mm/s (0.025 in/min).

Impact Compaction

Equipment and procedures were as specified by AASHTO T 99 procedure, except as noted. In the basic series of impact tests, only the compactive effort was varied. In addition to the standard 25 blows/layer, 12 and 55 blows/layer were also used. The moisture content versus unit weight curves obtained from these tests are shown in Figure 1, and the stress versus displacement curves obtained from the undrained strength tests of the specimens compacted at standard conditions are shown in Figure 2.

To investigate the effects of rammer velocity and force on the impact test method, a special rammer was made that allowed varying the height of drop and the force. The general design, clearances, and shape and area of the rammer face were the same as the standard rammer. The compactive effort was held constant at 592.5 kJ/m^3 (12 375 ft·lbf/ft^3), which is the energy of the standard test. The number of blows per layer, the heights of drop, and the rammer forces used are listed in Table 1.

For the impact tests, the gross energy applied per unit volume was calculated directly from the product of the force, the height of drop, the number of blows per layer, and the number of layers divided by the volume of soil.

Static Compaction

Specimens were compacted to the desired moisture content and unit weight by mixing the soil to as nearly the desired moisture content as possible, weighing the required amount of moist soil into the compaction mold, and compressing it to a known volume. After compaction, the sample was extruded from the mold, weighed, a moisture sample taken, and the moisture and unit weight computed. The moisture versus unit weight relationships obtained by the basic impact tests were duplicated as nearly as possible by static compaction, and strength tests were performed on these specimens. The results of typical strength tests are shown in Figure 3.

The soil was compacted in a steel cylinder by compression from both ends. The compacted specimen was the same size as that obtained in the impact method. The compression force was recorded at each 2.5 mm (0.1 in) of displacement, and the total energy required for compaction was computed as the area under the force versus displacement curve. The energy relationships are shown in Figures 4 and 5. The normal procedure was to compact at a constant rate of 5 mm/min (0.2 in/min). Tests of the effect of the rate of compression showed that the compaction energy did not increase significantly until the compaction rate was more than doubled.

Kneading Compaction

The kneading compaction tests were performed with a manual press similar to the University of California type (2). The soil was compacted in a standard AASHTO compaction mold, which was placed on a rotating base under the ram of the press. A triangular tamping foot on the ram was pressed into the soil, the foot was raised, the cylinder rotated 30°, and the foot again pressed into the soil. This process was repeated as required. The soil was compacted in three layers with 24 tamps/layer at a foot pressure of 3861 kPa (185 lbf/ft^2). These conditions were selected experimentally to approximately duplicate the moisture versus unit weight curve obtained by the standard impact method.

A hydraulic cylinder and pressure gauge in the ram assembly indicated the force on the foot, and an Ames displacement dial measured the foot penetration into the soil. The foot was pressed into the soil as rapidly as the displacement and the corresponding forces could be read manually. The energy for each tamp was computed as the area under the force versus displacement curve. The total energy was the sum of the energies of the individual tamps.

The strength results for the kneading compaction method are shown in Figure 6, and the energy relationships for this method are shown in Figures 4 and 5.

DISCUSSION OF RESULTS

The compaction results of the basic impact tests at the three energy levels and the undrained, as-compacted strength data are typical of this method. The data given in Table 1 for constant energy with different rammer forces, velocities, and energies per blow, however,

show that the way the energy is applied is significant. With respect to the maximum dry unit weight, the maximum variation is only about 0.5 kN/m^3 (3 lbf/ft^3). However, when this is translated into energy considerations, it becomes significant. Figure 7 shows the relationship between the maximum dry unit weight and the compactive effort for the basic procedure and the range of unit weights obtained at 592.5 kJ/m^3 (12 375 ft·lbf/ft^3) of energy with various rammer forces and drop distances. The least efficient combination gives a dry unit weight that could have been obtained with only about 402.2 kJ/m^3 (8400 ft·lbf/ft^3) by the basic method, and the most efficient combination corresponds to a unit weight that would have required about 790.0 kJ/m^3 (16 500 ft·lbf/ft^3) by the basic method. These are relative efficiencies of 68 and 133 percent respectively. On this basis, the most efficient combination is approximately twice as efficient as the least efficient procedure.

With respect to dry unit weight, the most efficient method was the use of the heaviest rammer with the lowest velocity and the highest energy per blow, and the least efficient was the use of the lightest rammer with the highest velocity and lowest energy per blow. Energy per blow was the most important factor: The lower the energy per blow, the lower the efficiency.

The strength test data show that these are also significantly affected by the details of the compaction procedure. Table 1 shows that the peak strength at the optimum moisture conditions for the specimen compacted with the lightest rammer with the highest velocity and the lowest energy per blow is about equal to that for the

Figure 1. Impact compaction: moisture content versus unit weight.

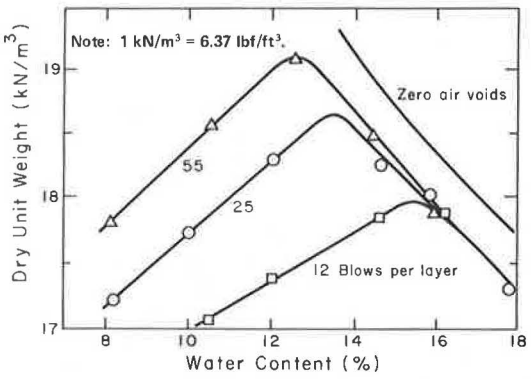

Figure 2. Shear stress: displacement relations for AASHTO T 99 compaction.

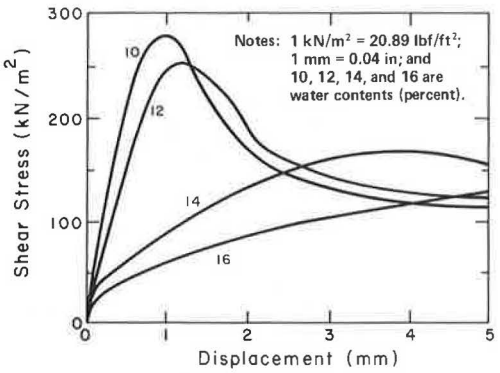

Figure 3. Shear stress: displacement relations for static compaction equivalent to AASHTO T 99 compaction.

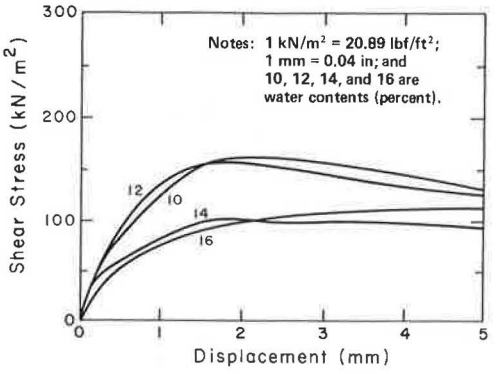

Table 1. Impact compaction variables and results.

Blows per Layer	Height of Drop (mm)	Rammer Force (N)	Optimum Conditions: Water Content (%)	Optimum Conditions: Dry Unit Weight (kN/m^3)	Optimum Conditions: Peak Strength (kN/m^2)
55	610	5.6	13.7	18.2	173
55	305	11.1	13.6	18.3	212
55	152	22.2	13.6	18.3	218
25	610	12.2	13.6	18.6	239
25	305	24.5	13.4	18.7	205
25	152	49.0	13.5	18.6	205
12	610	25.5	13.9	18.5	217
12	305	51.0	13.4	18.7	165
12	152	102.0	13.2	18.8	174

Note: 1 mm = 0.04 in; 1 N = 0.22 lbf; 1 kN/m^3 = 6.37 lbf/ft^3; 1 kN/m^2 = 20.89 lbf/ft^2.

Figure 4. Compactive effort required to obtain AASHTO T 99 dry unit weight.

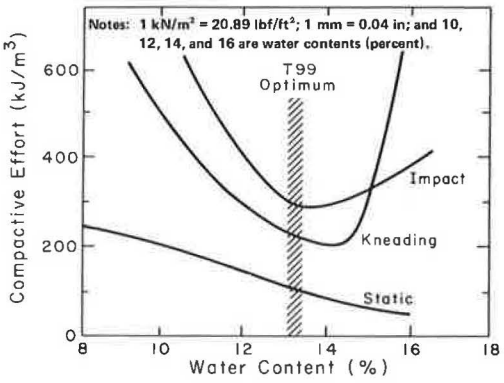

Figure 5. Compactive effort required to obtain dry unit weight of 17.9 kN/m^3 (114.0 lbf/ft^3).

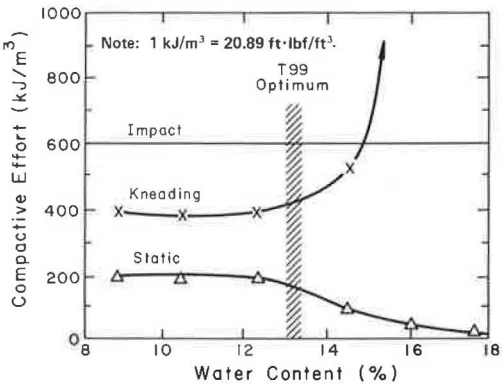

heaviest and slowest rammer and the highest energy per blow, even though this condition yields higher density. The highest peak strengths were those of intermediate conditions. Evidently, the high-energy rammer accomplishes more remolding and shear of the soil and develops a more ordered arrangement of the soil particles that reduces the strength.

The table below for measurements made at a compactive effort of 526 kJ/m^3 (11 000 ft·lbf/ft^3) shows that there were significant differences in the energy applied to the different layers in the kneading test (1 N·m = 0.74 lbf/ft).

	Energy (N·m)		
Tamp No.	Layer 1	Layer 2	Layer 3
1	15.8	17.2	19.7
4	7.5	7.6	9.8
8	5.9	5.9	9.4
12	4.6	6.6	7.8
Subtotal	88.1	93.8	117.6
16	4.6	6.1	6.5
20	3.8	5.3	8.0
24	2.8	4.8	7.0
Total	131.7	159.2	205.5

Layer one consumed less energy because it is underlain by the unyielding metal plate, but the other layers are over soil, which deforms when the foot is applied to the soil. This trend is much greater under conditions wetter than optimum.

Figure 6. Shear stress: displacement relations for kneading compaction equivalent to AASHTO T 99 compaction.

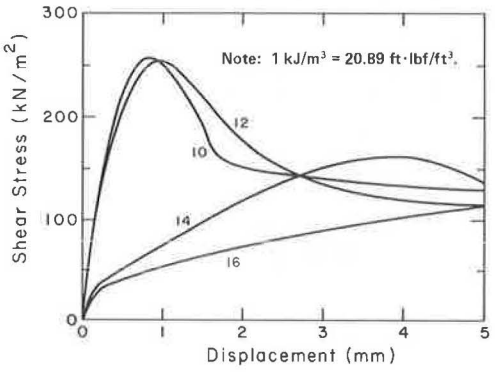

Figure 7. Maximum dry unit weight versus compactive effort for impact compaction.

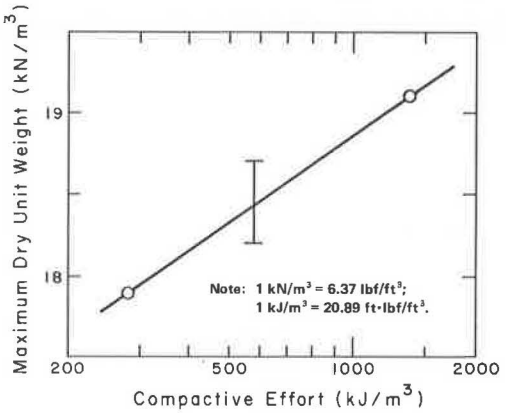

This table also shows that in the kneading method, the greatest energy is applied by the first tamp. There is a great difference between the first and second tamp and then a steady decrease with succeeding applications of the tamping foot: Approximately two-thirds of the total energy was applied during the first 12 tamps (one coverage of the soil). For the conditions of this kneading method, the energy applied during the first coverage accomplished about 97 percent of the compaction under moisture conditions drier than optimum and virtually 100 percent of the compaction under moisture conditions wetter than optimum. The energy in the second application was consumed almost entirely in remolding at constant volume.

Figure 4 shows the energies required to obtain the standard AASHTO T 99 moisture versus unit weight relationships by the three compaction procedures studied, and Figure 5 shows the energies required to obtain a dry unit weight of 17.9 kPa (114 lbf/ft^3) by the three methods. For the soils compacted under moisture conditions drier than optimum, the energies required to approximate AASHTO T 99 compaction are constant for all methods. Of course, for the impact method, the energy available for compaction is held constant, but for the other methods, more energy is available if required. Under moisture conditions drier than optimum, the density obtained for a constant energy input is essentially a linear function of the water content for all methods, and the static method is the most efficient, with respect to the dry unit weight, and the impact method is the least efficient of the methods. The difference between the kneading and impact methods is probably due, for the most part, to the different rates of loading in the two procedures. The kneading load is applied more slowly and is, therefore, more efficient. If the kneading loads were applied more rapidly and the dwell times reduced, the energy required by this method would be about the same as that in the impact method. As discussed previously, changing the energy per blow in the impact method will change the efficiency of this method.

Under moisture conditions wetter than optimum, the relationships are quite different. The efficiency of the static method compared to that of the impact method with respect to density becomes somewhat higher. This may be because the soil tested has a relatively high permeability and some of its water was squeezed out during static compaction. This trend might be slowed or even be reversed if a more impermeable soil were tested.

Under moisture conditions wetter than optimum, the efficiency of the kneading method is lower than that of the impact method. This is due to the greater remolding of the soil, which consumes energy, but does not increase the density. This greater remolding is also due to the slower rate of loading. If the tamping foot of the kneading compactor is pressed into the soil more rapidly and the dwell time is reduced, there will be less remolding, and the relative efficiency will probably be increased. It is also probable that efficiency could be increased by reducing the foot pressure so that the shear resistance of the soil is not exceeded.

In all cases, the most efficient method is at least three times as efficient as the least efficient method with respect to the compactive effort required to produce the same dry unit weight at a given moisture content.

For both the impact method and the kneading method, there are distinct optimum moisture contents. These optimums are well defined in Figure 5 where they correspond to the point of minimum energy required to obtain the specified dry unit weight. This figure also shows that there is no optimum moisture content for the static compaction method. Efficiency increases with increase in moisture content all the way to complete saturation.

Figure 8. Relative peak strength per unit compactive effort for compaction equivalent to AASHTO T 99.

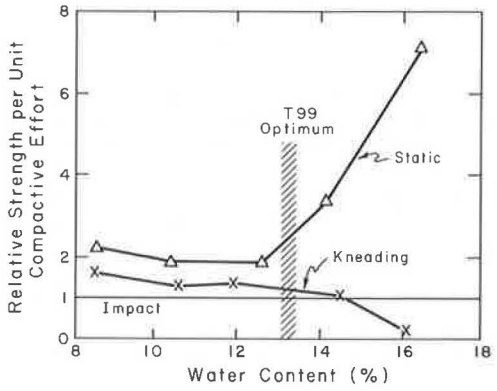

Figure 9. Idealized force versus penetration curve for compactable cohesive soil.

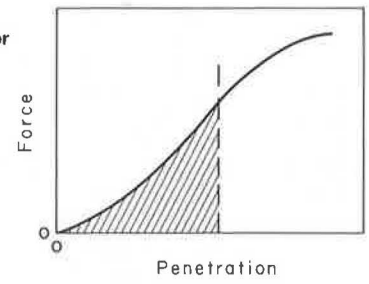

This is a logical extension of the tendency of the line of optimums to move toward the line of zero air voids with increased dwell time during kneading compaction (8).

The optimum moisture content is a function of the compaction procedure and can, for a given soil, be varied by changing the procedure. It appears to correspond closely to the highest moisture content at which there is no significant remolding of the soil at constant volume during compaction. If all of the factors were fully understood, it might be possible to adjust the kneading compaction procedure so that the optimum could be made to correspond to any soil moisture content.

For the procedures and soil used in this study, the peak strength for the same conditions of moisture versus unit weight was very nearly the same for the impact and kneading tests at all moisture contents. This does not agree with the results of Sankaran and Muthukrishnaiah (9) who found their impact method more efficient with respect to both density and strength for moisture contents below optimum. Evidentially their soil, which was more plastic than the one used in this study, and their procedures resulted in more remolding in the kneading method at low moisture contents.

Under moisture conditions drier than optimum, in this study, the kneading method yielded about the same strength with a lower energy input; therefore, it is more efficient with respect to strength than is the impact method. Under moisture conditions wetter than optimum, however, the strength ratio remained near unity, but the energy requirements increased for the kneading method, and the impact method became more efficient. These relationships are shown in Figure 8 in terms of the relative strength per unit energy input per unit volume with respect to the impact method. This was calculated by dividing the strength of a given specimen by the strength of a corresponding impact specimen and then dividing the answer by the corresponding ratio of the compactive efforts.

All of the static compaction specimens have lower strengths than do the corresponding impact specimens. This is inconsistent with the work of Seed, Mitchell, and Chan (10). The reasons for this were not investigated. However, even though the strengths were low, the low energy required by the static method made it the most efficient with respect to strength as well as to dry unit weight.

With respect to strength, the question of efficiency is very complex, and the data of different investigators are contradictory. However, with respect to dry unit weight, the trends appear to be fairly well established. These trends suggest a view of the compaction process for cohesive soils that may be helpful in understanding field as well as laboratory compaction.

As a compaction device is applied to a loose cohesive soil, the load overcomes the ability of the soil to support it, and it sinks into the soil. As it penetrates, the soil directly under the compaction device is densified. Large deformations are restricted to the zone directly beneath the device. Almost all of the input energy is used to densify the soil. As the soil is compacted, its bearing capacity is increased, and if that becomes equal to the applied load, penetration and compaction stop. An idealized force versus penetration curve is shown in Figure 9. The process described above is represented by that portion of the curve to the left of the dashed vertical line. In this region, almost all of the energy applied (which is equal to shaded area) is used to compact the soil. As long as densification is the dominant process, the penetration curve will be concave upward.

If the compaction pressure is increased, compaction will continue until the resistance to densification is approximately equal to the shear resistance to plastic deformation. If the pressure is increased further, the curve will become concave downward, and penetration will be largely the result of shear of the soil beneath the compactor at essentially constant volume. The energy represented by the area beneath the curve to the right of the dashed line is largely expended in remolding at constant volume and is wasted as far as compaction is concerned. For a given soil, the exact shape of the curve, the area under the curve, and the position of the inflection point depend on the moisture content and the details of the compaction procedure. The greatest efficiency is achieved when compaction is accomplished by a few slowly applied loads without excessive remolding. From the standpoint of equipment design and operation, it is necessary to obtain combinations of factors to allow compaction in the region represented to the left of the inflection point in Figure 9. In general, it appears that the most efficient will be that which uses heavy equipment with large contact areas, high contact pressures, and low rates of travel (which approximates static loading).

For dry conditions, the use of slow, heavy, high-pressure compaction equipment does not have serious inherent problems. However, for wet soils, high, slowly applied contact pressures cause inefficient remolding. If it is not possible to approach static compaction for wet conditions, then an impact procedure is the next most efficient. This could be approximated by compacting at high rates of travel, but heavy equipment is difficult to operate at high speeds; therefore, lighter equipment with smaller contact areas is better for compacting wetter cohesive soils. If constant contact pressure is used, efficiency will probably be improved by operating at slower speeds with subsequent passes of the roller. Or if more than one roller were used, the use of higher contact pressures on subsequent passes would increase efficiency. [These general observations are supported by numerous reports of actual field compaction (11).] Specific procedures for selecting appropriate contact pressures and

travel speeds do not, however, yet exist.

In real situations it is necessary to consider practical factors other than energy efficiency in the selection of the best equipment and procedures for a given job. Also, in compactor design, the mechanical efficiency in applying the energy to the soil may be more important than the compaction energy required by the soil, but the results of this study suggest that there are opportunities for significant improvements in design.

CONCLUSIONS

Much more information than is available from the literature or from this limited investigation is necessary to provide a thorough understanding of the energy requirements of soil compaction. Nevertheless, some preliminary conclusions about the compaction of cohesive soils appear justified.

1. For all moisture conditions, static compaction is the most efficient.
2. Either impact or kneading compaction may be next most efficient, depending on the details of the procedures used.
3. The optimum moisture content is apparently the lowest at which excessive shear of the soil occurs during compaction.
4. The most important factors controlling the compactive effort required to obtain a specified density with a given cohesive soil at a given moisture content are (a) the magnitude of the compactor-soil contact pressures (the highest contact pressure that does not cause excessive shear is most efficient) and (b) the rate at which the load is applied and the length of time the load is held on the soil (the slower the rate and the longer the load is applied, the higher the efficiency).
5. The data for energy efficiency with respect to the strengths of compacted soils are contradictory. This question needs more study.
6. Much more information is needed, but significant improvements in compaction equipment design could be made that would increase efficiency of operation and yield a compacted soil with better engineering properties. The problem is certainly worthy of additional study.

ACKNOWLEDGMENTS

This paper has been prepared from the results of research on soil compaction funded by the Hyster Company, Portland, Oregon, and conducted in the Department of Civil Engineering at Oregon State University, Corvallis.

REFERENCES

1. T. W. Lambe. The Engineering Behavior of Compacted Clay. Journal of Soil Mechanics and Foundations Division, Proc., ASCE, Paper No. 1655, May 1958.
2. A. W. Johnson and J. R. Sallberg. Factors Influencing Compaction Test Results. HRB, Bulletin 319, 1962.
3. C. L. Dhawan and J. C. Bahri. Stable Density. Proc., 4th International Conference on Soil Mechanics and Foundation Engineering, London, Vol. 1, 1957, p. 149.
4. G. G. Sowers and C. M. Kennedy. Effects of Repeated Load Applications on Soil Compaction Efficiency. HRB, Bulletin 93, 1954, pp. 61-64.
5. R. R. Proctor. Relationship Between the Foot Pounds per Cubic Foot of Compactive Effort to Soil Density and Subsequent Consolidation Under Various Loadings. Proc., 2nd International Conference on Soil Mechanics and Foundation Engineering, Rotterdam, Vol. 5, 1948, p. 223.
6. D. J. Maclean and F. H. P. Williams. Soil Mechanics for Road Engineers. Her Majesty's Stationery Office, London, 1952.
7. H. B. Seed and C. L. Monismith. Relationship Between Density and Stability of Subgrade Soils. HRB, Bulletin 93, 1954, pp. 16-32.
8. J. L. McRae and P. C. Rutledge. Laboratory Kneading of Soil to Simulate Field Compaction. Proc., HRB, Vol. 31, 1952, pp. 593-600.
9. K. S. Sankaran and K. Muthukrishnaiah. Efficiency of Compaction of Soil Structure. Journal of Materials, Vol. 5, No. 4, Dec. 1970, p. 739.
10. H. B. Seed, J. K. Mitchell, and C. K. Chan. The Strength of Compacted Cohesive Soils. In Shear Strength of Cohesive Soils, ASCE, June 1960, p. 877.
11. A. W. Johnson and J. R. Sallberg. Factors that Influence Field Compaction of Soils. HRB, Bulletin 272, 1960.

Publication of this paper sponsored by Committee on Compaction.

Mix Design, Durability, and Strength Requirements for Lime-Stabilized Layers in Airfield Pavements

John J. Allen, Department of Civil Engineering, Engineering Mechanics, and Materials, U.S. Air Force Academy
David D. Currin, Strategic Air Command, U.S. Air Force
Dallas N. Little, Jr., Texas A&M University

Laboratory and field evaluation programs leading to the development of a design process for lime-stabilized airfield pavement layers are described. The entire process can be completed in 3 to 7 d. The design procedure, which includes selection of the optimum percentage of lime, rapid cure,

durability testing, and residual strength requirements, uses common laboratory tests and requires no sophisticated equipment. It is appropriate for expedient and nonexpedient construction situations. Residual-strength curves were constructed from the results of a computer study that used a nonlinear finite-element code capable of simulating multiple wheel-gear loadings.

Mixture design procedures for stabilized pavement layers must consider the type of stabilizing agent, the optimum amount of it, and the strength and durability. The design sequence should be applicable to a wide variety of types of soil and relate to the strength requirements of the structural layer.

The Soil Stabilization Index System (SSIS) (2) was developed for the U.S. Air Force as a basis for a stabilized soil-mix design. It was conceptual in nature and required validation for a wide range of soil types. The SSIS provides various alternatives for the selection of the stabilizer and the determination of the optimum amount.

OBJECTIVES

The overall objective was to validate the SSIS through laboratory testing and field evaluation. Other objectives were

1. To evaluate the pH test proposed by Eades and Grim (12) for estimating the optimum lime content;
2. To verify the correlation between accelerated curing and the normal curing of lime-stabilized soils and ascertain the validity of curing times and temperatures;
3. To evaluate the three-cycle, freeze-thaw strength as an indicator of the field durability in varied environments;
4. To evaluate the strength after vacuum soak as an indicator of the field durability in varied environments; and
5. To correlate the durability and residual strength requirements for stabilized airfield layers.

Ultimately, the purpose was to develop a design process that used simple laboratory tests and equipment and could be applied by military engineers in expedient and nonexpedient situations. The validation methods for lime, cement, and asphalt stabilization and a literature survey of previous research in stabilized mix design have been given by Currin and others (1).

LABORATORY TESTING PROGRAM

Materials

The soils listed in Table 1 were selected as representing a wide range of soil classifications and a variety of soil-forming processes. Many were taken from military bases where stabilized layers have been used.

Eades and Grim pH Test

The analysis of the Eades and Grim pH test (12) was an essential phase in the testing program. Theoretically, the percentage of lime that gives a pH of 12.4 for the lime-soil mixture can be used to obtain the optimum strength conditions.

The percentage of lime obtained by the Eades and Grim test was compared to that obtained by using standard 28-d unconfined compressive-strength tests. For 3 of the soils (Craig, Moody, and Cannon), the inconclusive strength data available prohibited determination of the optimum percentage of lime. The pH test predicted the optimum percentage of lime within 1 percent of that obtained by using strength data for 16 of the soils and within 2 percent for the other 3 soils (Tyler, Coari, and Robbins). Regression analysis showed an excellent correlation between the percentages of lime determined by the two tests.

The majority of the soils investigated in this program could not be considered problem soils as a result of high sulfate or organic concentrations. Although the Tyler soil had high sulfate and organic contents (3.5 and 3.0 percent respectively), no conclusions could be reached about the effects of these on the pH test. The Robbins soil, which had low sulfate and organic contents (0.04 and 0.22 percent respectively), showed similar variations between the pH lime percentage and the strength lime percentage.

These results indicate that the Eades and Grim pH test is acceptable for the determination of an initial percentage of lime to be used in stabilization analysis.

Strength Development Using Rapid Cure

Both curing time and curing temperature affect the strength of soil-lime mixtures (3). Higher than normal temperatures activate the strength-producing pozzolanic reactions, which shortens the curing time required for strength development. Generally, higher temperatures produce higher strength over a given time interval, and the strength gain at a particular temperature initially increases at a rapid rate and gradually decreases with increasing curing time.

Dunlap and Biswas (3) have tried to correlate normal 28-d curing with accelerated curing. They found the curing times given below to be equivalent to a 28-d normal cure for lime-soil mixtures [°C = (°F - 32)/1.8].

Temperature (°C)	Time (h)
40	65
49	30
60	10

They also found that accelerated curing temperatures appeared to produce chemical reaction products similar to those obtained in normally cured specimens.

For this study, the unconfined compressive strengths of lime-soil mixtures molded at the optimum percentage of lime, the optimum moisture content, and the maximum dry density were measured after 28 d of cure at 23°C (73°F) and 100 percent relative humidity. Identical specimens were cured at 49 and 40°C (120 and 105°F) until the 28-d normal cure strength was duplicated.

Although the 60°C (140°F) curing temperature produces chemical reaction products similar to those produced by a normal cure, the 40 and 49°C temperatures are more realistic and conservative. The 49°C curing temperature gave more consistent data than did the 40°C curing temperatures and reduced the curing time appreciably with what seemed to be very little risk of altering the chemical reaction products. Therefore, the 49°C curing temperature was used.

Unconfined compressive strength versus hours of curing at 49°C data were collected. The curing time to produce the equivalent of a 28-d normal cure for all soils tested was determined statistically to be 30 h, although the data varied over a wide range.

The correlation obtained by regression analysis between the rapid and normal cures showed that a 30-h cure at 49°C is a valid substitute for a normal cure and may be used before durability or strength tests. Rapid-cure values are generally slightly conservative.

Freeze-Thaw Test as Durability Indicator

Both exposed-surface and vacuum-flask freeze-thaw tests were used. However, the vacuum-flask method appears to be more realistic and thus is discussed here. The strength loss was determined at 3, 6, and 9 freeze-thaw cycles. A second-order regression curve relating the strength loss to the number of cycles was then plotted for each soil.

The mean of the points on the best fit curves for all of the soils at which the slopes were equal to zero (i.e., zero strength loss with increasing number of cycles) is 6.74 cycles. There is remarkably little scatter about the mean dy/dx = 0 value for the various soils. The data show that after approximately 7 cycles of freeze thaw, there is no further significant reduction in strength.

A family of second-order curves of the general equation of $y = ax + bx^2$ was developed on the basis of the shape of the actual data curves. These curves represent the freeze-thaw behavior of lime-soil mixtures that are within 2 percent of the optimum percentage of lime as the difference between their 28-d strength and their strength after a certain number of freeze-thaw cycles. Figure 1 was developed from the family of design curves and shows the strength loss over the range of 3 to 7 cycles.

On the basis of these data, the freeze-thaw strength loss can be predicted from knowledge of the 28-d normal cure strength of a lime-soil mixture and the 3-cycle freeze-thaw strength. The following example is illustrative: unconfined compressive strength (q_u) after 28-d cure = 1448 kPa (210 lbf/in^2) at 23°C (73°F) and 100 percent relative humidity, and q_u after 3 freeze-thaw cycles = 827 kPa (120 lbf/in^2). Therefore the strength loss is 621 kPa (90 lbf/in^2). If Figure 1 is entered with a 621-kPa (90-lbf/in^2) freeze-thaw strength loss at 3 cycles and projected to 7 cycles, a freeze-thaw strength loss of 880 kPa (127 lbf/in^2) is predicted. The 28-d q_u minus the 7-cycle freeze-thaw strength loss = residual strength = 568 kPa (83 lbf/in^2).

Table 1. Soils tested.

Soil	AASHO Classification	Unified Classification
Dyess, Texas	A-7-6(12)	CL
Altus, Okla. (subgrade)	A-7-6(12)	CL
Tyler, Texas	A-7-5(15)	OH
Houma, La.	A-7-6(20)	CH
Perrin A, Texas	A-7-6(20)	CH
Perrin B, Texas	A-7-6(20)	CH
Perrin AB, Texas	A-7-6(20)	CH
Bergstrom, Texas	A-6(7)	CL
Kelly, Texas	A-7-5	CL
Carswell, Texas	A-7-6(20)	CH
Tinker, Okla.	A-6	CL
Ellington, Texas	A-7-6(20)	CH
Barksdale, La.	A-2-4	CL-ML
Ellsworth, S.D.	A-2-7	SW-SC
Craig, Ala.		CH
Moody, Ga.	A-2-5	SM
Robbins, Ga.	A-2-4	ML
LeMoore, Calif.	A-7-6(16)	CH
Malmstrom, Mont.	A-6	CL
Cannon, N.M.	A-1-b	SM
Estirado, Equador-Brazil	A-7-5(8)	CL
LaBrea, Brazil	A-7-5(14)	CH
Coari, Brazil	A-7-5(4)	CL
Eirunepe, Brazil	A-7-5(1)	CL

Immersed Strength as Durability Indicator

Another objective was to substantiate whether or not immersion testing, particularly vacuum saturation, can be used as an alternative to freeze-thaw testing.

The vacuum immersion test may be conducted after a normal 28-d cure at 23°C (73°F) or a rapid cure of 30 h at 49°C (120°F). If a rapid cure is used, a 2-h equilibrium period is required to permit the stabilized mixture to cool. The specimens must be sealed during this period to prevent moisture loss.

To remove air from the voids, the specimens are placed in an upright position within the vacuum vessel and the chamber evacuated to 81.6 kPa (24 in of mercury) for 30 min. The specimens are placed on a perforated plexiglass plate so that all surfaces will be equally exposed to the chamber environment. After the 30-min period, the vacuum vessel is flooded with water to a depth sufficient to cover the soil specimens. The vacuum is removed, and the specimens are soaked for 1 h at atmospheric pressure.

At the end of the soak period, the specimens are removed from the water and allowed to drain for approxi-

Figure 1. Design chart.

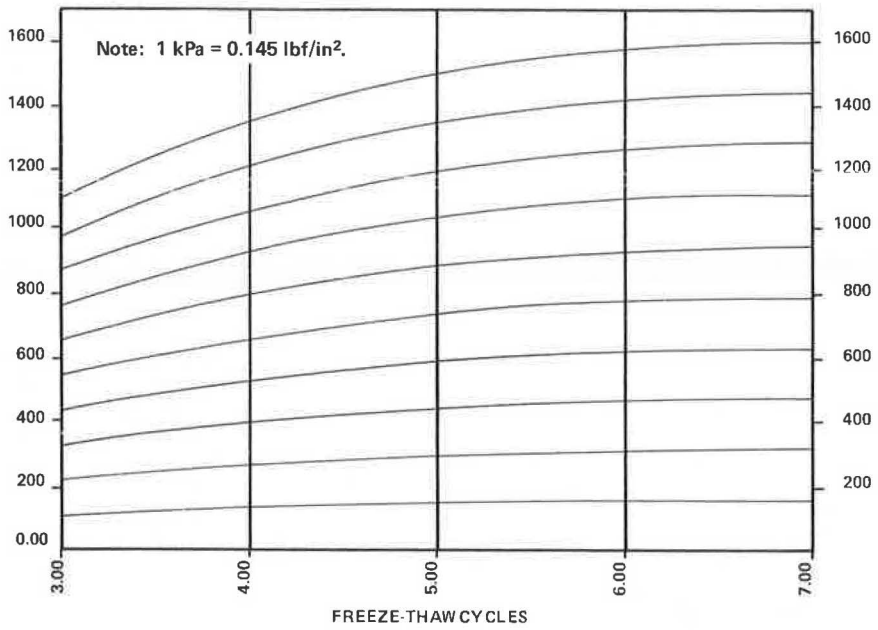

mately 2 min on a nonabsorptive surface. After the free surface water is drained away, the specimens are immediately tested for unconfined compressive strength. The entire immersion or saturation procedure can be carried out in less than 4 h after the rapid cure.

The strength after vacuum saturation was compared to the strength after 3 cycles of freeze-thaw testing. Preliminary regression analysis showed that there was a distinct change in slope of the regression line at a vacuum-saturation strength of 945 kPa (137 lbf/in^2) [a 3-cycle freeze-thaw strength of 345 kPa (50 lbf/in^2)]. On the basis of this, separate regression lines were constructed for vacuum-saturation strengths between 0 and 945 kPa (segment 1) and for vacuum-saturation strengths between 945 and 3792 kPa (550 lbf/in^2) (segment 2). The correlation coefficients of segments 1 and 2 are 0.82 and 0.79 respectively.

Figure 2 shows the design chart. From the vacuum-saturation strength, by using the proper segment of the design curve, the 3-cycle freeze-thaw strength is obtained. This value is then used with Figure 1 to determine the 7-cycle freeze-thaw strength loss.

Long-term (21-d) immersion as well as short-term (8-d) immersion were considered as alternatives to the vacuum-saturation test. However, 21-d immersion was not considered to be a suitable alternative because of the length of the test and the probability of unconservative results because of hydration while the specimens are submerged. Limited data on 8-d immersion showed that this test may possibly be used as an alternative to vacuum immersion or 3-cycle freeze-thaw, but no conclusive statement can be made yet. The vacuum-saturation test seems to be the most acceptable alternative to freeze-thaw durability testing because it is expedient and requires no sophisticated equipment.

RESIDUAL-STRENGTH REQUIREMENTS FOR AIRFIELD PAVEMENTS

Analysis of the stresses and strains in pavements subjected to moving wheel loads can be correlated with the performance of those pavements (4, 5, 13). Full-scale tests conducted at the Waterways Experiment Station indicate that, despite the present limitations in computational techniques and materials characterization, it is possible to predict the performance of a pavement from the results of computer analyses (5). Such procedures hold promise for the development of rational design schemes.

Indicators of Pavement Performance

Five factors that are indicative of the response of a pavement to moving loads were studied. The surface deflection and tensile strain in asphalt concrete can be correlated with the fatigue cracking of asphalt surface courses. In addition, the vertical stress and strain within the subgrade can be correlated with subgrade rutting, which can ultimately relate to distress of the pavement surface. Limiting values of the vertical subgrade strain are the basis for the design procedure for flexible pavements developed by the Koninklijke-Shell Laboratorium in Amsterdam (6).

Because stabilized layers in most pavement sections act in flexure, it was necessary to investigate the tensile stresses in such layers. Flexural cracking in stabilized layers leads to loss of strength and increased stresses applied to the subgrade.

A nonlinear, finite-element analysis technique (AFPRE-AFPAV) capable of simulating multiple wheel loadings was used.

To correlate the performance of pavement sections with the calculated indicators, it was necessary to devise a method of quantitatively assessing the present condition of the section. Accordingly, a rating form was devised that considered the major types of distress mechanisms that could be linked to the structural adequacy of the pavement (1, 7, 8). Each distress category was measured at a particular section, and the summation was used to determine the relative condition of the section. Those sections with higher numerical ratings were considered to be in poorer condition than those with lower ratings.

The test sections were selected from Air Force and Navy bases having stabilized and nonstabilized pavement sections that had been subjected to approximately the same traffic loadings. Information about their construction histories, layer thicknesses, and material properties

Figure 2. Design chart: 3-cycle freeze-thaw strength from vacuum-immersion strength.

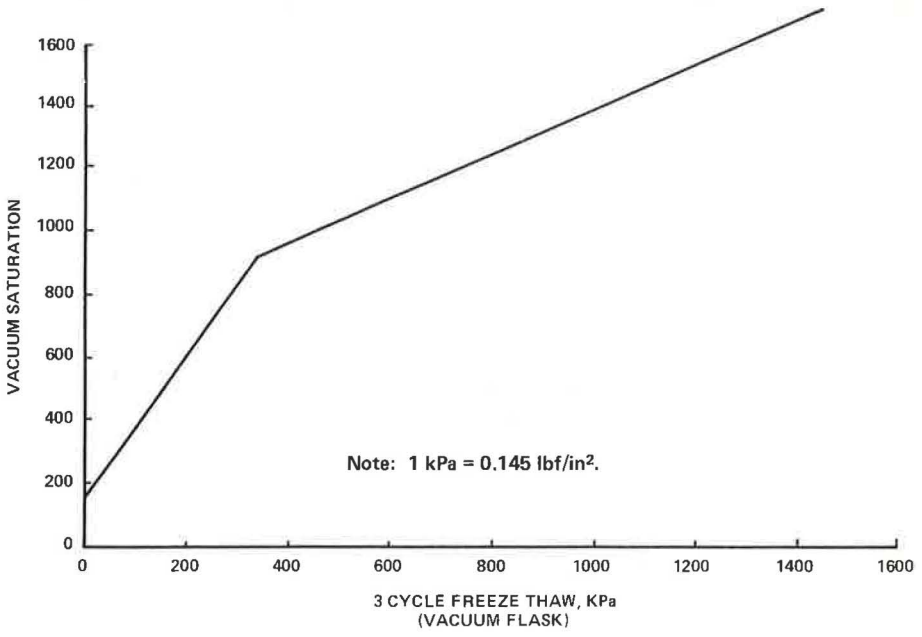

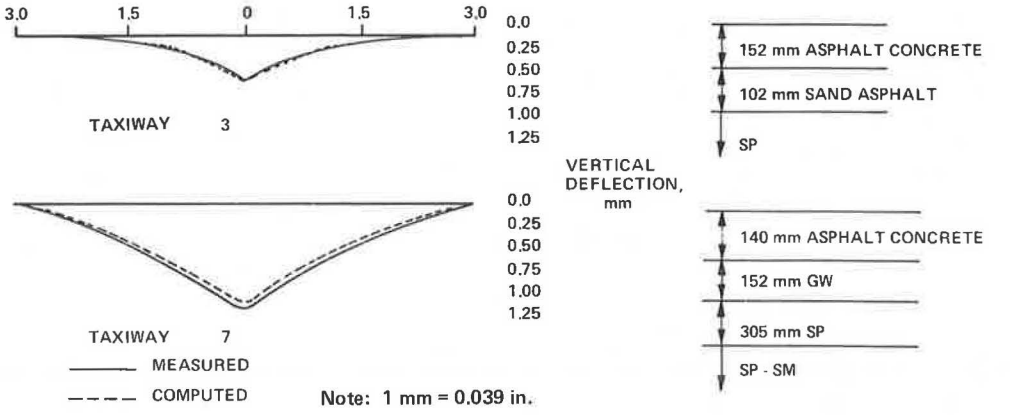

Figure 3. Deflection basins at Seymour Johnson Air Force Base.

Table 2. Computed responses.

Section	Max Deflection (mm)	Max Subgrade Stress (kPa)	Max Tensile Strain in Surface Course (mm/mm)	Max Tensile Strain in Stabilized Layer (mm/mm)
Taxiway 3	0.86	90	0.000 240	0.000 542
Taxiway 7	1.65	56	0.000 697	—

Note: 1 mm = 0.039 in; 1 kPa = 0.145 lbf/in^2; 1 mm/mm = 1 in/in.

was taken from the Airfield Pavement Evaluation and Condition Survey Reports published by the Corps of Engineers and the Air Force Civil Engineering Center.

The evaluation procedure consisted of the following steps:

1. The test sections were selected from the survey reports,
2. The present conditions of the sections were evaluated by using the rating forms,
3. The deflections under aircraft loadings were obtained by using a precise level capable of measuring vertical motions to 2.5 μm (0.0001 in), which was sighted on a target placed along the outer edge of the wheel path of the main gear as the aircraft was towed along the predetermined path, and
4. The pavement sections from selected bases were analyzed by using the AFPRE-AFPAV code. Measured and computed deflection basins were matched, and calculated indicators of pavement performance were compared.

Pavement sections at five airfields—Reese, Cannon, Kelly, and Seymour Johnson Air Force bases, and Point Mugu Naval Air Station—were evaluated.

Seymour Johnson Air Force Base

Although lime-stabilization had not been used at this base, the data are illustrated and show the effectiveness of computer structural analysis of pavement sections.

Taxiways 3 and 7 were evaluated. The nonstabilized section (taxiway 7) had extensive transverse and longitudinal cracking, intermittent rutting, and some alligator (fatigue) cracking. It received a rating of nine. The stabilized section (taxiway 3) had only isolated rutting and cracking and received a rating of three. The deflections were obtained under an F-4 aircraft [gross weight = 114 Mg (52 000 lb) and tire pressure = 1724 kPa (250 lbf/in^2)]. The deflections were measured and computed along a line offset 25.4 cm (10 in) from the center of the tire.

Figure 3 shows the measured and computed deflection basins for the two sections. Table 2 summarizes the computed responses of the two sections.

The significantly smaller deflections and strains in taxiway 3 account for its better surface condition as opposed to that of taxiway 7. The high subgrade stress calculated for taxiway 3 may account for the isolated rutting observed. The higher subgrade stress for this section compared to that of taxiway 7 can be attributed to the much smaller thickness of pavement.

The field performance evaluation showed the accuracy with which a powerful analytical tool such as the AFPRE-AFPAV code can be used in computing deflection basins.

Development of Residual-Strength Curves

The strength requirements for highway pavements and their associated loadings derived by linear analytical techniques have been given by Dempsey and Thompson (9). Because airfield pavement thicknesses and wheel loadings are significantly different from those of highways, it was necessary to determine the strength requirements for airfield pavement sections. Furthermore, because high-quality stabilized layers have greater stiffness than do underlying natural materials, they act in a flexural mode. The limiting value of strength for these layers to be investigated is the flexural strength.

The AFPRE-AFPAV nonlinear computer codes were used to account for the nonlinear stress and strain relations of paving materials, particularly natural subgrades and unbound granular layers.

The objective of this phase of the investigation was to determine the flexural strength required of stabilized pavement layers. These values were correlated with the unconfined compressive strengths (q_u) that would be required in the pavement after the first freeze-thaw season. The procedures described above were then used to determine the required q_u before freeze thaw on the basis of the anticipated number of freeze-thaw cycles.

Analysis Procedure: Lime-Stabilized Layers

Typical flexible and rigid pavements were analyzed for aircraft loading in the three design categories described in the Air Force Manual. The F-4E aircraft was used for the light-load category because it has the highest gear load in that category. The C-141 was used for the medium-load category, and the B-52 was used for the heavy-load category. Flexible pavements were not analyzed in the heavy-load category, nor were rigid pavements analyzed for the light-load category. A wide range

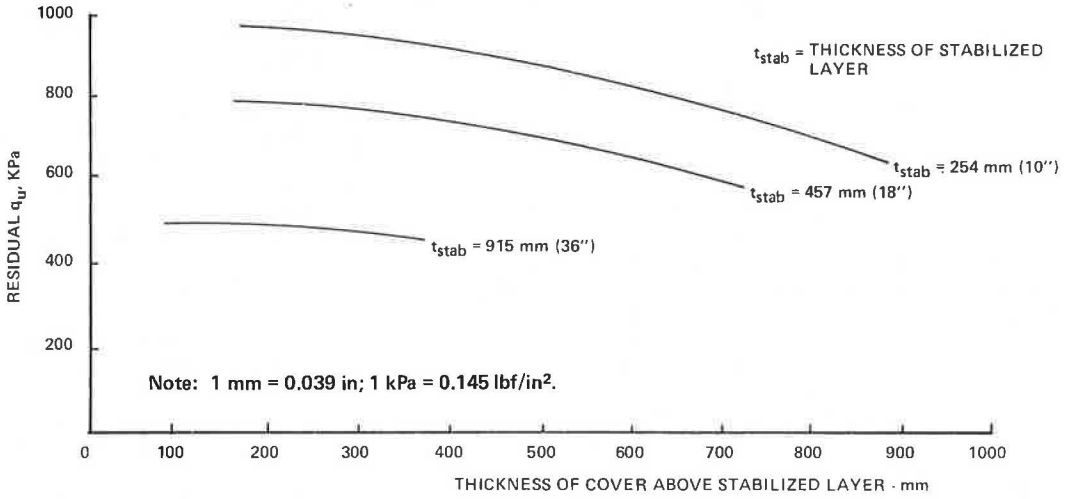

Figure 4. Residual-strength requirements for lime-stabilized layers in airfield pavements (flexible pavements: light-load design).

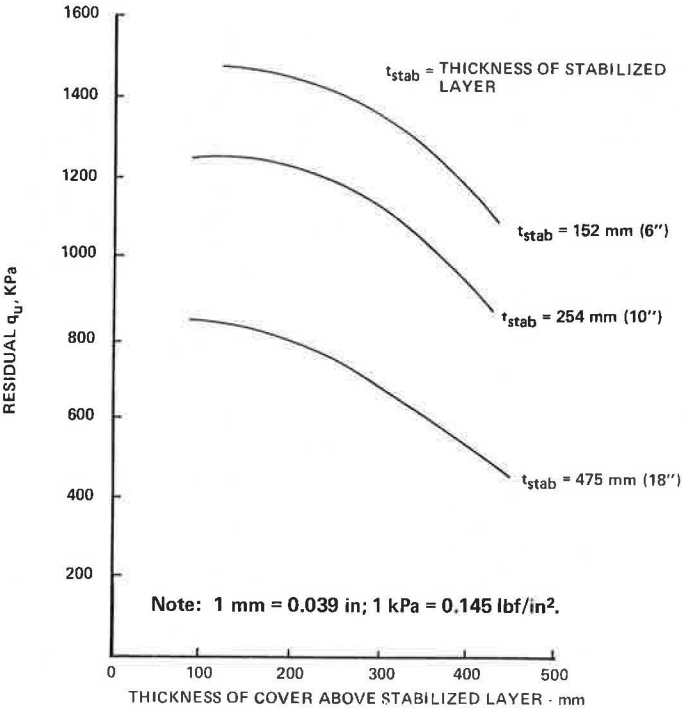

Figure 5. Residual-strength requirements for lime-stabilized layers in airfield pavements (flexible pavements: medium-load design).

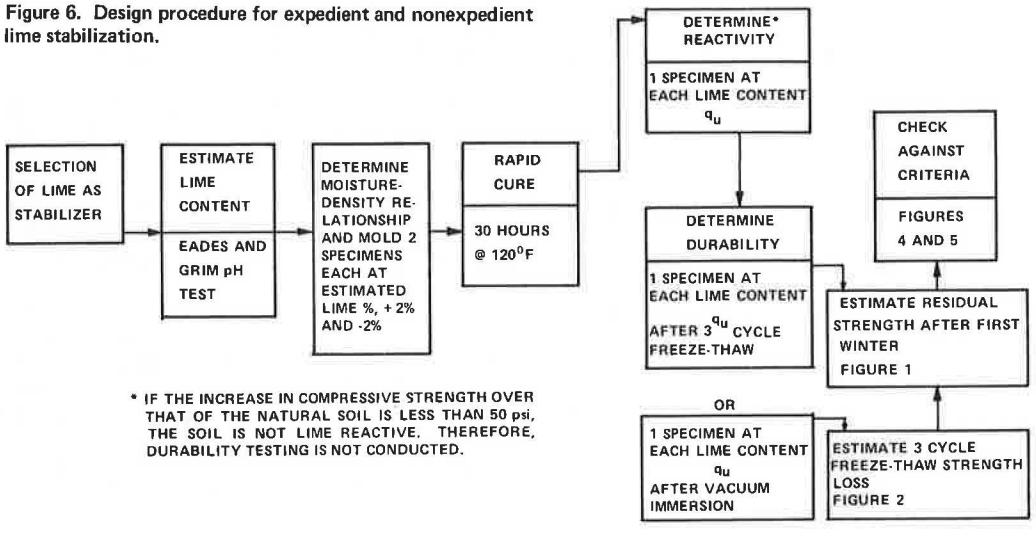

Figure 6. Design procedure for expedient and nonexpedient lime stabilization.

of subgrade types, pavement thicknesses, and stabilized-layer properties were investigated. The aircraft landing-gear configurations and wheel loads cover the range with which the military engineer is involved. The majority of civilian jetliners have similar characteristics.

Residual Strength

It is usually assumed that the most critical period in the life of a pavement containing stabilized layers occurs immediately after the first freeze-thaw period. This is the point at which natural subgrades may be least stable because of high moisture contents and stabilized layers will have suffered the deteriorating influence of the winter freeze-thaw cycles. However, Thompson and Dempsey (10) have shown that stabilized materials will continue to gain strength with increased curing time after the first winter and that the freeze-thaw damage occurring in subsequent winters is not cumulative. Therefore, the flexural strength required after the first freeze-thaw season may be regarded as the minimum necessary for satisfactory pavement performance. The flexural strength was converted to the unconfined compressive strength by using the relation flexural strength = $0.25q_u$. The values of q_u thus obtained represent the minimum required values of unconfined compressive strength (residual strength) that the stabilized materials must exhibit in the field immediately after the first freeze-thaw season.

Results: Flexible Pavements

Figures 4 and 5 show the residual-strength requirements for lime-stabilized layers for flexible airfield pavements. The design procedure using these figures should include the following steps:

1. Use the standard California-bearing-ratio design procedures to determine the required pavement thickness,
2. Select the individual layer thicknesses,
3. Enter the appropriate figure (design category and type of stabilizer) with the thickness of cover (thickness of material above the top of the stabilized layer) and read the required residual strength from the appropriate curve,
4. Use the procedures discussed above to determine the strength loss for the number of freeze-thaw cycles anticipated for the first season, and
5. Add the anticipated strength loss to the residual strength.

This value represents the q_u required in the field after construction and initial curing and before the first freeze-thaw season.

Results: Rigid Pavements

Because of the thickness and high modulus of concrete surface courses, the calculated flexural strengths varied over a small range [<69 kPa (10 lbf/in^2)]. Therefore, it is recommended that residual strength values of 410 to 550 kPa (60 to 80 lbf/in^2) be required for stabilized bases for rigid airfield pavements. These values are higher than would be indicated by the relation that flexural strength = $0.25q_u$. However, lower strength mixes have lower values of flexural modulus, which would allow larger strains and possibly more severe cracking in the stabilized layer.

The preceding discussion has been concerned with pavement response to repeated dynamic wheel loadings; i.e., flexural fatigue was the main consideration. However, stabilized pavement sections develop ultimate strengths far in excess of the stresses that lead to initial cracking. For situations where low traffic volumes are anticipated, e.g., the expedient construction case, the required strengths of the stabilized layers may be significantly overestimated by the use of Figures 4 and 5. The data given by Suddath and Thompson (11) indicate that ultimate strengths may be at least two to three times as large as those predicted by Meyerhof's ultimate-load theory. Clearly, for these situations, the designer is justified in accepting lower strengths than those indicated by Figures 4 and 5.

DESIGN SEQUENCE

The design procedure shown in Figure 6 was developed on the basis of the laboratory data and computer analysis. Selection of the stabilizing agent is determined by the grain-size distribution and the plasticity and is discussed by Currin and others (1).

The entire design process can be accomplished in approximately 1 week. If vacuum saturation is substituted for freeze-thaw testing, the time involved is shortened to 3 or 4 d.

CONCLUSIONS

The design process described here uses common laboratory tests and requires no sophisticated equipment. It can be accomplished in a short time and is appropriate for use by engineers untrained in stabilization technology. The adequacy of a proposed mix is ultimately determined by comparing its strength after durability testing with the required residual strength in the field. This process has been validated for a wide range of soil types.

ACKNOWLEDGMENT

The computer code was developed by John Crawford at the Naval Civil Engineering Laboratory at Port Hueneme, California, and was obtained from the Air Force Weapons Laboratory at Kirtland Air Force Base, New Mexico.

REFERENCES

1. D. D. Currin, J. J. Allen, and D. N. Little. Validation of Soil-Stabilization Index System With Manual Development. Frank J. Seiler Research Laboratory, U.S. Air Force Academy, Colorado Springs, Technical Rept. FJSRL-TR-76-0006, 1976.
2. J. A. Epps, W. A. Dunlap, and B. M. Gallaway. Basis for the Development of a Soil-Stabilization Index System. Air Force Weapons Laboratory, Kirtland Air Force Base, N.M., Technical Rept. No. AFWL-TR-70-176, 1971.
3. W. A. Dunlap and B. R. Biswas. Accelerated Laboratory Curing of Lime Stabilized Soils. Air Force Weapons Laboratory, Kirtland Air Force Base, N.M., 1974.
4. H. B. Seed, F. G. Mitry, C. L. Monismith, and C. K. Chan. Prediction of Flexible-Pavement Deflections From Laboratory Repeated Load Tests. NCHRP, Rept. 35, 1967.
5. W. R. Barker, W. N. Brabston, and F. C. Townsend. An Investigation of the Structural Properties of Stabilized Layers in Flexible Pavement Systems. Air Force Weapons Laboratory, Kirtland Air Force Base, N.M., Technical Rept. No. AFWL-TR-73-21, 1973.
6. G. M. Dorman and C. T. Metcalf. Design Curves for Flexible Pavements Based on Layered System Theory. HRB, Highway Research Record 71, 1965, pp. 69-84.

7. G. Y. Sebastyan. Discussion of Airfield Evaluation Procedures by Phillip P. Brown. Journal of the Aerospace Transport Division, Proc., ASCE, April 1965.
8. R. V. LeClerc and T. R. Marshall. Washington Pavement Rating System: Procedures and Applications. HRB, Special Rept. 116, 1971, pp. 112-121.
9. B. J. Dempsey and M. R. Thompson. Durability Properties of Lime-Soil Mixtures. HRB, Highway Research Record 235, 1968, pp. 61-75.
10. M. R. Thompson and B. J. Dempsey. Final Report on Durability Testing of Stabilized Materials. Civil Engineering Studies, Transportation Engineering, Univ. of Illinois, Urbana, Series No. 11, June 1974.
11. L. P. Suddath and M. R. Thompson. Load-Deflection Behavior of Lime-Stabilized Layers. U.S. Army Construction Engineering Research Laboratory, Champaign, Ill., Technical Rept. M-118, 1975.
12. J. L. Eades and R. E. Grim. Quick Test to Determine Lime Requirements for Lime Stabilization. HRB, Highway Research Record 139, 1966, pp. 61-72.
13. J. P. Nielsen and G. T. Baird. Nondestructive Pavement Load Rating. Proc., Symposium on Nondestructive Test and Evaluation of Airport Pavements. U.S. Army Waterway Experiment Station, Corps of Engineers, Vicksburg, Miss., May 1976.

Publication of this paper sponsored by Committee on Lime and Lime-Fly Ash Stabilization.

Frost Action in Cement-Stabilized Colliery Shale

R. J. Kettle, Department of Civil Engineering, University of Aston in Birmingham, England
R. I. T. Williams, Department of Civil Engineering, University of Surrey, England

This paper describes a laboratory investigation of frost action in cement-stabilized colliery shales in which their performance is evaluated in terms of the heave developed during prolonged freezing. Tests of nine unburnt and four burnt shales showed that the addition of cement reduced heave, except in the case of some fine-grained unburnt shales. These results are discussed in relation to the effect of cement on pore size, on permeability, and on strength. Of the strength tests undertaken, only the direct tensile test provided data that could be related to the behavior observed during a freezing test. Significant heave occurred only when the heaving pressure generated at the freezing front was greater than the tensile strength. It is concluded that freezing behavior is consistent with an energy balance between the work done in heaving and the energy liberated by supercooled freezing.

In recent years, there has been increasing interest in the use in road construction of nontraditional materials, such as industrial waste. A major source of such material in Great Britain is in the colliery tips that are probably the greatest single cause of dereliction of industrial land, so that their removal is also desirable in environmental terms. The material in these tips is the residue after coal has been removed in the washery and is generally referred to as colliery shale. It is customary to further describe the material as either unburnt or burnt because burning occurs in some tips under certain conditions. Broadly, burning converts the clay-like shale into a brick-like material having greatly changed properties.

Selected burnt shale has been used extensively in highway construction in Great Britain for many years as fill and as subbase material, but unburnt shale has been used significantly only during the past 8 years, following the issue of technical memoranda (1, 2) by the Department of the Environment that allow its use as common fill. However, because of its clay-like nature, it is unlikely that unburnt shale in its natural state will be suitable for use in pavement structures; the work reported in this paper is part of an investigation that examined its value when stabilized with cement. A preliminary study (3) showed that some unburnt shales could produce an acceptable soil-cement in terms of the strength criteria imposed in practice (4), and this prompted an extension of the work to the effect of frost action on materials of this type (5).

OVERALL APPROACH

The aim of the investigation was to test colliery shales in their natural state and when stabilized with cement to identify the characteristics that influence their behavior when subjected to prolonged freezing. Because the principal interest was in the effect of cement treatment, the emphasis was on the measurement of tensile strength as specimen fracture appears to be an essential prerequisite for the growth of substantial ice lenses. Samples of nine unburnt and four burnt shales were studied to compare the behavior of the two types of shale and to evaluate their response to cement treatment.

The behavior of test specimens subjected to frost action was evaluated by the heave that occurred and by the pressure generated when the heave was restrained. Permeability tests were made to obtain data on the water-transport potential of the various materials.

Preparation of Test Specimens

Cylindrical specimens, 152.4 mm high by 101.6 mm in diameter, were produced in constant-volume molds by using static compaction (6). To permit comparison among the results, the cement-stabilized specimens were made at the same moisture content as the unbound specimens [the optimum value determined on the unbound shale by using the 2.5-kg hammer in the British standard compaction test (7)]. The dry densities were adjusted so that the total air voids were the same for both the unbound and the cement-stabilized specimens of each shale.

The stabilized specimens were wax-coated immediately after extrusion from the mold and cured at 20 ± 2°C for the period between preparation and the test procedures.

Tests Undertaken

Frost-Heave Test

The Transport and Road Research Laboratory test (6) was used to measure the frost susceptibility and was performed either in a cold room or in a modified deep-freeze cabinet, as reported in detail elsewhere (8). The procedure involved positioning the specimens with their lower surfaces just in contact with water at room temperature and their upper surfaces unsealed. In this position, they were allowed to take up water by capillary flow for 24 h. They were then subjected to an air temperature of -17°C above their upper face with lateral insulation provided by a hardboard disc, so that the freezing front penetrated from the top to simulate field conditions. A heating system maintained the water-bath temperature at 4°C, so that water is available to support ice growth for the 250-h test period. The change in length of the specimens was monitored daily; the total increase in length during freezing is known as the frost heave. Standards based on experience in the severe winters of 1940 and 1947 in Great Britain classify materials heaving less than 13 mm as satisfactory, materials heaving 13 to 18 mm as marginally frost susceptible, and those heaving more than 18 mm as very frost susceptible.

The results given in Table 1 are of particular interest in relation to the suggestion (9) that the addition of 5 percent cement overcomes the frost susceptibility of burnt shale. Two of the four burnt shales remained marginally frost susceptible when stabilized with 5 percent cement and, of the nine unburnt shales tested, the addition of 5 percent cement increased rather than decreased the heave in two instances and had a negligible effect in another. Typical relationships for materials that respond satisfactorily to cement treatment and for materi als that do not so respond are shown in Figure 1. The critical factor, especially for the unburnt shales, appears to be the amount of material finer than 75 μm in the raw shale: This is consistent with the known effect (10) of fine particles on the freezing behavior of engineering soils. This is especially evident in Figure 2, which shows that adding 5 percent cement will reduce heave if the amount of fine material is less than about 30 percent. This provides a tentative basis for predicting the effect of cement on the heaving characteristics of shales.

Restrained-Heave Test

The experimental method adopted (11) was similar to

Table 1. Frost heave, restrained heave, and permeability tests.

Sample					
Location	Amount Finer Than 75 μm (%)	Cement Content (%)	Average Heave (mm)	Heaving Pressure (MN/m^2)	Coefficient of Permeability (nm/s)
Unburnt shale					
Snowdown	3	0	4.1	0.09	1 100
		5	0.0	–	–
		10	-0.7	–	–
Chislet sample A	5	0	9.5	–	43
		5	3.0	–	–
		10	2.0	–	–
		15	-1.0	–	–
Betteshanger	6	0	5.0	0.20	49
		5	1.0	0.21	–
		10	-1.0	0.20	–
		15	-1.1	–	–
Chislet sample B	10	0	10.7	0.21	22
		5	1.0	0.19	16
		10	0.0	–	29
		15	-1.0	–	60
Tilmanstone	19	0	50.8	0.59	5.6
		5	16.5	0.48	24
		10	6.2	0.43	–
Bedlay	21	0	7.9	0.36	8.1
		5	2.5	–	1.2
		10	0.9	–	3.6
Rothwell	31	0	12.7	0.50	1.6
		5	12.4	–	–
		10	4.3	–	–
Peckfield	38	0	6.4	0.60	0.34
		2.5	14.1	–	3.9
		5	11.5	0.48	35
		7.5	9.6	–	31
		10	7.2	0.44	39
		15	4.4	–	15
		20	3.6	–	4.1
Bullcroft	43	0	7.3	0.79	0.74
		5	21.8	–	45
		10	8.1	–	88
Burnt shale					
Newdigate	6	0	16.0	–	70
		5	5.5	–	–
		10	2.4	–	–
Thornley	9	0	30.9	0.26	380
		5	8.0	–	–
		10	-1.0	–	–
Tilmanstone	11	0	42.5	0.36	19 000
		5	16.4	0.36	–
		10	2.5	0.40	–
Wheatley Hill	13	0	27.5	–	170
		5	14.1	–	210
		10	5.1	–	150

that used by Hoekstra, Chamberlain, and Frate (12). In this method, the specimen remains within the compaction mold for the 24-h water-uptake period and also during the subsequent freezing procedure. Unidirectional freezing is achieved by placing a thermoelectric device on the top of the specimen and is restrained by the heaving tendency of a steel reaction frame. The restraining force is monitored electrically. The heaving pressure is defined as the value at which the rate of increase is less than 0.001 $MN/m^2/h$ (Table 1).

Permeability

The movement of water to the freezing front generally takes place under conditions of unsaturated flow (13), although the soil immediately below the ice will become saturated if water is available (14). Thus, while the results of saturated permeability tests may not be directly applicable to frost action, they offer a convenient basis for examining the effects of cement stabilization and were therefore undertaken by using an experimental technique based on that of Bjerrum and Hoder (15).

The results given in Table 1 showed that cement treatment increased the coefficient of permeability so that for tests begun after 7-d curing, reduced heave after cement stabilization cannot be attributed to the anticipated reduction in permeability as the pores become filled with the hydration products.

Strength

Values of compressive strength have been reported in many papers dealing with cement-stabilized materials and provide a basis for comparison with the work of others and with the current performance requirements for soil cement. Care should be exercised, however, in interpreting the results obtained in this investigation because the test specimens had a height to diameter ratio of 1.5:1 rather than the more usual value of 2:1 and because the specimens were produced at moisture content and dry density values based on the British standard compaction test, which probably led to a compactive state inferior to that associated with current practice.

The tensile strength was considered to be especially important: Uniaxial tests were made because they allow the properties to be determined without the assumption of elastic behavior under load. However, the test specimens must be held in such a way that the failure load is not significantly influenced by local stress concentrations or by eccentricity. Ultimately, a glued end-plate system based on the work of Hughes and Chapman (16) was used in which the glue could be applied to a damp surface. The system worked well, with the failure locations being well distributed throughout the length of the specimens and with very few end failures (5). The success is attributed partly to the inherent tendency of the end zones of specimens produced in constant-volume molds to be marginally more dense and partly to the fact that the modulus of elasticity and Poisson's ratio for the glue and the stabilized shale were sufficiently close so that the differential lateral strains were not excessive.

The cylinder-splitting test was included in the work, despite of its known limitations (17) as a measure of tensile strength, because the program formulated included measuring the strength after the pretest soaking period, and this was not possible with glued end plates. The splitting test, through its simplicity, allowed this to be done and at least provided a broad indication of the relative behaviors of the materials examined.

Table 2 includes the results of estimating the 8-d direct tensile strength by evaluating the effect of the 24-h pretest soaking on the indirect tensile strength and multiplying the ratio so determined by the 7-d direct tensile-strength values. This defines the strength at the beginning of the freezing treatment and effectively throughout the test because additional hydration during the 250-h freezing period will probably be limited by the low temperature.

Table 2 shows that the cylinder-splitting strength is always greater than the direct tensile strength, the ratio varying between fairly wide limits but being typically 1.7:1. The direct tensile strength for a given cement content also varies with the source of the shale, and there is a trend for the shales having larger amounts of material finer than 75 μm to have lower strengths. Table 2 also shows that the 24-h soaking leads to an increase in strength in some materials but produces a severe loss in strength with others, with the largest reductions occurring with the shales containing a large proportion of material finer than 75 μm.

INTERPRETATION OF TEST RESULTS

Correlation of Tensile Strength and Frost Heave

Typical relationships (5) among heave, estimated 8-d direct tensile strength, and heaving pressure are shown in Figure 3 for two shales. These show that no positive heave occurs when the direct tensile strength of the stabilized material exceeds the heaving pressure and support the hypothesis that significant heave occurs only when the specimen has fractured, which confirms the results based on cylinder-splitting tests of Sutherland and Gaskin (18).

Effect of Frost Heave on Residual Strength

If the frost susceptibility of cement-stabilized materials is evaluated by using heave criteria established for soils (6, 19), it is necessary to consider the changes that accompany only a small amount of heave. The initial cooling of the specimen produces a thermal contraction of approximately 1 mm and, because heave is measured from a datum defined by the height of the specimen before exposure to freezing, the total heave is this movement plus that to overcome the thermal contraction. Measurements taken throughout the test period are plotted in Figure 4 for a selection of cement-stabilized materials that display significantly different behavior patterns.

To measure the disruptive effects of heave, strength tests were performed on the specimens after completion of the heave test. On removal from the heave equipment, the specimens were placed in polythene bags and stored at 20°C for 3 d, and end caps were glued to those intended for the direct tension test. The results of testing at an age of 22 d are given in Table 3.

The results of the direct tension test show that many specimens suffered a substantial (often total) loss of strength in one direction as a result of the freezing test. The amounts of positive movement, which indicate the severity of damage, are plotted in Figure 5. In contrast, neither the compression test nor the cylinder-splitting test discriminate in this decisive way because the direction of fracture during frost heaving is unlikely to greatly influence the failure load either in compression or in cylinder splitting unless there is a general breakdown of the material.

Effect of Existing Damage

Cement-stabilized materials may contain discontinuities

arising from the presence of a plane of weakness caused during compaction or by an earlier exposure to frost. The effects of prefracture were therefore examined by freezing cement-stabilized shale specimens that had a plane of zero tensile strength formed by sawing at the expected equilibrium location of the zero isotherm. The results given in the following table show that the sawed specimens heaved more than the full specimens, but less than the unbound material: Unrestricted ice growth occurs at the discontinuity in the sawed specimens while lensing above this point is still restricted by the cementing action [Sutherland and Gaskin (18) found similar results with cement-stabilized pulverized fuel ash].

Sample	Cement Content (%)	Average Heave (mm) Full	Sawed	Unbound
Unburnt shale				
Chislet sample B	5	1.0	5.6	10.7
Snowdown	5	0.0	2.3	4.1
Tilmanstone	10	6.2	13.6	50.8

The effect of successive severe winters was simulated by subjecting some of the cement-stabilized specimens to two frost-heave tests with thawing for 7 d at room temperature between the two tests. The values given in the following table show that once the material has fractured, subsequent freezing leads to increased heave, which confirms the results obtained with the sawed specimens.

Figure 1. Relationship between heave and cement content for two unburnt shales showing notably different responses to cement stabilization.

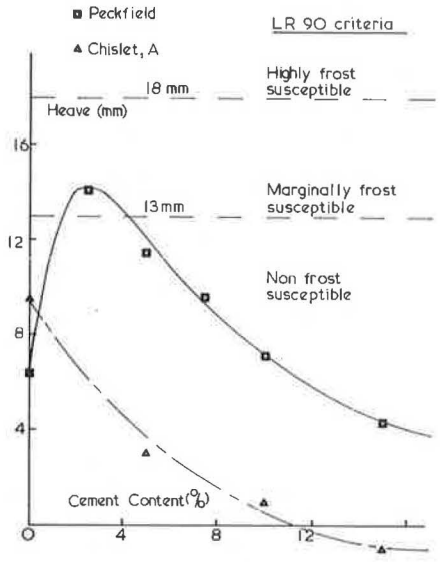

Figure 2. Relationship between heave ratio and amount of fine material in unbound shale.

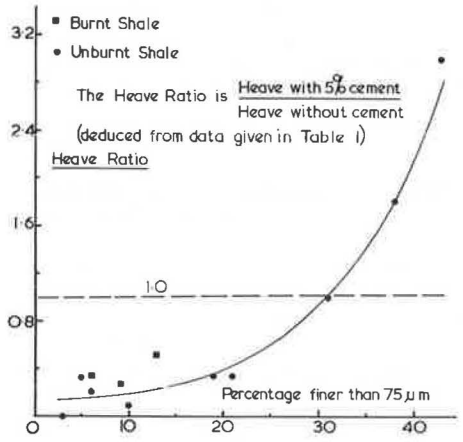

Table 2. Strength tests.

Sample	Cement Content (%)	7-d Compressive Strength (MN/m^2)	Tensile Strength (MN/m^2) Indirect 7-d (A)	Indirect 8-d (B)	Indirect Ratio [C = (B/A)]	Direct 7-d (D)	Estimated Direct 8-d (C × D)
Unburnt shale							
Snowdown	5	1.61	0.19	0.15	0.79	0.13	0.10
	10	2.91	0.38	0.36	0.95	0.20	0.19
Betteshanger	5	1.71	0.22	0.22	1.00	0.16	0.16
	10	3.38	0.44	0.45	1.02	0.30	0.31
	15	4.93	0.62	0.66	1.06	0.39	0.39
Chislet sample B	5	2.29	0.33	0.30	0.91	0.17	0.15
	10	4.11	0.58	0.56	0.97	0.27	0.26
	15	5.65	0.83	0.86	1.04	0.33	0.34
Tilmanstone	5	1.74	0.21	0.17	0.81	0.13	0.10
	10	3.02	0.38	0.36	0.95	0.21	0.20
Bedlay	5	2.50	0.30	0.30	1.00	0.13	0.13
	10	3.77	0.53	0.57	1.07	0.22	0.24
Rothwell	5	1.50	0.22	0.02	0.09	0.13	0.01
	10	2.63	0.40	0.12	0.30	0.16	0.05
Peckfield	2.5	1.18	0.13	0.00	0.00	0.08	0.00
	5	1.41	0.18	0.01	0.06	0.11	0.01
	7.5	1.92	0.23	0.05	0.22	0.15	0.03
	10	2.10	0.27	0.08	0.30	0.17	0.05
	15	2.64	0.35	0.13	0.37	0.19	0.07
	20	3.15	0.44	0.22	0.50	0.20	0.10
Bullcroft	5	1.30	0.15	0.06	0.40	0.09	0.04
	10	2.19	0.27	0.17	0.63	0.14	0.09
Burnt shale							
Thornley	5	1.88	0.26	0.28	1.08	0.17	0.18
	10	3.65	0.51	0.55	1.08	0.33	0.37
Tilmanstone	5	1.39	0.14	0.13	0.93	0.13	0.12
	10	3.14	0.56	0.55	0.98	0.39	0.38

Sample	Cement Content (%)	Average Heave (mm) 250 h	500 h	Unbound 250 h
Unburnt shale				
Chislet sample B	5	1.0	4.1	10.7
Chislet sample B	15	-1.0	-1.0	10.7
Snowdown	5	0.0	2.1	4.1
Tilmanstone	10	6.2	14.9	50.8

Effect of Prolonged Hydration on Subsequent Frost Heave

Continuous hydration produces changes in the properties of cement-stabilized materials so that the heave of specimens tested at 7 d may not accurately predict the frost resistance of material subjected to freezing at a greater age. The effect of curing for 3 months before the frost-heave test is shown below.

Sample	Cement Content (%)	Average Heave (mm) Cured for 7 d	Cured for 3 Months
Unburnt shale			
Snowdown	5	0.0	-0.5
Tilmanstone	10	6.2	5.6
Burnt shale			
Tilmanstone	5	16.4	12.9

This indicates that testing after 7 d provides a factor of safety because field performance is also affected by the time lapse between construction and the onset of severe freezing conditions.

Figure 3. Interrelationships among heave, heaving pressure, and direct tensile strength for cement-stabilized shale.

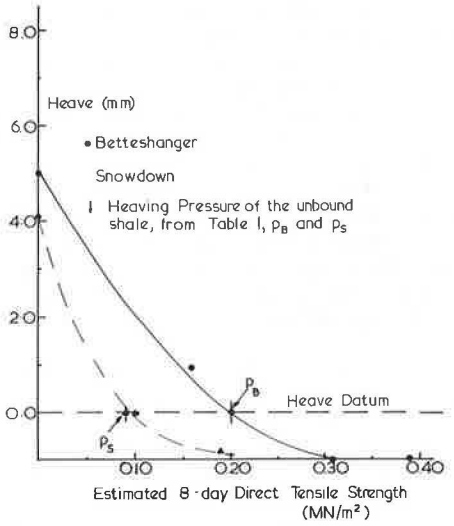

MECHANISM OF FROST ACTION IN CEMENT-STABILIZED MATERIALS

To understand the freezing behavior of cement-stabilized shales, it is essential to consider not only the cementing action, but also the changes in pore structure produced by the addition of cement. These changes arise from the aggregation (20) of the cement particles and the soil grains by a mechanism similar to the action of lime on clay soils. As hydration proceeds, secondary cementation (21) causes further agglomeration and leads to the formation of clusters. The amount of aggregation depends on the cement content and the nature of the clay minerals. The aggregation reduces the pore space between the clay colloids and increases the size of the pores between the aggregate. It also increases the permeability as determined from saturated flow tests (although other factors, including reduced surface activity, should also be considered).

However, account must also be taken of the relationship between pore size and the free energy available (13). It has been suggested that the forces associated with frost heave arise from supercooled freezing of the thin films of water present within the smaller pores (10) and that the degree of supercooling and the magnitude of the associated forces are inversely proportional to the pore size (10, 22). Thus, if aggregation occurs, the forces developed during ice lensing will be less, which will reduce the heaving activity. This is supported by the observation that the heaving pressure of the finer graded unburnt shales is less for stabilized samples than for unbound samples (11). It is therefore clear that the increase in pore size accounts for some of the change in heave associated with the addition of cement.

Another factor to be considered when dealing with cement-stabilized materials is the tensile strength because this must be overcome by the expansive heaving pressure before appreciable heave can occur. Energy will be consumed in fracturing the material, which means that less will be available for water transport and for vertical uplift. This is consistent with the increased heave of cut specimens and of refrozen specimens.

The addition of 5 percent cement did not affect the heave of Rothwell unburnt shale and caused a marked increase in the heave of Peckfield and Bullcroft unburnt shales. Of all the shales tested, these had the finest gradings and the lowest permeability in the unbound state so that cement-induced aggregation should be most marked. The evidence for their increased permeability and decreased heaving pressure after stabilization is given in Table 1. It follows that the effect of aggregation on fine-graded shales is to reduce the free energy liber-

Figure 4. Movement versus time under test for selected, unburnt cement-stabilized shales.

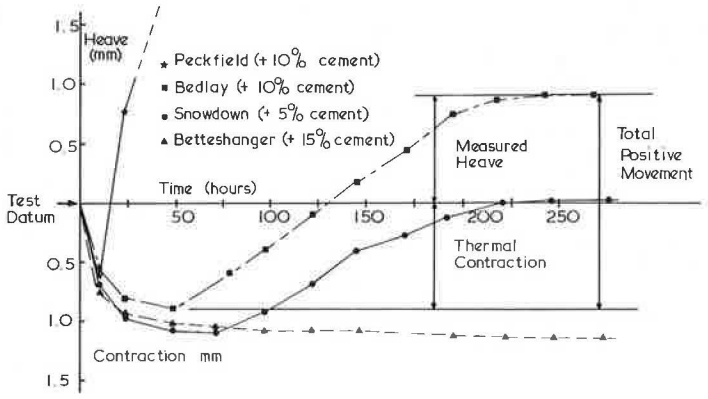

Table 3. Strength tests on cement-stabilized specimens after frost-heave test.

Sample	Cement Content (%)	Measured Heave (mm)	Total Movement (mm)	Strength After Freezing/Strength Before Freezing		
				Compressive	Indirect Tensile	Direct Tensile
Unburnt shale						
Snowdown	5	0.0	1.1	0.83	0.87	0.00
	10	-0.7	0.4	1.05	1.00	0.65
Betteshanger	5	1.0	2.1	0.85	0.73	0.00
	5[a]	-0.3	0.7	—	—	0.31
	10	-1.0	0.1	0.95	—	0.98
	15	-1.1	0.0	1.18	1.02	1.05
Chislet sample B	5	1.0	2.1	0.97	1.03	0.00
	5[a]	-0.4	0.6	—	—	0.45
	10	0.0	0.9	1.06	1.00	0.25
	10[a]	-0.7	0.3	1.08	1.01	0.79
	15	-1.0	0.0	1.20	1.08	1.04
Tilmanstone	10	6.2	7.1	0.75	—	0.00
Bedlay	10	0.9	1.8	1.00	0.68	0.00
	10[a]	-0.5	0.4	—	—	0.58
Peckfield	5	11.5	12.4	0.08	—	0.00
	10	7.2	8.1	0.30	0.13	0.00
	20	3.6	4.6	0.65	0.30	0.00
Bullcroft	10	8.1	9.0	0.95	—	0.00
Burnt shale						
Thornley	5	8.0	9.0	—	—	0.00
	10	-1.0	0.1	1.15	1.07	0.95
Tilmanstone	5	21.4	22.5	0.45	—	0.00
	10	2.5	3.5	0.75	—	0.00

[a]Specimens tested for 100 h.

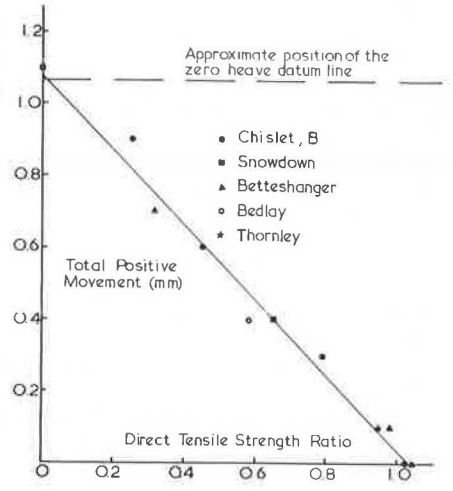

Figure 5. Movement during frost-heave test versus direct tensile-strength ratio for cement-stabilized shales.

ated during freezing. Consider the manner in which the free energy liberated is consumed: The initial strength of these shales is low, and there is a subsequent loss in strength during soaking (Table 2), so that relatively little energy is required to fracture the material. There is also an increase in permeability of at least two orders of magnitude and therefore less energy is required to lift water to the growing lens. Thus, more of the available energy can be used for heaving, and the behavior will be governed by the balance between the reductions in the free energy liberated and in the energy required for water transport and for fracture.

As the cement content was further increased, all three fine-graded shales showed reduced heave, in common with the other materials tested. This is attributed partly to the increase in strength and partly to the possibility that the more open pore structure caused by aggregation is offset by the pore-filling action of the hydration products. In some cases, there may be an overall increase in free energy, but the strength of the material may then be sufficient to either prevent or limit heave. Such cement contents would also reduce permeability and thus further limit heaving activity. The reduced heave of specimens cured for 3 months can be explained in the same manner.

CRITERIA FOR JUDGING FROST SUSCEPTIBILITY OF CEMENT-STABILIZED MATERIALS

The reduction in the direct strength after a frost-heave test is indicative of the disruption that can result from even a relatively limited heave and supports the view (23) that the direct tension test detects minute cracks and localized weaknesses that are not detected by other strength parameters. Cement-stabilized shales that developed positive heave lost all tensile strength across the fracture, although the material above and below the crack appeared to be comparatively sound. It is therefore necessary to reconsider the heave criteria for cement-stabilized materials: Positive movement during the test is evidence of a nonreversible breakdown within the specimen, which emphasizes the need to evaluate the behavior of cement-stabilized materials in terms of their tensile strength.

In North America, where freeze-thaw tests are used, the change in compressive strength is used for assessing the frost susceptibility of cement-stabilized and lime-stabilized materials. The formulation of dual criteria based on a limiting change in length and a limiting loss of compressive strength has been considered (23, 24), but the main emphasis is usually on changes in compressive strength (25). Other work (26) has included studies of frost susceptibility in terms of the effect on the cylinder splitting strength.

Heave criteria are also used in North America for evaluating the frost susceptibility of cement-stabilized and lime-stabilized materials. A dimensional criterion that limits the change in length within the frozen zone to 1 percent is considered appropriate for subbase materials because the wheel-load stresses are low. For the specimens tested in this investigation, this requirement would correspond to a movement of 1 mm, which agrees with the finding that a total heave of more than about 1 mm resulted in complete loss of tensile strength in the stabilized specimens. Other workers (23) have suggested that the expansion should be limited to 0.1 percent, but this may be unduly exacting for a subbase material (al-

though it may be applicable to road-base materials where the tensile stresses induced by wheel loads and by restrained movement are higher). Separate criteria may be required for subbase and road-base materials, and separate test procedures may also be necessary. A continuous freezing test with a heave criterion is probably appropriate for subbase materials because the prolonged periods of low temperature may induce failure by water transport to the stable freezing front. For road-base materials, a testing regime that subjects specimens to cycles of freezing and thawing, so as to simulate short duration but repeated damage, may be more relevent. This approach to durability evaluation requires careful consideration of the field environment, both with respect to the thermal regime and to the assessment of damage (27).

CONCLUSIONS

The freezing behavior of cement-stabilized colliery shale is a complex phenomenon that can be tentatively explained in terms of an energy balance. In both unbound and cement-stabilized shales, the forces associated with frost action arise from the supercooled freezing that occurs in the soil pores. These forces are then responsible for transporting water to the freezing front and for lifting the frozen soil plus any imposed load. In cement-stabilized shales, the tensile strength of the materials is analogous to an imposed load that must be overcome before heaving can occur, so that considerable energy may be consumed before appreciable lensing occurs. Stabilization also causes changes in pore structure that affect both the permeability of the material and the degree of supercooling that occurs (so that stabilization influences freezing behavior both directly and indirectly).

Significant heave develops only in materials in which the heaving pressure is greater than the direct tensile strength, so that massive ice lensing is preceded by fracture of the material at the freezing front. With certain exceptions, the addition of cement reduces the heave of colliery shale, which is attributed to the tensile strength imparted and to the changes in pore structure that result from cement stabilization. The exceptions to this are the fine-graded, unburnt shales in which the addition of cement leads to aggregation of the clay colloids. These materials developed only very limited tensile strength, and the changes in pore size produced large increases in permeability, so that the energy liberated is largely available for heaving.

Both the compressive strength test and the cylinder-splitting test have limitations as means of quantifying the damage suffered during a freezing test, but this is not so for the direct tension test. In particular, the increase in length during freezing that is evidence of a nonreversible breakdown is clearly reflected only in the direct tension test results.

The current heave criteria for the frost susceptibility of cement-stabilized materials should be reconsidered. A tensile strength criterion may be especially relevant for road-base materials, although a heave criterion may be acceptable for subbase materials.

ACKNOWLEDGMENTS

This study formed part of a research project financed by the National Coal Board. We wish to express our thanks for the support given and for permission to publish the paper. The views expressed are ours and not necessarily those of the National Coal Board. We also wish to express our thanks to the U.K. Department of the Environment, Engineering Intelligence Unit, who kindly loaned the equipment used for measuring the restrained heaving pressures. Finally, we wish to thank our colleague, D. J. Hannant, for his many useful comments during the course of the investigation.

REFERENCES

1. Use of Unburnt Colliery Shale as Filling Material in Embankments. U.K. Ministry of Transport, Technical Memo T4/68, 1968.
2. Use of Unburnt Colliery Shale as Filling Material in Embankments. U.K. Department of the Environment, Technical Memo H4/74, 1974.
3. R. J. Kettle and R. I. T. Williams. Cement-Stabilized Unburnt Colliery Shale. Roads and Road Construction, Vol. 47, No. 559, 1969, pp. 200-206.
4. Specification for Road and Bridge Works. U.K. Department of the Environment, Her Majesty's Stationery Office, 1969.
5. R. J. Kettle. Freezing Behavior of Colliery Shale. Univ. of Surrey, PhD thesis, 1973.
6. D. Croney and J. C. Jacobs. The Frost Susceptibility of Soils and Road Materials. U.K. Transport and Road Research Laboratory, Crowthorne, England, Rept. LR90, 1967.
7. Methods of Testing Soils for Civil Engineering Purposes. British Standards Institution, London, BS 1377, 1967.
8. R. J. Kettle and R. I. T. Williams. The Development of Frost-Heave Testing Equipment. Materiaux et Constructions, Vol. 6, No. 34, 1973, pp. 299-306.
9. J. R. Lake and C. K. Fraser. A Laboratory Investigation of the Physical and Chemical Properties of Burnt Colliery Shale. U.K. Transport and Road Research Laboratory, Crowthorne, England, Rept. LR 125, 1967.
10. E. Penner. Heaving Pressure in Soils During Unidirectional Freezing. Canadian Geotechnical Journal, Vol. 4, No. 4, 1967, pp. 398-408.
11. R. J. Kettle and R. I. T. Williams. Frost Heave and Heaving-Pressure Measurements in Colliery Shales. Canadian Geotechnical Journal, Vol. 13, No. 2, 1976, pp. 127-138.
12. P. Hoekstra, E. Chamberlain, and T. Frate. Frost-Heaving Pressures. HRB, Highway Research Record 101, 1965, pp. 28-38.
13. B. Chalmers and K. A. Jackson. Experimental and Theoretical Studies of the Mechanism of Frost Heaving. Res. Rept. 199, U.S. Army Cold Regions Research and Engineering Laboratory, Hanover, N.H., 1970.
14. A. E. Z. Wissa and R. T. Martin. Behavior of Soils Under Flexible Pavements: Development of Rapid Frost-Susceptibility Tests. Department of Civil Engineering, MIT, Cambridge, Res. Rept. R68-77, 1968.
15. L. Bjerrum and J. Hoder. Measurement of the Permeability of Compacted Clays. Proc., 4th International Conference on Soil Mechanics and Foundation Engineering, London, Vol. 1, 1957, pp. 6-8.
16. B. P. Hughes and G. P. Chapman. Direct Tensile Test for Concrete Using Modern Adhesives. Rilem, Bulletin 26, 1965, pp. 77-80.
17. M. Walker. Is Anyone for Cylinder Splitting? New Civil Engineer, May 2, 1974, pp. 28-31.
18. H. B. Sutherland and P. N. Gaskin. Factors Affecting the Frost-Susceptibility Characteristics of Pulverized Fuel Ash. Canadian Geotechnical Journal, Vol. 7, No. 1, 1970, pp. 69-78.
19. P. T. Sherwood. The Properties of Cement-Stabilized Materials. U.K. Transport and Road Research Laboratory, Crowthorne, England,

Rept. LR 205, 1968.
20. L. R. Chadda. The Phenomenon of Aggregation in the Stabilization of Soils With Cement. Indian Concrete Journal, Vol. 44, No. 5, 1970, pp. 210-212.
21. A. Herzog. Evidence for Skeleton-Matrix Structure in Clays Stabilized With Portland Cement. Proc., 5th Australian-New Zealand Conference on Soil Foundation Engineering, Petone, 1967, pp. 55-61.
22. D. H. Everett and J. M. Haynes. Capillary Properties of Some Model Pore Systems With Reference to Frost Damage. Rilem, Bulletin 27, 1965, pp. 31-38.
23. R. G. Packard and G. A. Chapman. Developments in Durability Testing of Soil-Cement Mixtures. HRB, Bulletin 36, 1963, pp. 97-122.
24. L. T. Norling. Standard Laboratory Tests for Soil-Cement Development: Purpose and History of Use. HRB, Highway Research Record 36, 1963, pp. 1-10.
25. M. R. Thompson. Durability and Frost Resistance of Lime and Cement-Treated Soils. Proc., Symposium on Frost Action on Soils, Organization for Economic Cooperation and Development, Vol. 2, 1973, pp. 377-393.
26. D. L. Townsend and T. W. Klym. Durability of Lime-Stabilized Soils. HRB, Highway Research Record 139, 1966, pp. 25-39.
27. B. J. Dempsey and M. R. Thompson. Effects of Freeze-Thaw Parameters on the Durability of Stabilized Materials. HRB, Highway Research Record 379, 1972, pp. 10-18.

Publication of this paper sponsored by Committee on Soil-Portland Cement Stabilization and Committee on Frost Action.

Tensile-Strength Determinations of Cement-Treated Materials

L. Raad, Department of Civil Engineering, University of Illinois at Urbana-Champaign
C. L. Monismith and J. K. Mitchell, Department of Civil Engineering and Institute of Transportation Studies, University of California, Berkeley

Differences in values of the tensile strength of cement-treated materials measured by using flexure, direct tension, and split tension tests are explained analytically by using Griffith failure theory; and predicted values are shown to agree well with the strength data available in the literature. The results indicate that the direct tension test provides the most reliable values of tensile strength of cement-treated materials, even when the failure surface is close to the interface between the cap and the specimen. Flexural strengths deduced from beam tests can be as much as twice the actual tensile strengths, depending on beam geometry, moduli in tension and compression, and degree of fixity at support and load-application points. The split tension test appears most suitable for practical use in evaluation of the tensile strength of cement-treated materials because it is simple to perform and yields measured values that do not deviate by more than 13 percent from the actual tensile strength.

Cement-treated bases used in pavement structures are subjected to tensile stresses caused by applied wheel loads, shrinkage, and internal temperature gradients. When these stresses exceed the tensile strength of the material, cracking takes place (1, 2, 3), which results in increased deflections and stress transmissions to the subgrade (4). In addition, the presence of open cracks permits the entry of water into the subgrade, which leads to decreased subgrade support and thereby hastens pavement deterioration. Determination of the tensile strength of cement-treated materials is therefore a desirable part of the design process for pavement structures containing these materials.

Tensile strength has been measured by using flexure tests, direct tension tests, and split tension tests (e.g., 2, 5, 9). The estimation of tensile strength from flexural-beam tests and split tension tests is usually made by using simplifying assumptions about the stress-deformation characteristics of the material, i.e., linear-elastic behavior with the modulus in tension (E_t) equal to the modulus in compression (E_c). The values of tensile strength obtained on this basis vary and depend on the kind of test used. The split tension test gives lower values of tensile strength than do the flexure and direct tension tests (5, 6), and the flexure test gives higher values than does the direct tension test (2, 5).

Experimental work on the stress and strain behavior of cement-treated soils has shown that the modulus in compression is greater than the modulus in tension (2, 3, 5). Bofinger (5) has suggested that the flexural-beam and the split tension tests do not measure the actual tensile strength of the cement-treated soil because E_c and E_t are not equal and concluded that the direct tension test is the only method that can directly measure the tensile strength of the material. On the other hand, Pretorius (2) has shown that there are stress concentrations at the ends of the specimen in a direct tension test, so that the measured tensile strength measured by this test could also be unreliable.

In this paper, an attempt has been made to explain the differences observed in the three types of tests by using analytic simulations and actual experiments.

METHOD OF ANALYSIS

The cement-treated material was assumed to be linearly elastic with a modulus in compression that might differ from the modulus in tension. The finite-element method of analysis was used to determine the stresses and deformations for a specific test configuration (Figures 1 and 2) resulting from particular load. A planar stress condition was assumed, and a successive-approximation technique was used to include the bimodular material properties (i.e., $E_c \neq E_t$). In this procedure, the modulus in compression was used for all elements on the first

iteration. On successive iterations, the modulus in tension was substituted in the directions of principal tension. Three or four iterations were usually sufficient to attain reasonable convergence.

For the specific test under consideration (i.e., flexural beam, split tension, or direct tension), the failure load is calculated as follows:

1. The applied load is incremented until the most critically stressed element fails. Failure, as defined by the Griffith criterion (7), which is applicable for tension and small compressive-stress fields, takes place when

$$(\sigma_1 - \sigma_3)^2/8(\sigma_1 + \sigma_3) = T_a \quad (\sigma_1 + 3\sigma_3 \geq 0)$$
$$\sigma_3 = -T_a \quad (\sigma_1 + \sigma_3 \leq 0) \tag{1}$$

where

σ_1 = major principal stress,
σ_3 = minor principal stress, and
T_a = actual tensile strength of the material and corresponds to the uniaxial uniformly applied tensile stress required to cause fracture in the material.

(Tensile stresses are negative; compressive stresses are positive.)

2. The failed element is removed from the system, and a new state of stress for each element is determined.
3. This process is continued until complete fracture of the specimen occurs. A failure load (P_f) in terms of the actual tensile strength of the material can then be determined.

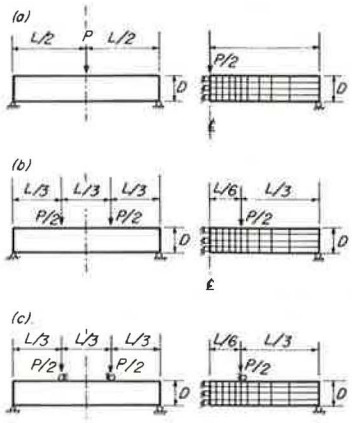

Figure 1. Finite-element representation of flexural-beam test.

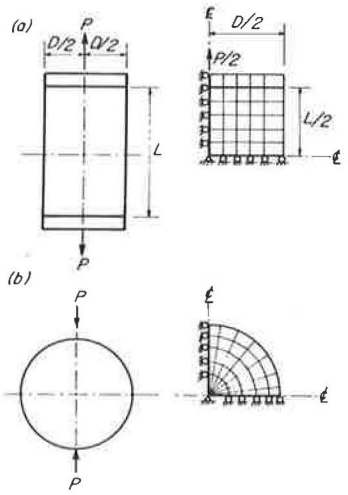

Figure 2. Finite-element representation of direct and split tension tests.

By using this value of P_f, a tensile-strength value (T_c) of the material is then calculated on the assumptions that

1. The material is linearly elastic ($E_c = E_t$),
2. Simple beam theory holds true in the flexure test,
3. Lateral restraints that may exist at the points of application of the load in the flexure test [Figure 1(c)] have negligible effects on the stress distribution in the beam, and
4. In the direct tension test, the stress concentration at the ends of the specimen where the loads are applied is negligible.

For the flexural-beam test,

$$T_c = M_f c/I \tag{2a}$$

where

M_f = moment that corresponds to P_f and acts at a section through the center of the beam,
c = half the depth of the beam, and
I = moment of inertia of the beam section.

For the split tension test,

$$T_c = P_f/\pi R \tag{2b}$$

where R = radius of the sample. For the direct tension test,

$$T_c = P_f/A \tag{2c}$$

where A = cross-sectional area of the sample.

The value of P_f in all of these tests corresponds to the load per unit thickness that is required to cause complete fracture. P_f is expressed in terms of the actual tensile strength of the material. T_c can be expressed in terms of T_a, and the ratio T_c/T_a for a given E_c/E_t can be calculated.

RESULTS

The variation of T_c/T_a as a function of E_c/E_t has been determined for all three tests. The results are summarized in the following sections.

Flexure Test

Three loading conditions were investigated: (a) central loading [Figure 1(a)], (b) third-point loading with no lateral restraints [Figure 1(b)], and (c) third-point loading with lateral restraints [Figure 1(c)]. The results are shown in Figures 3 and 4 for different length-to-depth beam ratios (L/D); the variation of T_c/T_a as a function of E_c/E_t is also plotted in Figure 3 by using simple beam theory. The derivation of the following expression for T_c/T_a in terms of E_c/E_t by using simple beam-theory assumptions has been given by Raad (3).

$$T_c/T_a = 2\left\{1 - [(R^{1/2} - 1)/(R - 1)]\right\} \tag{3}$$

where $R = E_c/E_t$.

Analysis of the results shows that

1. T_c/T_a increases as E_c/E_t increases for all of the cases studied;

Figure 3. Analytically predicted values of measured tensile strength in terms of actual tensile strength.

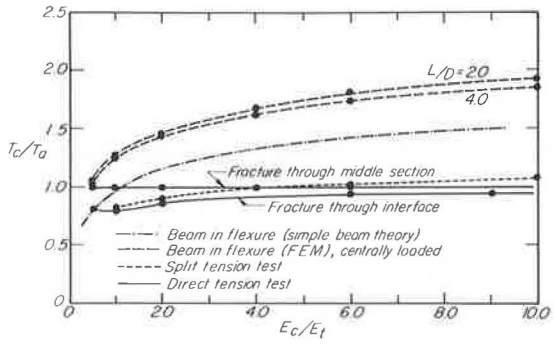

Figure 4. Effect of lateral restraints of applied vertical load on measured values of tensile strength in flexural-beam test.

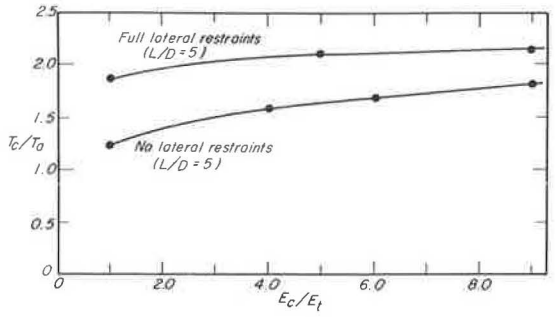

Figure 5. Stress concentrations in direct tension test.

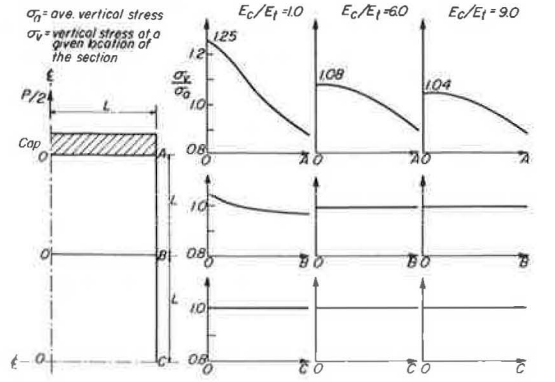

Table 1. Predicted values of tensile-strength ratio of cement-treated materials using different laboratory tests.

		Failure Near Interface[a]				Failure Through Midsection[a]				
		T_t/T_a				T_t/T_a				
		L/D[b] = 5				L/D[b] = 5				
E_c/E_t	T_a/T_a	FR[d]	NR[e]	L/D[b,c] = 4	L/D[b,c] = 2	T_a/T_a	FR[d]	NR[e]	L/D[b,c] = 4	L/D[b,c] = 2
1	1	2.32	1.52	1.52	1.57	0.80	1.85	1.25	1.25	1.26
10	1.11	2.28	1.94	1.96	2.04	1.04	2.15	1.85	1.84	1.92

[a] Refers to the position of the failure surface in the direct tension test.
[b] L/D = length of beam/depth of beam in flexure test.
[c] A central or a three-point loading system with no lateral restraint is used in the flexure test.
[d] Full lateral restraint of the applied vertical load in the flexure test.
[e] No lateral restraint of the applied vertical load in the flexure test.

2. The value of T_c/T_a corresponding to a given E_c/E_t will be greater if the applied load is laterally restrained from movement than if there are no restraints;
3. Both simple beam theory and the finite-element method of analysis predict higher values of strength than the actual measured tensile strength of the material for $E_c/E_t > 1$ (i.e., $T_c/T_a > 1$); and
4. The values of measured tensile strength, T_c, obtained in the flexural-beam test are higher than those obtained in the direct or the split tension tests.

Direct Tension Test

In this test, the load is applied through rigid caps (i.e., made of a material having a high modulus of elasticity compared to that of the cement-treated material) bonded to the specimen (i.e., with no relative movement of the interface between the caps and the specimen allowed). The effect of this kind of restraint on the stress distribution and on the measured tensile strength of the material was investigated. The predicted values of the tensile strength are shown in Figure 3, and the stress concentrations are shown in Figure 5. The results can be summarized as follows:

1. If the failure surface is located at the center of the specimen, then the measured tensile strength (T_c) will be the same as the actual tensile strength (T_a) for all values of E_c/E_t;
2. If the failure surface occurs at the interface between the cap and the material, then the measured tensile strength will vary from 0.8 to 0.94 T_a, depending on the value of E_c/E_t (for $E_c/E_t > 4.0$, T_c/T_a will be equal to 0.94); and
3. Stress concentrations occur near the interface of the cap and the specimen and increase with the decrease in the radial distance from the center of the specimen (the normal tensile stress at the interface near the center of the cap could have values of 1.25 and 1.04 times the average applied normal stress for E_c/E_t = 1.0 and 9.0 respectively.

Split Tension Test

The results of analysis of this test configuration are given in Figure 3 and can be summarized as follows: (a) T_c/T_a increases as E_c/E_t increases (the measured tensile strength varies from 0.8 T_a at E_c/E_t = 1.0 to 1.04 T_a at E_c/E_t = 9.0) and (b) the values of tensile strength measured by using this test are smaller than those given by the flexural test, but can be either smaller or larger than those measured by the direct tension test, depending on the value of E_c/E_t and on the position of the failure surface.

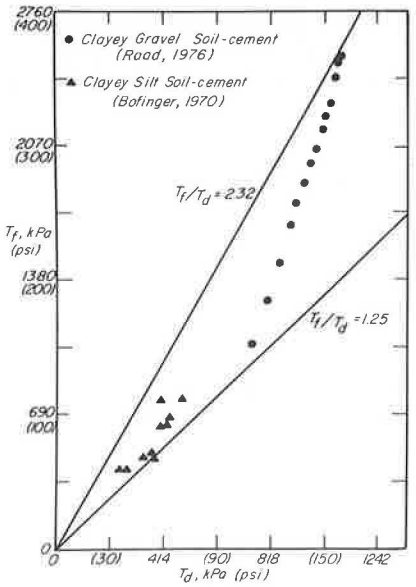

Figure 6. Measured and predicted values of direct tensile and flexural strengths.

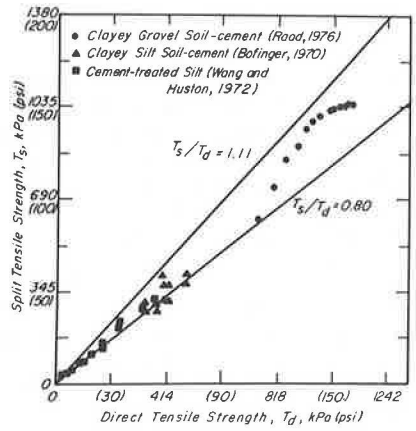

Figure 7. Measured and predicted values of direct and split tensile strengths.

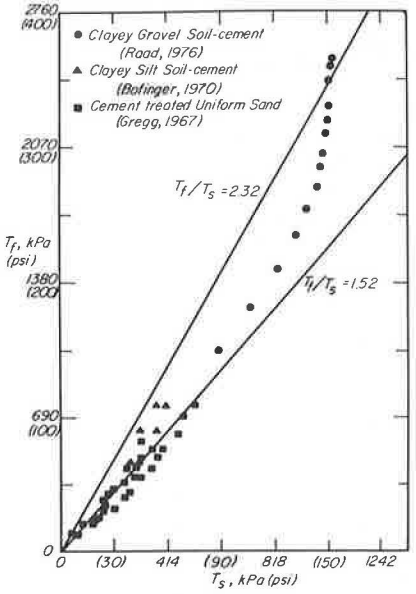

Figure 8. Measured and predicted values of flexural and indirect tensile strengths.

EXPERIMENTAL VERIFICATION

Previously published test data for flexural strength, direct tensile strength, and split tensile strength can be compared with the values predicted by using the suggested analytical procedure. A clayey, gravel soil-cement and a cement-treated, clayey silt were tested in tension and in compression using metal caps bonded to the specimens with an epoxy resin to apply the tensile loads. The values for initial tangent moduli and secant moduli from these tests are given by Raad (3) and Bofinger (5); E_c/E_t varied from 5 to 11. Analytical predictions for the ratios of the split tensile strength (T_s) to the direct tensile strength (T_d) and of the flexural strength (T_f) to T_d for E_c/E_t = 1 and 10 are summarized in Table 1.

Measured values of tensile strength for cement-treated soils using the direct tension test, the split tension test, and the flexural test have been given by a number of investigators (4, 5, 6, 8). Comparisons between the measured and the predicted values are shown in Figures 6, 7, and 8. Figure 6, for example, shows that the measured values of the flexural strength (T_f) and of the direct tensile strength (T_d) should vary, according to the results of analysis (Table 1), such that T_f/T_d will be in the range of 1.25 to 2.32. This figure also shows that the correspondence between the actual and the predicted results is actually obtained. Figures 7 and 8 indicate similar results.

SUMMARY AND CONCLUSIONS

In this paper, an attempt has been made to explain analytically the differences in measured tensile strength for cement-treated soils. The analyses showed that the direct tension test gives reliable values of the actual tensile strength of such materials. Even if the failure surface is near the interface between the cap and the tested specimen, the measured tensile strength will be about 0.94 times the actual tensile strength. The flexural strength deduced from beam tests by using simple beam theory and assuming that $E_c = E_t$ can be as much as twice the true tensile strength, depending on the beam geometry, the value of E_c/E_t, and the degree of fixity at the support and load-application points. The split tension test would seem best for the practical evaluation of tensile strength because of its simplicity. The true tensile strength can be estimated as 1.11 times the split tensile strength. On this basis, the error in the estimated value would not exceed 13 percent.

REFERENCES

1. K. P. George. Shrinkage Characteristics of Soil-Cement Mixtures. HRB, Highway Research Record 255, 1968, pp. 42-58.
2. P. C. Pretorius. Design Considerations for Pavements Containing Soil-Cement Bases. Univ. of California, Berkeley, PhD dissertation, 1970.
3. L. Raad. Design Criterion for Soil-Cement Bases. Univ. of California, Berkeley, PhD dissertation, 1976.
4. P. E. Fossberg, J. K. Mitchell, and C. L. Monismith. Cracking and Edge-Loading Effects on Stresses and Deflections in a Soil-Cement Pavement. HRB, Highway Research Record 379, 1972, pp. 25-38.
5. H. E. Bofinger. The Measurement of the Tensile Properties of Soil-Cement. British Road Research Laboratory, Crowthorne, England, Rept. LR 365, 1970.
6. J. S. Gregg. The Significance of Compressive, Tensile, and Flexural Strength Tests in the Design of Cement-Stabilized Pavement Foundations. Proc., 4th Regional Conference for Africa on Soil Mechanics

and Foundation Engineering, Capetown, South Africa, Dec. 1967.
7. A. A. Griffith. Theory of Rupture. Proc., 1st International Congress for Applied Mechanics, Delft, Netherlands, 1924, pp. 55-63.
8. M. C. Wang and M. T. Huston. Direct Tensile Stress and Strain of a Cement-Stabilized Soil. HRB, Highway Research Record 379, 1972, pp. 19-24.
9. J. N. Anagnos, T. W. Kennedy, and W. R. Hudson. Evaluation and Prediction of the Tensile Properties of Cement-Treated Materials. Center for Highway Research, Univ. of Texas at Austin, Res. Rept. 98-8, Oct. 1970.

Publication of this paper sponsored by Committee on Soil-Portland Cement Stabilization.

Performance Study of Asphalt Road Pavement With Bituminous-Stabilized-Sand Bases

Claude P. Marais and Charles R. Freeme, National Institute for Transport and Road Research, Council for Scientific and Industrial Research, Pretoria, South Africa

The possibility of using the windblown sands that occur in the northern areas of South West Africa for the construction of all-weather roads to carry heavy truck traffic has been investigated. Laboratory investigations and field trials in Pretoria, South Africa, showed that bituminous stabilization of these sands was promising, and a full-scale road experiment to test a limited number of bases of bituminous-stabilized sand was constructed in the homeland of Owambo, South West Africa. This paper describes the laying of the experiment and the construction techniques and control measures used. A new technique that establishes the optimum time for the compaction of a cutback bituminous-stabilized sand mixture after aeration by using a vane shear apparatus is described. The vane shear apparatus was also used to measure the in situ shear strengths of the various experimental bituminous-stabilized sand bases after compaction and during service; the results of these measurements, together with performance data after 8 years service with respect to deformation and cracking, are discussed. Laboratory and field studies are described and predictions about the performance of a bituminous-stabilized sand base under varying traffic conditions are made by using the best known techniques available at this time.

Vast areas of the southern subcontinent of Africa are covered with a deep blanket of aeolian sand. Probably these sands were originally derived from preexisting sedimentary rocks in the general area and first emplaced by wind during the lower most Pleistocene epoch (approximately 2 000 000 years ago). They were subsequently redistributed by wind and water during the Pleistocene; the latest major redistribution was brought about by wind action, probably some 10 000 to 15 000 years ago, although some minor redistribution is still occurring (1).

Because of their widely spread occurrence, these sands, apart from various types of calcrete (caliche), are sometimes the only natural building material available to the civil engineer. From an economic point of view, they are therefore extremely important and have been studied for use in concrete structures, building construction, and, more recently, pavement construction by the National Institute for Transport and Road Research (NITRR) of the Council for Scientific and Industrial Research in Pretoria, South Africa (2, 3, 4).

This paper describes the use of these aeolian sands as the base layer of a road pavement in the recently proclaimed homeland of Owambo, in the northern part of South West Africa (SWA). It discusses the performance results of the experiment and relates these to the probable performance that might be expected under much heavier traffic on a normal freeway.

The accelerated development of the infrastructure of Owambo during the past decade necessitated upgrading the existing gravel road linking Owambo to the more developed, southern part of SWA to an all-weather, 8-m-wide, black-topped facility. The construction of the R60 000 000 ($84 000 000) hydroelectric facility at Ruacana Falls and other major building schemes in Owambo have resulted in a significant increase in heavy freight vehicles using this, the only surface transportation route to the south.

Initial laboratory work by the NITRR in the early 1960s showed that the most suitable method of improving the engineering properties of the in-place sand was to blend it with 15 percent calcareous filler (mechanical stabilization) and then to bind the blend with a bituminous binder. Both the hot-mix and cold wet-mix processes were studied; the latter was adopted as the more practical because of the length of road required and the problems associated with the establishment of a hot-mix facility in this remote area.

After extensive preliminary research into the wet-sand process of bituminous stabilization of fine-grained wind-blown sands, a full-scale road experiment was carried out in May 1965 in Owambo to test the techniques developed during the preliminary study (3, 4).

DETAILS OF EXPERIMENT

The experiment was designed and constructed with the following objectives:

1. To demonstrate in the field the feasibility of in situ bituminous stabilization of sand by using cutback binders and a cationic bitumen emulsion;
2. To investigate the stability and durability, under the traffic conditions and climatic environment of the site, of various bituminous-sand mixtures containing cutback bitumens, a cutback tar, and a cationic bitumen emulsion at binder contents considered suitable from

laboratory work and previous experimental trials;

3. To investigate the effect on stability of adding a proportion of calcareous filler to the natural sand before stabilization;
4. To investigate the effect of laying the bituminous-stabilized sand mixtures over a compacted sand-clay subbase of low strength [California bearing ratio (CBR) approximately 30 percent];
5. To investigate the relative performances of 76.2 and 152.4-mm compacted layers of bituminous-stabilized sand bases;
6. To obtain data on the temperature distribution throughout a bitumen-sand mixture on the road under the climatic conditions of Owambo; and
7. To study the setting up of bitumen-sand mixtures on the road over a period of 2 years.

The experimental pavement was constructed in Owambo from April 27 to May 26, 1965, on the alignment of the road route from Oshivelo to Oshakati. The experiment consisted of eighteen sections each 91.4 m long by 7.3 m wide (width of carriageway). The stabilized sand bases were supported by 3.7-m-wide shoulders on either side of the carriageway. The layout of the experiment with details of the base compositions and compacted thicknesses is given in Figure 1. All of the experimental sections, with the exception of sections 1 and 2, were laid over a firm foundation comprising a number of layers of approved subbase and base material consisting of silcrete and calcrete to which binding material was added. These layers were designed to obviate any deformation distress below the bituminous-sand base layer.

The area in the vicinity of the experiment consists of flat to slightly undulating plains with shallow, localized depressions that have been prospected for calcrete (5). As distinct from river channels, there is a network of shallow watercourses (oshanas). These watercourses drain the level country and do not reach the sea. The center of the drainage system is the Etosha pan. During years of good rainfall, large quantities of slowly flowing water are carried southward along this network of oshanas; this phenomenon is of great importance for the underground water of Owambo (6). The annual rainfall of the area is approximately 500 mm, but it is very variable and results in frequent droughts. Rain falls during a period of less than 60 d/year, mainly during January to March. The area is about 1000 m above sea level, has a subtropical climate, and is composed of open grasslands with scattered palms (Hyphaene ventricosa) in various stages of development in the area near Ondangwa; it changes to Mopani veld near the experimental site. In this region, Mopani (Colophospermum mopani) displays an interesting tendency to form large copses of even-sized trees varying from scrub bush 1.2 m high to large trees 6 to 12 m high (7).

Since the opening of the experimental sections, the traffic pattern has increased significantly, as was anticipated because of the large development program initiated in Owambo at about the same time as the experiment. The table below gives the traffic counts recorded over the 8-year period and the calculated equivalent 80-kN axle loads per day (8).

Date of Survey (year)	Vehicles per Day	Equivalent 80-kN Axles per Day
1965 to 1967	100	4
1971	147	6
1972	195	8
1973	226	9

This traffic is light by normal standards in developed countries, where the equivalent 80-kN axle loads per day would be expected to vary between 200 and 500 for freeways carrying medium to medium-heavy traffic.

MATERIALS

Windblown Sand

The local sand used for the stabilization was cohesionless and had an average particle-size distribution as given in Figure 2. The particle shape, as seen by microscopic examination, can be described as subrounded to subangular with relatively few well-rounded grains. The color is grey-white to a light reddish-brown caused by iron oxide stains on the grains. In the dry state, the sand has very poor inherent stability. Its apparent relative density is 2.60.

Blend of Windblown Sand and Calcareous Filler

The calcareous filler added to the windblown sand was selected from a natural powder-calcrete deposit in the vicinity of the experimental site. Its maximum particle size was generally 4 mm and approximately 50 percent passed a 0.074-mm sieve (Figure 2). The properties are as follows:

Property	Value
Liquid limit, %	50.9
Plasticity index, %	17.0
Linear shrinkage, %	8.0
Apparent relative density	3.61

The blend of windblown sand and 15 percent (by volume of dry sand) of calcareous filler was nonplastic, with an average particle size distribution as shown in Figure 2.

Bituminous Stabilizers

The following bituminous binders were used:

1. Cutback bitumens—A special cutback bitumen manufactured from an 80 to 100 penetration bitumen (MX) and a cutback bitumen manufactured from a 40 to 50 penetration bitumen and cutback to an intermediate grade of rapid-to-medium cure (250) were used. Both were straight-run bitumens, refined in South Africa from Middle East crudes (9, 10). The nominal binder contents were 4.0 and 6.0 percent (by mass of dry sand) for the 152.4-mm-thick compacted bases and 6.0 and 8.0 percent for the 76.2-mm-thick compacted bases (MX only).
2. Cationic bitumen emulsion—The cationic bitumen emulsion used was manufactured from an 80 to 100 penetration bitumen that was fluxed with 10 percent (by mass of emulsion) of a fluxing oil having a boiling point of 160°C. The base bitumen was straight-run and refined in South Africa from a Middle East crude. The nominal binder contents were 4.5 and 6.5 percent.
3. Cutback tar—The cutback tar was manufactured from a high-temperature coke-oven tar and cut back to a 30 to 35°C Evt grade. The nominal binder content was 6.0 percent.

All of the binders were tested with the windblown sand only and with a blend of wind-blown sand and 15 percent calcareous filler. The results of laboratory tests on samples of the binders used are reported elsewhere (4).

Borehole Water Used for Wetting Sand and Sand-Calcrete Filler Blend

The local borehole water used for wetting the sand and the sand-calcrete filler blend before the addition of the bituminous stabilizers had a total dissolved solids content of 52 800 ppm with an alkalinity of residue as carbonate of 3980 ppm.

TECHNIQUES OF CONSTRUCTION

A working platform was constructed to correct the longitudinal and transverse levels and ensure that, once the stabilized sand base was laid, the final road profile would be in accordance with the design requirements. Two 3.66-mm-wide shoulders were constructed to give a 7.32-m-wide trough into which the sand could be spread before treatment. The full experimental length of working platform was primed with a medium-cure (30) cutback bitumen at a rate of 0.72 L/m^2.

In situ CBR measurements were made on the primed platform. The length of platform constructed with calcrete had an average value of 142 percent (dry), and that constructed with sand-clay had an average value of 78 percent (dry) and 28 percent after 24 h soaking.

Where a blend of sand and calcareous filler was required, the correct quantity of sand was spread over the section, and then the calcareous filler was spread uniformly over the sand layer with a mechanical gritter. The sand and calcareous filler were mixed with a disc harrow and a motor grader to form a homogeneous blend.

Watering of Sand and Sand-Filler Blend Before Addition of Binder

The laboratory work carried out before the beginning of the experiment showed that water in the fine sand aids in coating of the sand particles by the cutback binder. It also showed that an initial excess of fluids gave a mixture that, after a specified period of aeration, had the highest density and shear strength when compacted (11).

For these reasons, the moisture content of the sand was increased to approximately 10 to 12 percent before stabilizing with binder. At this range of moisture content, after arbitrary compaction of the wet sand with a pneumatic-tired vehicle, the inherently poor stability of the dry sand improved to such an extent that the stabilization plant was able to move over the sandbed at the required speed without undue slippage.

The watering was done with a water tanker fitted with a gravity-feed spray bar. The moisture content of the sand was controlled by a nuclear gauge that was very useful in obtaining a rapid result. After the required quantity of water had been added, motor graders mixed the water into the sandbed to uniformly distribute the moisture throughout the sand layer.

Heating of Binders

The binders were supplied in drums. The contents of the drums were transferred to four 2300-L binder heaters, which were fired with liquid petroleum gas.

The heating of cutback binders is a fire hazard, and because of this, the temperature to which the cutback bitumens were raised in the binder-heating tanks was limited to approximately 5°C below that required for spraying. This procedure was satisfactory, and no fires occurred.

The heated binder was then pumped into a 4500-L distributor and further heated to a temperature that gave a Saybolt-Furol viscosity of 30 to 40 s, which was satisfactory for spraying.

Spraying and Mixing of Binder Into Wet Sand

The stabilization train consisted of a tractor, pulvimixer, and 1370-L binder-storage tanker. The 4500-L distributor pumped hot binder into the storage tanker during the stabilization process, thus enabling the work to proceed with a minimum of delay.

The binder was sprayed through a specially fitted spray bar located in front of the rotor of the pulvimixer. The depth of cut of the pulvimixer rotor blades was set

Figure 1. Diagrammatic layout of bitumen-sand stabilization experiment in Owambo, South West Africa.

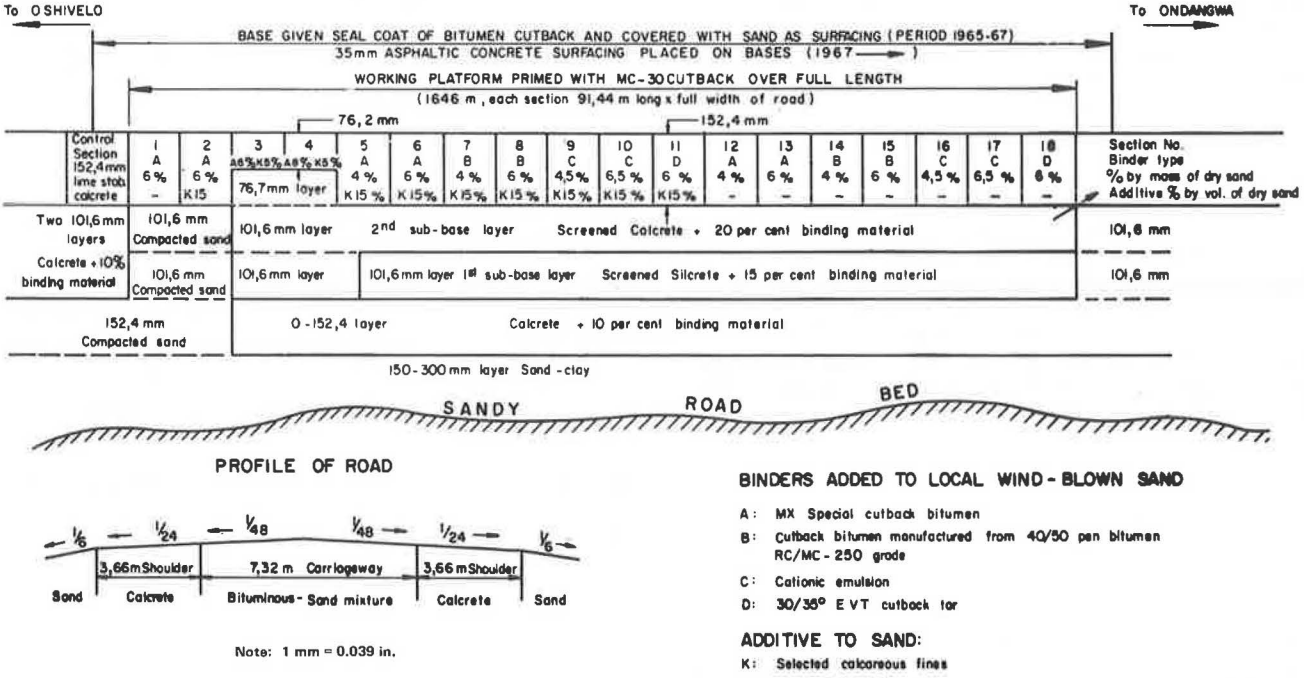

Figure 2. Grading analysis of materials.

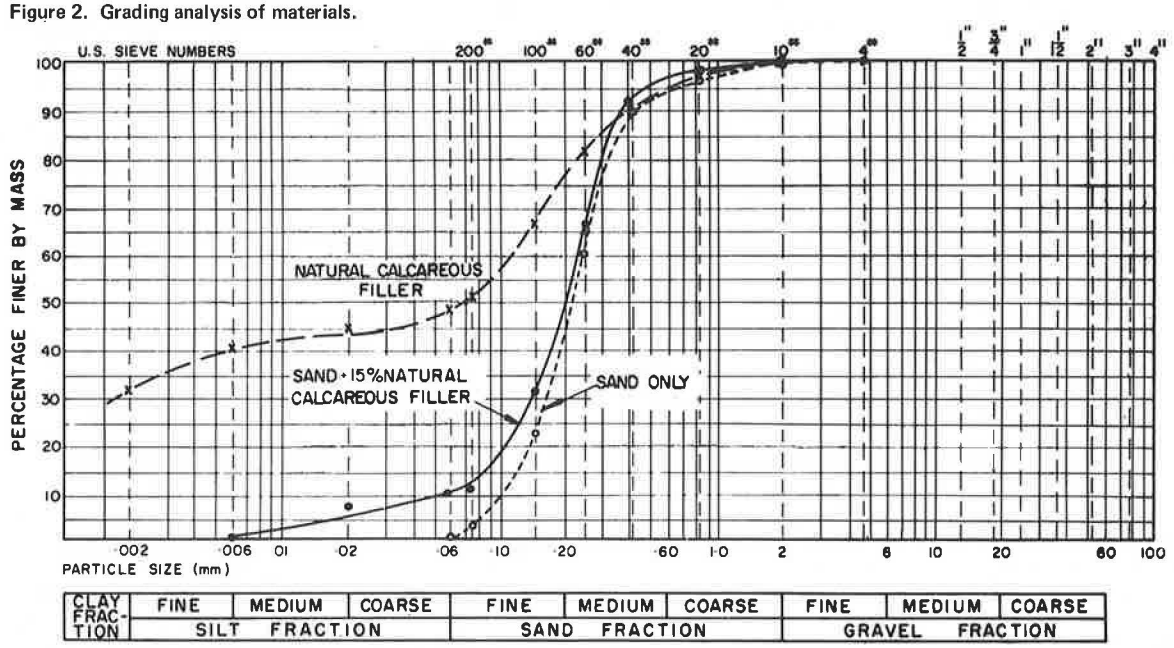

to just touch the working platform, thus ensuring that the full depth of sand layer was mixed with the binder. The spray bar nozzles were adjusted so that the hot binder was sprayed just ahead of the rotor to obtain an intimate mix while the binder was still in a relatively fluid state. The distribution of the binder after this spraying pass was inadequate, and a second mixing pass was necessary to improve the overall distribution of the binder through the sand mass.

A single pass of the pulvimixer covered a width of approximately 2 m, which made five passes over the full width of the carriageway necessary to give an adequate overlap between successive passes.

Control of the quantity of binder introduced was achieved by calibrating the spray bar to give a known output at a particular pump speed and by operating the train at the forward speed required to give the desired binder content. The relative density of the hot binder was used to convert the amount sprayed from a volume to a mass basis. The forward speed of the mixing train was controlled by charts relating the true forward speed to the various tractor gears and engine revolutions that could be selected. The times taken over measured distances during each mixing run were determined with a stopwatch and, where necessary, adjustments were made to the forward speed. This method of speed control gave very satisfactory results.

At the outset of the experiment, it was intended to dilute the cationic emulsion with 30 percent (by volume of emulsion) of water so that it could be sprayed in a cold condition because a trial experiment had shown that the best distribution and coating were obtained with this dilution (after a spraying and mixing pass of the pulvimixer alone). The highly alkaline water available on the site, however, precluded any form of dilution because the acidic emulsifier reacted immediately with the water, which caused the emulsion to break. The viscous, cationic bitumen emulsion was therefore heated to lower its viscosity and sprayed in the same manner as the cutback binders.

Mixing of Stabilized Sand With Motor Grader

An inspection of the stabilized sand after the mixing operation with the pulvimixer showed that the coating of the sand particles was still not adequate. Further mixing with the pulvimixer would have delayed the progress of the work and so mixing by means of a motor grader was begun as soon as possible after the pulvimixer had completed the last mixing run. The high shearing action of the motor blade, producing a spiraling motion of the material during the cutting operation, was very effective in improving the coating of the sand particles. There was a significant improvement in the appearance of the mixture after each passage of the grader, and adequate coating resulted after two movements of the material from one side of the carriageway to the other.

Finally, the grader leveled the now homogeneous mixture to an even, loose thickness.

Aeration of Mixtures

The laboratory control measures used during this experiment indicated that aeration was essential to obtain the high stabilities required for the traffic that would use the road.

Controlled aeration was therefore carried out with a disc harrow pulled by a pneumatic-tired tractor. The discs were set to cut to the full depth of the loose layer. During aeration, the resistance of the mixture to the movement of the discs increased; this became evident when the tractor required more power to maintain a constant forward speed.

The aeration was continued until laboratory tests showed that the mixture had reached the condition at which maximum stability would be obtained on compaction.

Compaction of Mixtures

The most satisfactory compaction plant was a 30-Mg pneumatic-tired compactor (fully ballasted), used with a sheepsfoot roller. The sheepsfoot roller was fitted with a cleaning device to avoid excessive pickup of material during compaction. The individual feet measured

21 by 13.5 cm and were arranged in 24 rows of four, around the periphery of each roller drum. If it is assumed that four feet made contact at one time, the pressure per foot was 1.31 MPa when the roller drums were fully ballasted.

Various methods of compaction were tried, but since they all resulted in similar densities, the most practical method was chosen. This consisted of compacting in approximately 50-mm lifts by using the pneumatic-tired compactor and the sheepsfoot roller while a motor grader spread uncompacted material over the already compacted layer. It is important to obtain a good bond between the successive lifts, and the impressions left by the sheepsfoot roller assisted in this. Compaction was achieved by a continuous operation with a final leveling of each section with the motor grader. Each section was given a minimum of eight complete coverages with each compactor.

The sections containing calcareous filler and sand were compacted to such high stabilities that the motor grader had difficulty in trimming the material to the final profile required and, in some cases, an imperfect finish resulted. This difficulty was not experienced where only sand was stabilized, as these mixtures were more workable.

On completion of the experiment and before opening the sections to traffic, in situ density measurements of each section were made in duplicate by the sand replacement method. The densities obtained on the 152.4-mm-deep sections were fairly consistent, varying generally between 1794 and 1826 kg/m^3. Sections 3 and 4, which were 76.2 mm deep, however, had densities of between 1700 and 1715 kg/m^3, i.e., significantly lower than those for the 152.4-mm-deep sections.

Surfacing and Opening of Sections to Traffic

On completion of the stabilized base sections, the type of surfacing to be used to protect the base material was considered. Because of the high stability of most sections, it was decided that initially only a light sand seal should be provided; the position could be reviewed if the traffic caused serious rutting of the weaker sections.

Sufficient cutback bitumen binder was available on site for all of the surfacing and so a blend of equal quantities of the two types of cutback bitumen used for the stabilization work was used for the sand seal. The rate of application varied between 1.37 and 1.76 L/m^2. The application of the sand to the binder film was delayed to enable the cutback binder to penetrate into the stabilized sand base and to allow the viscosity of the binder remaining on the surface to increase, which gave a more stable surfacing layer. The same wind-blown sand that was used for the base stabilization was used for the surfacing and was spread at approximately 0.0065 m^3/m^2 and then well-rolled with a 15-Mg self-propelled pneumatic-tired roller.

Traffic was not allowed onto the sections until June 21, 1965, so that the sections laid toward the latter part of the experiment could set sufficiently and thus not be at a disadvantage during the initial trafficking. This light surfacing was overlaid with a 30-mm thick asphalt-concrete surfacing in mid-1967; it was therefore in service for a period of 2 years.

Placing of Level Pegs for Future Observations

Purpose-made pegs were placed in lines transversely across each section at distances of 30.5 and 61 m from the beginning of each section. The pegs were spaced at 304-mm intervals.

Level observations were made before trafficking and at regular intervals after trafficking. A number of permanent bench marks were installed so that all precise level observations could be compared in relation to a common datum. When the asphalt-concrete surfacing was placed in 1967, the level pegs were replaced in exactly the same positions as the original pegs and releveled.

LABORATORY CONTROL DURING LAYING OF EXPERIMENT

Sampling Mixtures

Representative samples of the mixed material were taken with a sampling tool that consisted of a 75-mm-diameter thin-walled aluminum tube that was introduced vertically into the loose mixture to make contact with the firm working platform. On withdrawal, the mixture remained in the tube and could be extruded into a suitable container. Samples were taken at the following times: (a) after blade mixing (before the beginning of the aeration) and (b) before compaction (after the aeration was complete). These samples were analyzed for the residual binder and fluid contents, and generally close agreement with the designed binder content was found.

A certain amount of intermixing of material from adjacent sections was unavoidable during construction; the first and last 15 m of each section were therefore not sampled.

Field Test to Establish When to Compact Mixtures

In the field, the strength of the mixtures produced could be evaluated by a vane shear apparatus. These tests also made it possible to establish when a particular mixture was in the optimum condition for compaction (11).

Accelerated Aeration of Field Sample

The technique followed was to first obtain a representative sample from the road as soon as the blade-mixing operation was complete. This sample was then divided into at least eight portions, each weighing approximately 6 kg. Each portion was placed in a tray of approximately 1-m^2 area and left to aerate in the sun. Gentle agitation of the mixture in the trays accelerated the aeration process. The material from each tray was tested after various periods of aeration by the following procedure:

1. The mixture from the tray was compacted in a CBR mold under modified AASHO compaction.
2. After compaction, the wet density of the compacted material was determined.
3. The compacted sample in the mold was introduced into the vane shear apparatus, which was fitted with a special base plate to retain the CBR mold.
4. The shear strength of the mixture was determined with the vane shear apparatus, and the temperature of the mix was measured at the middepth of the vane (Figure 3a).
5. After shearing, a representative sample of the mixture from the mold was analyzed for fluid content by evaporating the volatile oils and water.

The binder content of the mixture tested was determined from field measurements. The constitutions of the cutback binders and emulsion were known from previous laboratory tests in terms of residual binder and volatiles (oils or water) on a mass basis. From these

data, it was possible to calculate the dry density of the compacted bitumen-sand mixture.

The dry densities and the vane shear strengths converted to 40°C were then plotted against the fluid contents. Typical results for mixtures with 6.0 percent (nominal) cutback bitumen (80 to 100 penetration base) MX, sand, and 15 percent calcareous filler (section 6) are given in Figure 4. Both the density and the shear strength pass through maximum values. To achieve maximum stability of the mixture, the highest possible shear strength and density should be obtained when compaction takes place. However, the peak of the shear strength curve always occurs on the dry side of the maximum density, so that it is not possible to obtain both maximum shear strength and maximum density at a particular fluid content. Eighty to 90 percent of the maximum shear strength and 95 to 100 percent of the maximum density were chosen as a suitable compromise for the sand used, and this criterion was used to establish the time when compaction of the mixture on the road should take place.

Field Aeration Control and Subsequent Compaction

Control of the aeration process on the road was achieved by taking regular samples from the road mix and testing these for shear strength and density. The shear strengths were converted to 40°C values by using factors determined from laboratory and field tests. The values for section 6 shown in Figure 4 indicate the good correlation between field and accelerated test values. The fluid content at which compaction was begun on the road is also shown.

Temperature Records at Experiment Site

A clockwork temperature recorder was installed during the experiment and again later for obtaining long-term temperature records at the site. Thermocouples were

Figure 3. Measurement of vane shear strength of bituminous-stabilized sand: (a) in field laboratory and (b) on pavement.

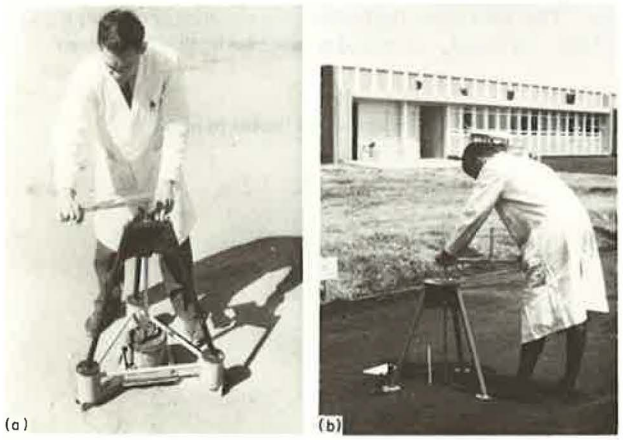

Figure 4. Dry density, vane shear strength, and fluid content relationships (section 6).

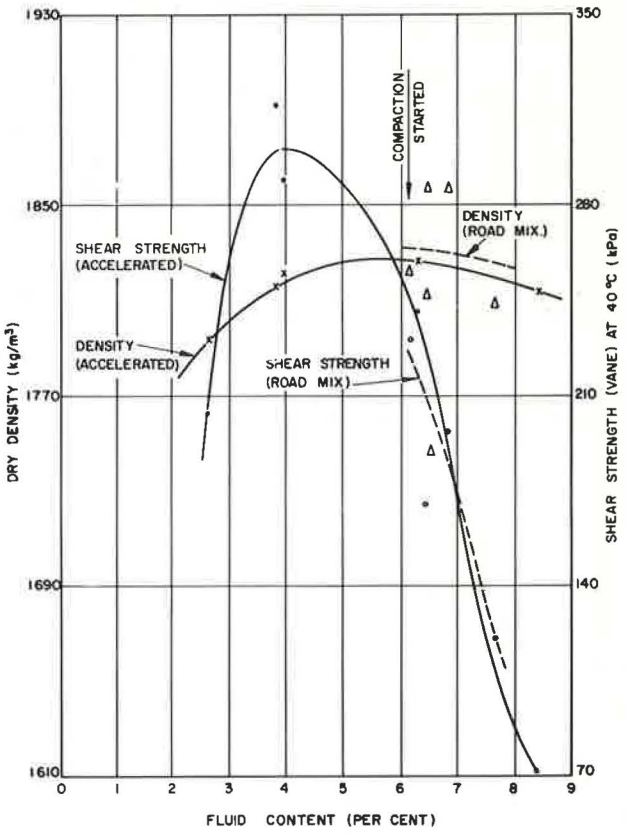

Table 1. Vane shear strength of experimental bituminous-stabilized-sand bases.

Stabilizer	Section No.	Binder Content (%)	Filler Content (%)	Vane Shear Strength (KPa) at 40°C After		
				Compaction	1 Year	2 Years
MX cutback bitumen	12	4.0	0	80	230	305
	5	4.0	15	125	346	415
	1	6.0	0	60	185	224
	13	6.0	0	60	178	255
	2	6.0	15	64	242	315
	6	6.0	15	90	286	405
Cutback bitumen [rapid-to-medium cure (250)]	14	4.0	0	68	240	318
	7	4.0	15	230	373	495
	15	6.0	0	54	210	305
	8	6.0	15	175	255	390
Cationic bitumen emulsion	16	4.5	0	50	170	235
	9	4.5	15	168	280	345
	17	6.5	0	25	180	242
	10	6.5	15	130	280	314
Cutback tar (30 to 35°C Evt)	18	6.0	0	44	150	226
	11	6.0	15	98	380	555

placed at depths of 0.75, 150, and 300 mm below the surface of section 6. Maximum and minimum road surface temperatures on a hot summer day in February 1966 were 70 and 24°C. On the same day, the maximum and minimum temperatures were 52 and 34°C at a depth of 150 mm.

FIELD STUDIES

Setting Up of Bituminous-Stabilized Sand Mixtures

To study the setting-up pattern of the bituminous-stabilized-sand mixtures, shear strength measurements were made on the sections with the vane shear apparatus (Figure 3b). These measurements were carried out at intervals after completion of the work, up to the time of laying the asphalt-concrete surfacings (1967), and all vane shear strengths were converted to values at 40°C (standard temperature).

The vane shear strengths of the mixtures for various periods of time are given in Table 1. All of the mixtures gained significantly in shear strength with time. This gain in strength was fairly linear over the 2-year period. On the average, the mixtures containing sand only increased in shear strength by a factor of approximately 5.3 and those with sand and calcrete filler by a factor of approximately 3.6, i.e., annual increases in shear strength of 225 and 125 percent respectively.

The change in binder content did not have a significant effect on either the shear strengths of the various mixtures or their rate of gain in strength with time. However, the addition of 15 percent powder calcrete to the sand had a significant effect on the shear strengths of the mixtures; mixtures with calcrete filler had shear strengths from 1.1 to 3 and about 1.5 times those of the sand-only mixtures after compaction and after the 2-year period respectively.

Figure 5. Relation between vane shear strength and deformation under traffic after 8-year service of bituminous-stabilized-sand bases.

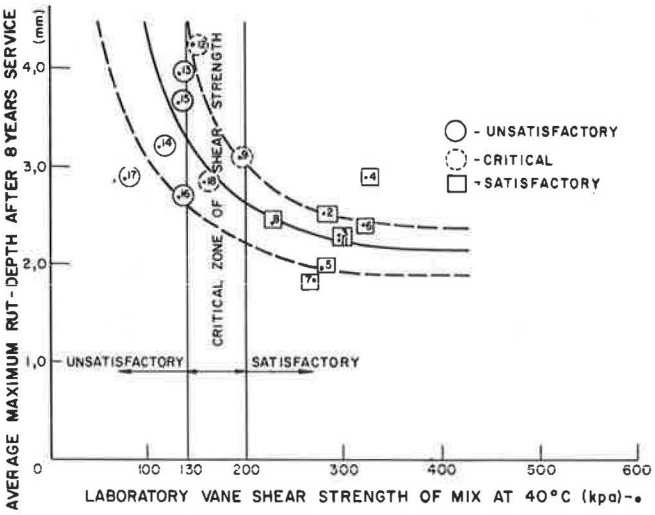

Figure 6. Crack indexes of sections.

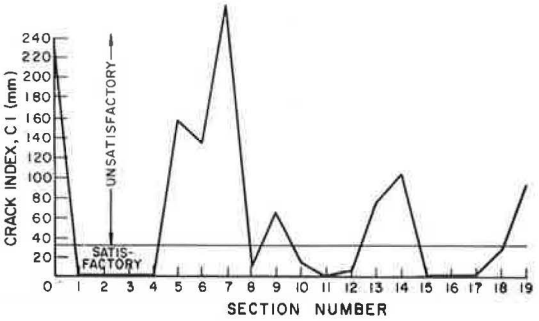

Structural Tests

Various structural tests were carried out on a selected number of these experimental sections toward the beginning of 1966; those results were reported by Gregg and others (13) and will therefore not be covered in this paper.

Deformation Measurements

The precise level observations for the 8-year service period have shown that, significantly, the deformation that occurred during the 6-year period after the laying of the 30-mm-thick asphalt-concrete surfacing was very much less than the deformation that occurred during the preceding 2-year period, particularly in those sections that deformed excessively (>10 mm), viz., sections 16 and 18.

To investigate whether there was any relationship between the laboratory, vane shear strengths of the mixtures at the time of construction and the subsequent permanent deformation (the average maximum rut depth between the inner and outer wheel tracks) measured after an 8-year in-service period, these results were plotted as shown in Figure 5. These data gave a reasonable envelope of laboratory, vane shear strength versus rut depth. The data also indicated which mixtures were satisfactory, critical, or unsatisfactory with respect to

Figure 7. Extrapolation of measured rut depths to higher axle-load regimes.

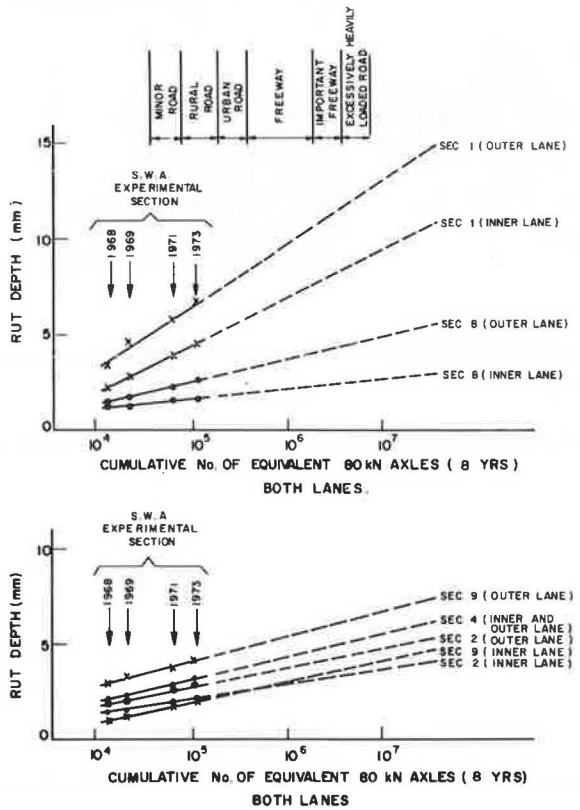

Figure 8. Prediction of maximum permissible tensile strain levels for different traffic categories.

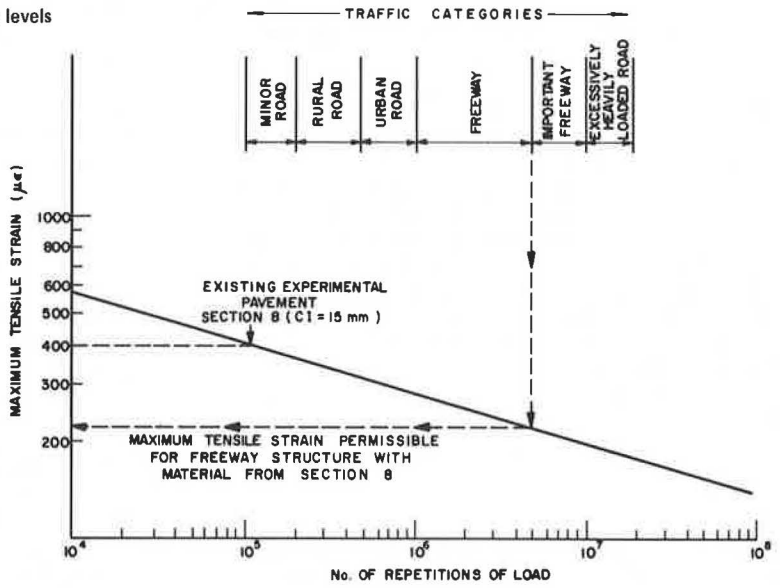

permanent deformation: Those with laboratory, vane shear strengths between 130 and 200 kPa were regarded as critical, those above 200 kPa as satisfactory, and those below 130 kPa as unsatisfactory. The major external factors affecting permanent deformation on a particular bituminous material are traffic, rate of loading, and temperature, and it is not a simple matter to extrapolate the results from a given condition to a new situation if one or more of these major factors is different. However, techniques have recently become available for this purpose if the material properties are well characterized. These techniques were applied to this experiment in an attempt to predict the deformation likely to occur in similar materials under the heavier traffic conditions of a rural freeway; they are discussed later.

Cracking of Sections

A visual survey of the sections was made in 1973 (after 8 years service) to assess the extent of cracking on the different sections. A crack index (CI) (14) was developed for this purpose where

$$CI = \sum_{\substack{\text{all} \\ \text{patterns}}} (\text{percentage of area covered by cracks}) (\text{average width of cracks in mm}) \quad (1)$$

The parameters of the spacing and the length of the cracks are not included in this definition. In the case of block and chicken-mesh cracking the area affected can usually be determined. However, a difficulty arises in the case of longitudinal and transverse cracks: When only a few such cracks appear, engineering judgment must be used to assess their effect on the pavement structure.

The CI gives an indication of the severity and area covered by cracks, regardless of the pattern. The CIs for the various sections, including the control sections (0 and 19) on which a lime-treated calcrete base was used, are shown in Figure 6.

It is interesting to compare the results shown in Figures 5 and 6 and to note the opposite trends in performance of some sections with respect to deformation and cracking; e.g., section 12 has the highest deformation and a very low CI and section 7 has a low deformation and a very high CI. This type of behavior is, of course, expected and points to the problem facing the highway engineer in selecting a suitable material that will give good performance in both deformation and crack resistance. Sections 2, 3, 4, 8, 10, and 11 performed acceptably and may be used with confidence for a pavement carrying similar traffic under a similar climatic environment.

CONCLUSIONS FROM EXPERIMENTAL PAVEMENT

In terms of the objectives of the experiment, it can be stated that

1. It is feasible to construct in situ bituminous-stabilized-sand bases that will give satisfactory performance for a highway pavement by using the following binders: (a) MX special cutback bitumen, (b) cutback bitumen manufactured from a 40 to 50 penetration bitumen [rapid to medium cure (250)], (c) cationic emulsion, and (d) cutback tar (30 to 35°C Evt grade), [if the sand is mechanically stabilized by the addition of 15 percent powder calcrete (calcareous filler)];
2. The two 76.2-mm-thick bituminous-stabilized-sand sections (3 and 4) gave excellent performances and stand out as the most successful sections laid, from the points of view of both economy and performance;
3. The performance of the section containing a blend of calcareous filler and sand laid on a sand-clay subbase (section 2) was acceptable, and for similar traffic conditions, this type of structure is worth serious consideration because it would be economically advantageous; and
4. All of the bituminous-stabilized-sand bases increased in shear strength with time (for the 2-year period that measurements were made).

EXTRAPOLATION OF PERFORMANCE RESULTS TO HEAVIER TRAFFIC CONDITIONS

The design and particularly the construction of existing pavements have already provided a wealth of experience and information. The extrapolation of analyses of existing material to new pavements should not be neglected simply because the test methods used are considered inadequate to characterize the pavement by current standards. In general, extrapolation has not been widely

used, primarily because new and more advanced methods of testing and evaluating materials are continually being developed.

An alternative approach is to use the results of in situ tests to characterize existing pavements as well as possible. These data can then be extrapolated to other conditions on the clear understanding that the extrapolations are guidelines with which engineers can supplement their existing knowledge. In this context, existing experimental and prototype test pavements are normally the best to use, because a number of variations are usually incorporated in the experiment and a well-defined program of testing is carried out. The experimental sections described in this paper are an example of this type. One of the main aims of these experimental sections was the determination of the behavior of bituminous-stabilized-sand bases under the environmental and traffic conditions pertaining to this road.

Pavement Deformation

Precise level determinations of permanent deformation were made for each of the experimental sections of the road. These measurements were originally made in 1967 to establish a datum line and then repeated in 1968, 1969, 1971, and 1973. The maximum rut depths in the inner and outer lanes were determined from the measurements. Semilog plots of rut depth versus cumulative number of equivalent 80-kN axle loads for some of the experimental sections are shown in Figure 7.

The amount of heavy traffic on these sections was small, about 0.1 million equivalent heavy axles over the 8-year test period. However, the few heavy axles borne by the section during this period were usually loaded more than the legal limit.

In Figure 7, the rut depth has been extrapolated to a higher number of 80-kN axles by using a linear-log relationship (14). From this relationship between rut depth and number of equivalent 80-kN axles, it appears that the base mixtures used would give reasonably acceptable values of rut depth even under freeway traffic conditions (i.e., 1 million to 10 million equivalent axles).

The conditions under which the extrapolation will remain valid are

1. That no major variations in the environmental conditions occur, other than those that have already occurred over the previous 8 years,
2. That the behavior of the bituminous materials does not go into the shear failure zone, and
3. That the deformation behavior of the bituminous materials used is not as dependent on their stress history as is that of, e.g., unbound granular materials.

The first condition is perhaps the most unpredictable. There are also other unpredictable factors, e.g., cracking of the surfacing and base, which could allow ingress of surface water to the subbase and result in excessive deformation.

Three zones can be identified in the deformation behavior of bituminous-based mixtures to repetitions of load. In zone 1, there is initial deformation, but no further increase; in zone 2, the deformation increases at a constant rate; and in zone 3, excessive shear begins to take place.

The conditions under which zone 3-type deformation will occur can be studied by investigating the cohesion (c) and the angle of internal friction (ϕ) of the material under the appropriate test conditions.

A study of this nature was carried out by using an extreme case of dual wheel loading with double the legal axle load (2 times 40 kN). Under these conditions, the base material should have a c-value greater than 35 kPa and a ϕ-value greater than 27° (at 40°C) to prevent zone 3 deformation. An analysis of the stress states of the 150-mm-thick bituminous layer showed that, except for a small area under the wheel loads at the 150-mm depth, the material remained in the satisfactory zones of deformation. This condition is not considered important from a practical point of view because of the extreme loading conditions chosen.

Fracture (Fatigue Cracking)

It is also desirable to estimate the cracking that can be expected if a similar base mixture is used in another pavement with different loading conditions. At present, the degree of cracking is known for specific sections of the SWA experiment after 8 years of trafficking. Section 8, for example, has a CI of 15 mm, which means that 15 percent of the area has cracks 1-mm wide, after 100 000 load repetitions. This degree of cracking is acceptable even for freeways. However, to achieve this level where there is a greater volume of equivalent 80-kN axles, the maximum tensile strain at the bottom of the base layer must be reduced. The amount by which it must be reduced can be determined from the fatigue behavior of the material, as shown in Figure 8. From knowledge of the tensile strain computed for the conditions at the pavement section (in the case of section 8, 400 microstrains) and of the traffic, a point on the strain-versus-load-repetitions (ϵ-N) line can be established. The slope of the (ϵ-N) line representing the material used for the base was taken to obey the formula given by Brown and Pell (15). This relationship can be determined either by measurement or by the average values used (14, 15). In Figure 8, the average value for the slope of the line was used. In the case of section 8, the maximum permissible strain level is approximately 210 microstrains.

A reduction in strain at the bottom of the base can be achieved either by increasing the modulus of the subbase (i.e., by increasing the CBR or by stabilization) or by increasing the thickness of the base layer. Structural analysis using elastic theory is an effective method of determining the upgrading of the pavement that is necessary to avoid fatigue cracking of the base material.

ACKNOWLEDGMENTS

The investigation was carried out as part of the National Institute for Transport and Road Research (South Africa) approved research program, and the paper is published by permission of the director.

The assistance of the South West Africa Roads Department is gratefully acknowledged.

REFERENCES

1. H. Korn and H. Martin. The Pleistocene in South West Africa. Proc., 3rd Pan-Africa Conference on Prehistory, Livingstone, Chato and Windus, London, 1975, pp. 14-22.
2. F. Netterberg. Calcrete in Road Construction. National Institute for Road Research, CSIR, Pretoria, South Africa, Bulletin 10, Res. Rept. 286, 1971.
3. C. P. Marais. Report on Small-Scale Experiment to Test Bases of Bituminous-Stabilized Sand at the NIRR Test Site, Silverton, Nov. 1964. National Institute for Road Research, CSIR, Pretoria, South Africa, Rept. RB/1/65, June 1965.
4. C. P. Marais. Report on a Full-Scale Road Experiment to Test Bases of Bituminous-Stabilized Sand on the Tsumeb-Ondangua Route, South West

Africa, Constructed in May 1965. CSIR, National Institute for Road Research, Pretoria, South Africa, Rept. RB/7/65, Oct. 1965.
5. J. A. Mabbutt. Report on Visit to Ovamboland, South West Africa, in Connection With Calcrete Problems, April 14 to 16, 1965. CSIR, National Institute for Road Research, Pretoria, South Africa, Rept. 1965.
6. Report of the Commission of Enquiry Into South West Africa Affairs (1962-1963), p. 15.
7. J. H. Mortimer. Summary of the Vegetation of Ovamboland and the Okavango Region. CSIR, National Institute for Road Research, Pretoria, South Africa.
8. Asphalt Pavement Design for National Roads, 1970. CSIR, National Institute for Road Research, Pretoria, South Africa, June 1971.
9. I. L. Jamieson and M. M. Hattingh. The Correlation of Chemical and Physical Properties of Bitumens With Their Road Performance. Proc., 5th Conference of the Australian Road Research Board, 1970.
10. C. P. Marais and I. L. Jamieson. The Performance of 80/100 Pen. Straight-Run and Air-Rectified Bitumens. Trans., South African Institute of Civil Engineers, Vol. 12, No. 9, Sept. 1970, pp. 203-210.
11. C. P. Marais. A New Technique to Control Compaction of Bitumen-Sand Mixes on the Road Using a Vane Shear Apparatus. Trans., South African Institute of Civil Engineers, Vol. 8, No. 3, March 1966, pp. 87-94.
12. R. H. Williamson and C. P. Marais. Pavement Temperatures in Southern Africa. Trans., South African Institute of Civil Engineers, Vol. 16, No. 8, Aug. 1975, pp. 203-214.
13. J. S. Gregg, G. L. Dehlen, and P. J. Rigden. On Properties, Behavior and Design of Bituminous-Stabilized Sand Bases. Proc., 2nd International Conference on the Structural Design of Asphalt Pavements, Ann Arbor, Mich., Aug. 1967, pp. 863-882.
14. C. R. Freeme and C. P. Marais. Traffic Load Associated With Cracking of Asphalt Pavements. Proc., 2nd Conference on Asphalt Pavements for Southern Africa, Durban, CSIR, Reprint 166, 1974, pp. 1-135 to 1-151.
15. L. Brown and P. Pell. Repeated Loading of Bituminous Materials. Proc., 2nd Conference on Asphalt Pavements for Southern Africa, Durban, CSIR, Reprint 166, 1974, pp. 3-28 to 3-50.

Publication of this paper sponsored by Committee on Soil-Bituminous Stabilization.

Ponding an Expansive Clay Cut: Evaluations and Zones of Activity

Malcolm L. Steinberg, Texas Department of Highways and Public Transportation

The use of ponding water on a clay subgrade of high swelling potential to cause soil heaves before pavement placement was successful on an expressway project outside San Antonio, Texas. Expansive soils are a worldwide problem and cause over $2 billion damages/year in the United States. Their effectiveness of controlling the clay was measured, and the depth of the movements was determined. Observations began in 1968 and continued through 1976, both inside and outside the ponded area. The elevation rods were set at depths of 0.6 to 5.8 m (2 to 19 ft), and the moisture measurements were taken in the same zones. The ponding generally resulted in an upward movement of the elevation rods. The maximum movement was that of the shallower set rods in all areas. It now exceeds 0.12 m (0.42 ft) in the area where the predicted vertical rise is 0.15 m (0.5 ft). The moisture variations were greatest at depths up to 3 m (10 ft), where the rods exhibited maximum movement. This was the zone of activity. Pavements in the ponded areas have shown less distress and less major cracking and have required less major maintenance work than those in the nonponded areas. The relation of rainfall measurements to rod movements is not definitive. A trend may be developing that shows upward movement to follow rainfall after prolonged dry periods. Ponding does seem to help curb the destructive movements of expansive clays.

Expansive soils are an international problem. They are also expensive problems, costing the United States more than $2.2 billion in 1973 (1). They have been studied extensively (2, 3, 4, 5, 6, 7). In Texas, expansive clays extend in a corridor from the northern borders with Oklahoma and Arkansas almost to the Rio Grande River and Mexico in the south. They usually lie along the Wichita Falls, Dallas, Fort Worth, Austin, San Antonio line. The clays present fewer problems in the eastern areas of the state, where higher rainfall rates tend to keep subsoil moistures uniformly higher. In the areas west of San Antonio and Austin, the Balcones escarpment and the upland area contain more limestone and less expansive clay.

In 1968, the Texas Highway Department, now the State Department of Highways and Public Transportation, began planning improvements to US-90 west of San Antonio. This highway lays over an expansive clay area, and multiple control measures were considered. Ponding and the installation of a lime-treated moisture seal and an underdrain were chosen. The department, in cooperation with the Federal Highway Administration and the Center for Highway Research at the University of Texas, also decided to measure the effectiveness of these techniques, and to find the depths at which the movements of these clays and the moisture changes take place. The work was initially reported as part of the center's series on expansive clays (8).

SITE AND ITS GEOLOGY

US-90 is a transcontinental route. It passes through the San Antonio area where the movement of expansive clays has long been observed. This highway project, where the ponding was used, begins at I-410 on the southwest

boundary of San Antonio and extends just beyond the city's outer loop (FM-1604).

The area is a Pleistocene high-terrace deposit overlying the Taylor formation. In the ponding areas, this formation is a greenish-gray calcareous nodular clay that extends at least 6.1 m (20 ft) below the bottom of the proposed FM-1604 cut. About 1.5 m (5 ft) of the terrace gravel was left on the site at the east boundary of the ponded area.

X-ray diffraction analyses were made of two samples within the ponded area by the Bureau of Economic Geology at the University of Texas at Austin. A sample of clay from the base of the gravel at station 242+00 was 35 percent calcium montmorillonite, 50 percent illite, and 15 percent kaolinite and chlorite. A second sample, taken from a depth of 4.6 m (15 ft) at the other end of the site, was 30 percent calcium montmorillonite, 60 percent illite, and 10 percent kaolinite and chlorite.

SOIL PROPERTIES

A soil profile developed from area sampling is shown in Figure 1. The following data reflect samples taken from stations 170 to 258:

Property	Range	Avg
Liquid limit, %	46 to 109	69
Plastic limit, %	20 to 44	28
Shrinkage limit, %	7 to 19	14

PROJECT

The contract called for building a four-lane divided highway with frontage roads, grade separations at three locations, and span structures at Medio Creek. The grade separation of US-90 and FM-1604 involved the construction of an underpass as a part of a diamond interchange. Exploratory core drilling reaffirmed the presence of expansive clays, and by using McDowell's method of determining the potential vertical rise (PVR), the expected movement was calculated. The removal of 8.2 m (27 ft) of material in the excavation added rebound to the reactions of the expansive clay. The area to be ponded extended from station 245 to station 270 and covered the section up to 0.9 m (3 ft) on the backslope. Ponding was to be continued for a 30-d period. A moisture seal was to be placed by using 0.15 m (0.5 ft) of lime-stabilized subgrade.

Two other measures were added to minimize pavement distress. A strata of gravel removed as part of the interchange excavation was stockpiled and spread 0.45 m (1.5 ft) deep over the lime-stabilized moisture seal in the ponded area. Where some of the gravel remained at the east end in the finished subgrade section, 0.15-m (0.5-ft) diameter underdrains were placed beneath the centerlines of the outside main-lane ditches.

Instrumentation

Different types of devices were used to make the elevation and moisture measurements. Elevations were developed from rods embedded at depths of 0.6, 1.4, 3.2, and 5.8 m (2, 4.5, 10.5, and 19 ft) and read with a level rod. The elevation rods were 1.2-cm (0.5-in) galvanized water pipes with a 7.5-cm (3-in) auger plate welded on the bottom. The pipes were placed in 0.2-m (8-in) casings which were set in holes drilled 0.23 m (9 in) in diameter to depths of 0.5, 1.2, 3.1, and 5.6 m (1.5, 4, 10, and 18.5 ft) below subgrade. The space around and inside the 0.2-m (8-in) pipe was packed with automobile-chassis grease. The auger plate and the 1.2-cm (0.5-in) pipe were advanced 0.15 m (6 in) into the ground at the bottom of the grease-filled hole, with the top of the pipe extending about 0.5 m (1.5 ft) above the casings. The entire assembly was protected by a 1.2-m (4-ft) long section of 0.3-m (1-ft) clay pipe, which was capped (Figure 2). A variety of evolutionary measuring rods and nuclear access tubes were also set for moisture and density readings. More conventional moisture measurements were made by drilling samples with a rotary bit and conducting laboratory tests.

Contract Work

Work on the contract began on January 21, 1969. Excavation for the FM-1604 interchange began in June 1969 and initially included only the northern two-thirds of the cut. The rest remained so that traffic could use the existing pavement. Frontage roads were built to carry the future detour route. The first sets of elevation rods were placed before the ponding. They were located in the median area at stations 241, 245, 250, and 255. Each set consisted of four rods set at the different depths. The first readings were taken in December 1969.

The first group of 33 dikes were built the following February. They were spaced 15 m (50 ft) apart, usually at a 45° angle with the centerline following the contour line of the section. The dikes were usually 0.9 m (3 ft) high and 1.2 and 0.3 m (4 and 1 ft) thick at their base and top respectively. They were about 53 m (175 ft) wide and filled with water from a 244-m (800-ft) deep well with a pump.

Ponding began on March 3, 1970, and was completed by draining on April 7. Liming operations for the moisture seal were completed by May.

The rod readings and the moisture determinations indicated substantial increases in elevations of the rods set at shallow depths and considerable moisture variations and so the limits of the ponding were increased by 91.4 m (300 ft) to cover another area of anticipated significant potential swell and to expand the test sites.

The three new test sites in the ponded areas were in the portion of the interchange excavation about 30 m (100 ft) south of those in the median. The control sites were located in the median outside the ponded areas. The excavation on the south side of the interchange was completed in January 1971, a year after the first sections. Ponding began shortly afterward, with the first section completed in February. The placement of the lime and the stockpiled gravel was completed in July, and the construction work was completed on November 12, 1971. The originally estimated quantities of ponding were 36 900 m^3 (9 733 000 gal) covering 72 000 m^2 (88 981 yd^2). After the field change, the estimate was revised to 46 300 m^3 (12 200 000 gal) covering 88 000 m^2 (110 621 yd^2) at a bid price of 0.16¢/m^3 (0.0006¢/gal). The final quantity was 71 300 m^3 (18 831 000 gal) costing $11 298.60.

OBSERVATIONS

The readings of the moisture data began in April 1968 and those of the elevations in December 1969 and have continued semiannually. Some of the measuring locations have been lost, and others have been destroyed. Among these were the nuclear tubes. Whether their thin shells were unable to resist the extensive pressures or whether the upward movements of the soils covered them over is unknown. Only the pipes with the protective jackets remain identifiable today. A road surface inventory has given further indications of the effectiveness of the pondings. A series of profilometer readings have also been made, but an analysis of their relationship among the sections has not been completed.

Rod Readings

Generally, the ponding caused an upward movement in the elevation rods. This was most pronounced in those set 0.6 and 1.4 m (2 and 4.5 ft) deep, i.e., the shallower rods, and most clearly indicated in the rods set in the ponded median areas. With time, this movement was reflected to a lesser degree in the deeper set rods. No movements greater than 1 cm (0.4 in) were read in the rods set at the 5.8-m (19-ft) depth for more than 4 years. This is typically shown in the group at station 245 (Figure 3).

The control rods have also developed upward movements. At station 241, this did not occur until 2 years after the subgrade was shaped and the pavement placed (Figure 4). The movement was greatest in the elevation devices set at the shallowest depths, 0.6 and 1.4 m (2 and 4.5 ft). In the other control group at station 173, no movement was recorded until 1972. There, readings were greater and continue to show more movement from the 1.4 and 3.2-m (4.5 and 10.5-ft) rods than from the shallowest one at 0.6 m (2 ft).

The movements generally take place in a zone of activity, which was usually to a depth of 3.0 m (10 ft) on this project. Readings for the rods set in the areas of the 1971 pondings indicated less upward movement than those in the previous year's ponding, but the patterns were generally the same.

In mid 1974, a pronounced change occurred in most readings. The direct reading indicated that the deepest rod had a decreased elevation. Either the movement had suddenly reversed itself or the bench marks were more affected by the clays than was the 5.8-m (19-ft) rod, which was insulated from movement by the grease. When the grades were adjusted so that the deepest rod reading reflected no change, the pattern of increased upward movement tended to be fairly uniform. (Anticipation of this problem of the movement of the standard bench marks was the reason why the program of calculating the adjusted reading was followed from the beginning of the project.)

Figure 1. Soil profile.

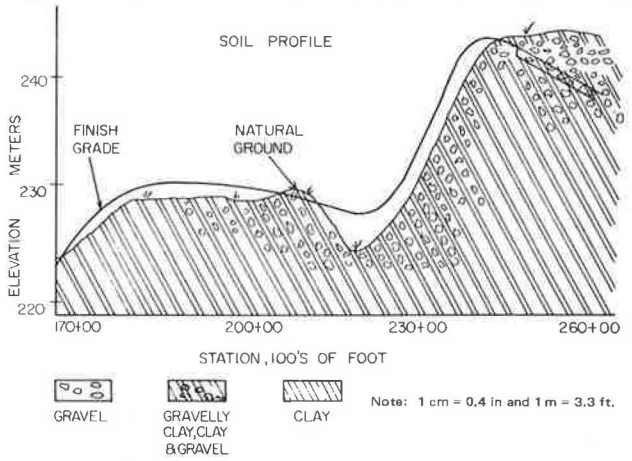

Figure 2. Elevation-rod device.

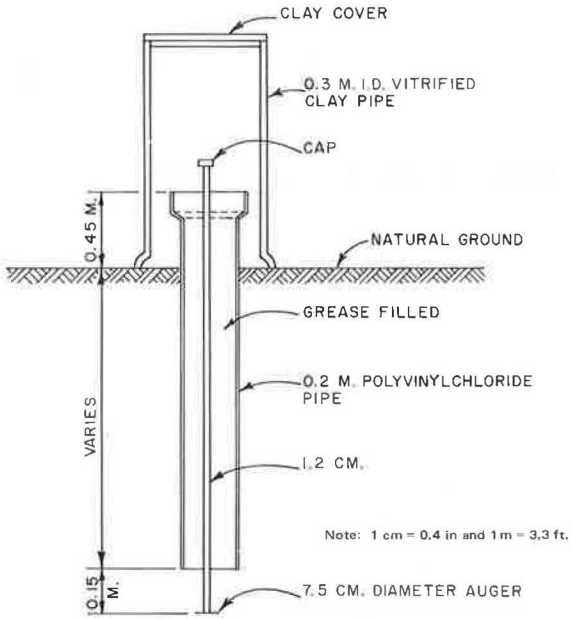

Figure 3. Vertical movement at station 245.

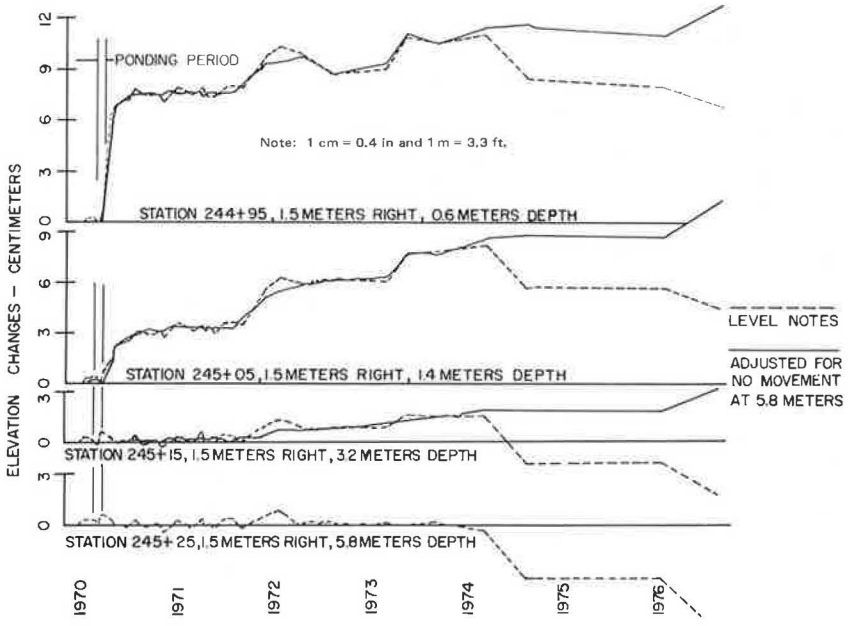

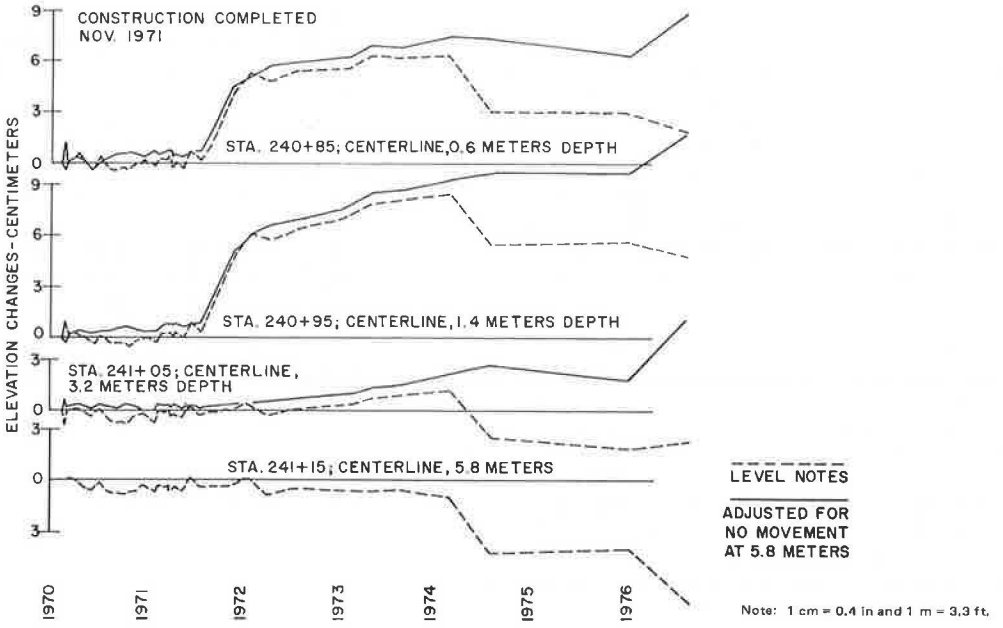

Figure 4. Vertical movement at station 241.

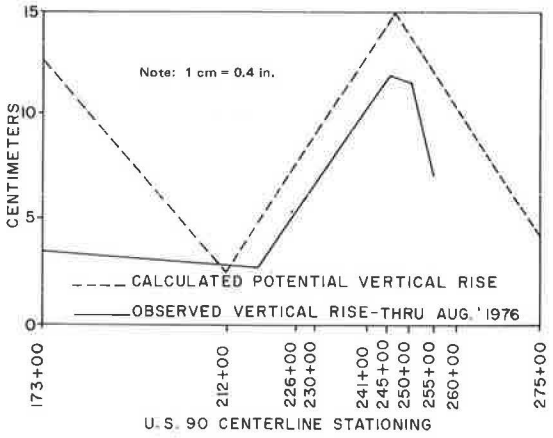

Figure 5. Vertical movements: calculated and observed.

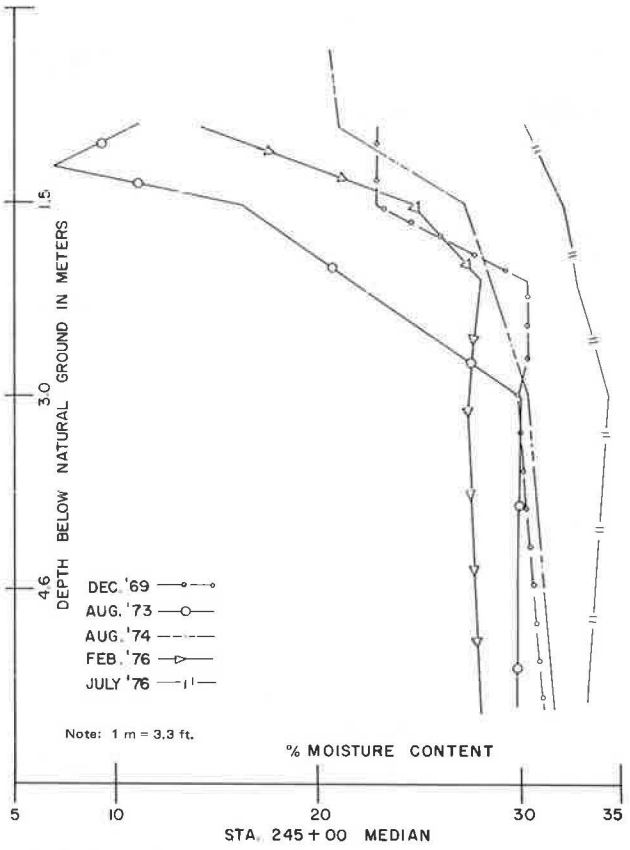

Figure 6. Moisture changes at station 245 (centerline).

Calculated Versus Observed Readings

On none of the rods has the actual maximum reading yet reached the calculated PVR. The movements seem to be approaching the calculated values if the adjustment to the 5.8-m (19-ft) rod is used. The rods in the stations 245 to 255 medians are now showing maximum upward movement close to the predicted PVR. The readings at station 173 have not come within that range, nor have the ones 30 m (100 ft) to the left of the centerline (Figure 5).

Moisture Contents and Depth

These readings cover a 9-year period. To avoid variations due to testing modes, they were all taken by the method of laboratory tests of drilled samples. They reflect a zone-of-activity pattern in which there is considerable change in the moistures (usually) down to 3 m (10 ft). They range from a low of close to 5 to a high of almost 35 percent (Figure 6). This was true for both the ponded and the unponded areas and as likely to occur in 1976 as in 1969. Below 3 m (10 ft), the samples showed much less variation. The range at that depth seemed to be from 24 to 28 percent at one site to 28 to 34 percent at others. Instead of the 30 percent moisture-content variations in the zone of activity, these deeper readings reflect changes of one-third that or less. Moisture changes seem to relate to elevation changes. Both have their maximums in the zone of activity.

Observations from the second ponded group, those set about 30 m (100 ft) from the median and first recorded in

Figure 7. Moisture changes at station 245 (30 m left of centerline).

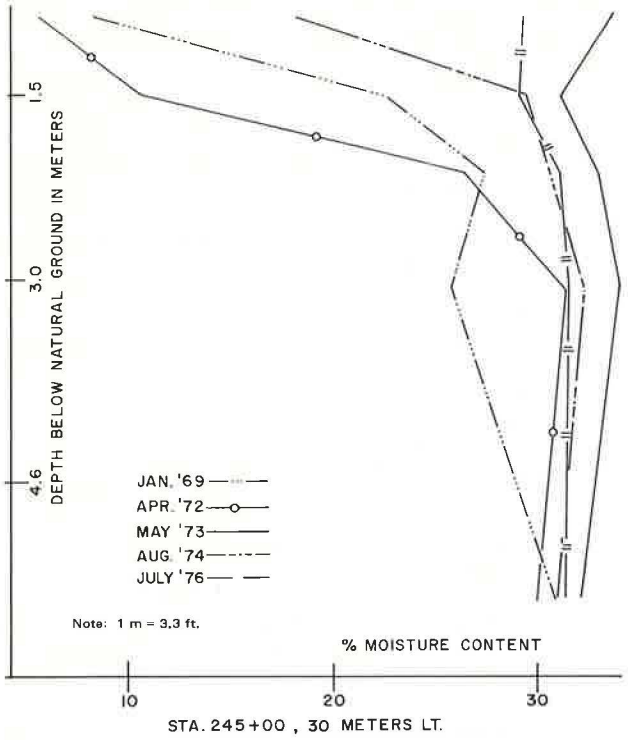

Figure 8. Road inventory.

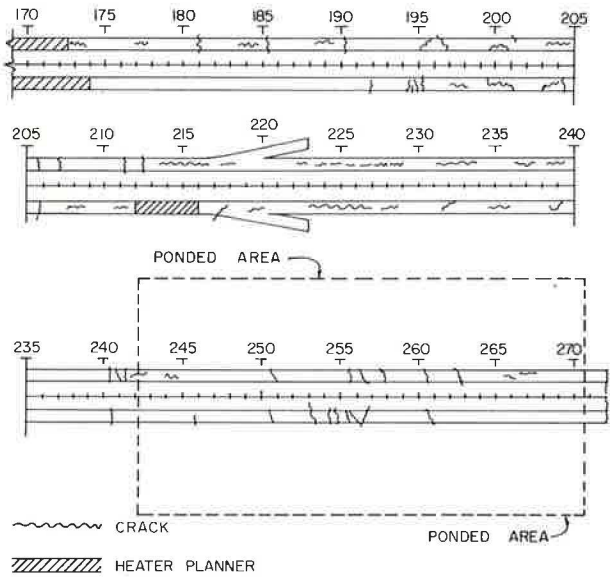

1969 indicate that they have less moisture variation below 3 m (10 ft) (Figure 7). Whether this diminished range of change is due to differences in the material has not been clarified. The soil profiles do reflect some variations. Other possible reasons are closeness to the slopes of the 6-m (20-ft) deep excavation and the fact that these latter sites were ponded shortly after excavation. However, the pattern is generally the same. Major moisture changes take place near the surface in the zone of activity, and the changes at the lower depths are relatively minimal.

The effect of ponding on these moisture contents was not clearly observed. This was due in part to the delay in testing that required moving heavy drilling equipment into the site. Nuclear measurements would have avoided this, but the loss of the tubes prevented them.

Road Conditions

A road inventory has been made through the test area in the last 2 years. The ponded area has shown less need for major repairs and less major cracking. Heater-planner work areas that indicate the need to reduce a significant swell in the roadway surface have been required only in nonponded areas.

Though cracking has occurred on roadway surfaces over the ponded subgrades, it has not been of a prolonged nature. The cracks that have occurred there are relatively short and usually transverse. The nonponded areas of the test section show more prolonged cracking, both longitudinal and transverse, and require heater-planner repair work. Recent records show the pattern that began to evolve in the first examination (Figure 8).

An attempt to relate some of these observations of roadway conditions to the elevation-rod movements showed that the greatest amount of pavement repair work and apparent distress was between stations 170 and 175, but that these sections had little rod movement compared to those from stations 242 to 255. However, the sections over the ponded areas had also made use of the select material of low plasticity index, which contributed to those pavements relative lack of distress.

The results of other ponding projects (8, 9) confirm the effectiveness of ponding in reducing pavement maintenance work. Roadway sections that are above ponded subgrades tend to have less pavement distress. In tests in Mississippi, the introduction of moisture by drilling reverse drains to put the water deeper into the clays indicated considerable benefits to the pavements in terms of low maintenance requirements.

Rainfall and Rod Readings

A pattern of upward elevation changes following rainfall is being examined by comparing plots of the rod readings to rainfall records from the U.S. National Weather Service at San Antonio International Airport, 32 km (20 miles) northwest of the project. Rains in this area are irregular with dry and wet periods, and those recorded at the airport are not necessarily the same as those at the site. With all of these limiting factors, the pattern is clouded. Surface cracking caused by an extended dry spell tends to allow rainfall to enter these openings, and the upward movements in the shallower rods can be attributed to these rains.

CONCLUSIONS

Ponding apparently caused the upward movement of elevation rods set at shallow depths. The movements continued in these clay soils after the ponding and in the nonponded areas. In the nonponded areas, the movements took place only after the pavement had been placed.

The moisture changes were greatest at the shallower depths. At depths below 3 m (10 ft), there was considerably less variation. The greatest rod movement generally took place in those set less than 3 m (10 ft) deep. This was also the area of maximum moisture change, the zone of activity.

In this area, pavement maintenance problems are occurring more frequently outside the ponded area. Problems in the ponded areas are less frequent and less serious than those outside. Ponding appears to have contributed to the reduction of these problems. This

confirms the reports of other engineers in other places. It appears that if the zone of activity could be isolated from moisture changes that affect its movements, then many maintenance problems might be avoided.

ACKNOWLEDGMENTS

The work in this study was performed cooperatively by personnel of the Texas State Department of Highways and Public Transportation, the Center for Highway Research of the University of Texas, and the Federal Highway Administration.

The contents of this report reflect my view, and I am responsible for the facts and the accuracy of the data presented. The contents do not necessarily reflect the official views or policies of any agencies or institutions mentioned.

Special note is made of the assistance of the late Gordon Watt, of Saskatchewan, Canada, who contributed a great deal in the first several years of this research.

The interest of all the agencies and their personnel involved is gratefully acknowledged.

REFERENCES

1. D. E. Jones and W. G. Holtz. Expansive Soils: The Hidden Disaster. ASCE, Civil Engineering, Vol. 43, No. 8, Aug. 1973, p. 49
2. G. E. Blight and J. A. DeWet. The Acceleration of Heave by Flooding. In Moisture Equilibria and Moisture Changes in Soils Beneath Covered Areas: A Symposium in Print, Butterworth, 1965.
3. G. M. Kassiff, M. Livneh, and G. Wiseman. Pavements on Expansive Clays. Jerusalem Academic Press, 1969.
4. T. A. Haliburton. Preliminary Planning. Interim Rept. 1, Subgrade Moisture Variations, School of Civil Engineering, Oklahoma State Univ., 1966.
5. C. O'Bannon and F. Mancini. Field Stabilization of Chinle Clay by Electroosmosis and Base Exchange of Ions. Arizona State Univ.; Arizona Department of Transportation; Federal Highway Administration, Rept. FHWA-A2-RD-13 (145), 1975.
6. D. R. Snethen and others. A Review of Engineering Experiences With Expansive Soils in Highway Subgrades. U.S. Army Engineer Waterways Experiment Station, Vicksburg, Miss.; Federal Highway Administration, Interim Rept., 1975.
7. M. L. Steinberg. Interceptor Drains in Heavy Clay Soils. Proc., ASCE, Transportation Engineering Journal, Vol. 96, No. TE 1, Feb. 1970, pp. 1-10.
8. R. Lytton and others. Study of Expansive Clays in Roadway Structural Systems. Center for Highway Research, Univ. of Texas, Austin, Repts. 118 1-8, 1969 to 1974.
9. P. T. C. Teng, R. M. Mattox, and M. B. Clisby. A Study of Active Clays as Related to Highway Design. Research and Development Division, Mississippi Highway Department, 1972.

Publication of this paper sponsored by Committee on Lime and Lime-Fly Ash Stabilization.